National Institute of Justice

[redacted]

COVER PAGE

Agency	**National Institute of Justice**
Award Number	**2017-IJ-CX-0026**
Project Title	**Security Crystals: NIR-To-NIR Upconverting Nanoparticles for Fingerprint Identification and DNA Extraction**
PI Name, Title and Contact Information	**Dr. William M. Cross, Ph.D.** **Professor, Materials and Metallurgical Engineering Department** **South Dakota School of Mines and Technology** **Rapid City, SD, 57701-3995** **Tel: (605) 394-2485; Fax: (605) 394-3369** **E-mail: William.Cross@sdsmt.edu**
Name of Submitting Official, Title, and Contact Information (Director/PI)	**Dr. William M. Cross, Ph.D.** **Professor, Materials and Metallurgical Engineering Department** **South Dakota School of Mines and Technology** **Rapid City, SD, 57701-3995** **Tel: (605) 394-2485; Fax: (605) 394-3369** **E-mail: William.Cross@sdsmt.edu**
Submission Date	**5/31/2022**
DUNS and EIN Numbers	**DUNS: ; EIN: N/A**
Recipient Organization	**South Dakota School of Mines and Technology** **501 East St. Joseph Street** **Rapid City, SD 57701**
Recipient Identifying Number or Account Number, if any	**N/A**
Project/Grant Period	**January 1, 2018 – December 31, 2020**
Project Amount	**$841,307**
Reporting Period End Date	**December 31, 2021**
Report Term or Frequency	**Final**

Signature of Submitting Official

William M. Cross

Summary of the Project

Major Goals and Objectives

The goal of the proposed research is to develop a safe, cost-effective portable field *system* for sensitive, interference-free latent fingerprint identification. The system will be based on near infrared (NIR)-to-NIR upconversion luminescence from optimized upconverting nanoparticles (UCNPs) and be capable of capturing highly resolved fingerprint images under full ambient lighting, even on highly fluorescent surfaces. In addition, the nanoparticles will be used to extract DNA from fingerprints. These goals will be accomplished by an interdisciplinary team with a confluence of expertise in photodynamics, nanoparticle synthesis, particle surface modification (for selective adhesion), interfacial phenomenon, and image analysis. The project builds upon significant prior team success in using upconverting nanoparticles for security printing applications.

The overall goal was met by achieving the following objectives: *a)* optimize UCNP synthesis, scale-up and particle-surface modification for NIR-to-NIR fingerprint imaging and DNA extraction, *b)* develop UCNP transfer procedures to minimize the airborne transport of nanoparticles, *c)* use statistical methods to evaluate UCNP fingerprints against standard procedures, and *d)* develop an optical-capture/image-processing device for implementation of a complete field system.

Research Questions

The primary research question answered was can our upconverting nanocrystals be used to develop latent fingerprints on a variety of surfaces (objective a). In addition to the first question, a second question related to the use of upconverting nanocrystals to collect DNA from the latent fingerprint was investigated (objective a). The third research question involved developing methods to utilize the upconverting nanoparticles in a manner that minimizes exposure of crime scene and laboratory personnel to airborne upconverting nanocrystals (objective c).

Research Design, Methods, Analytical and Data Analysis Techniques

The overall goal of this research was met by following research design: *a)* optimize UCNP synthesis, scale-up and particle-surface modification for NIR-to-NIR fingerprint imaging and DNA extraction, *b)* develop UCNP transfer procedures to minimize the airborne transport of nanoparticles, *c)* use statistical methods to evaluate UCNP fingerprints against standard procedures, and *d)* develop an optical-capture/image-processing device for implementation of a complete field system. The methods used were standard chemical techniques, such as zeta potential measurements, and Fourier transform infrared spectroscopy, along with surface modification techniques for the UCNPs. DNA was examined using polymerase chain reaction experiments. Modifications of standard fingerprinting techniques were used to develop fingerprints using dry UCNP powder, and various non-powder application methods used.

Expected Applicability of the Research

This work developed two complete systems for developing latent fingerprints, one using a laser for use in laboratory environments and one using a light emitting diode for use at crime scenes. In particular, forensic laboratories would have a new tool for obtaining latent fingerprints on surfaces that generally do not work well with either traditional fingerprinting powders or fluorescent fingerprinting powders. In addition, the nanoparticles can collect DNA if modified with acetic acid capping agent.

Participants and Other Collaborating Organizations:

Grant Personnel

Name	Project Role	Affiliation
Faculty and Research Associates		
William M. Cross	Principal Investigator (PI)	South Dakota Mines (SDM)
P. Stanley May	Co-PI	University of South Dakota (USD)
Jon J. Kellar	Co-PI	SDM
Mengyu Qiao	Co-PI	SDM
Linda DeVeaux	DNA Research Consultant	New Mexico Tech (NMT)
Aravind Baride	Research Associate	USD
Anjaneyulu Putta	Research Associate	USD
Students		
Ganesh Sigdel	Graduate Student	USD
Amit Chowdhuri	Graduate Student	USD
Sierra Rasmussen	Graduate Student	SDM
John Hillard	Undergraduate Student	SDM
Ben Ramseyer	Undergraduate Student	SDM
Dennis Kovarik	Undergraduate/Graduate Student	SDM
Casia Esparza	Undergraduate/Graduate Student	NMT
Zumruck Syed	Undergraduate Student	NMT
Michael Yoon	Undergraduate Student	SDM

Other Organizations

Organization Name: University of South Dakota (USD)
Location of Organization: Vermillion, South Dakota, USA
Partner's contribution to the project: Collaborative research
More detail on partner and contribution: Personnel at USD manufactured upconverting nanoparticles, performed experiments related to using these nanoparticles

Organization Name: New Mexico Institute of Mining and Technology (NMT)
Location of Organization: Socorro, NM, USA
Partner's contribution to the project: Collaborative research
More detail on partner and contribution: Personnel at NMT performed DNA extractions and PCR

Organization Name: South Dakota Forensics Laboratory (SDFL)
Location of Organization: Pierre, SD, USA
Partner's contribution to the project: Collaborative research
More detail on partner and contribution: Personnel at SDFL have discussed the project direction and results

Changes in approach from original design and reason for change, if applicable

No major changes in approach were undertaken.

Outcomes

Activities/accomplishments

Two complete systems were developed, one utilizing a laser to excite the upconverting nanoparticles (UCNPs) and a modified cellular phone as a camera to read the upconversion. The UCNPs were tested and worked excellently on a wide variety of substrates, including fluorescent surfaces and under room lighting. A platform for interpreting the fingerprint minutiae and matching fingeprints was also developed. A second light emitting diode (LED)-based system was also developed to read the upconversion from the UCNPs on fingerprints. This utilized a 100 Watt, 980 nm emitting LED and a modified camera to collect the upconversion light. The LED system also included a water-cooling setup to keep the LED emitting light for longer.

Finally, UCNPs were modified to be more attractive to DNA molecules. Acetic acid was used to modify the surface of the UCNPs. Acetic acid modification allowed the UCNPs to pick up DNA at low pH and to shed this DNA when the pH was raised sufficiently. This resulted in the recovery of 15-20% of the DNA. In addition, at low DNA concentrations, polymerase chain reaction (PCR) of the DNA seemed to be inhibited by the presence of UCNPs or contaminants from the UCNPs that are present when UCNPs are used.

Results and findings

Results and finding are given in the accompanying Appendix.

Limitations

The primary limitation to use of the products developed in this study is likely the need to use the reader system to find the latent fingerprints. This is required as the nanocrystals being so small require considerable excitation energy to generate sufficient luminescence. In addition, the complete system would cost in the range of $500-$5,000, while the nanocrystals cost at least $20,000 for 20 grams, and can cost consider4ably more depending on the source. The primary limitation related to the research was the pandemic which resulted in the schools at which the research was performed to be partially or fully closed for much of 2020.

Artifacts

List of products

1. Baride, A.; Sigdel, G.; Cross, W. M.; Kellar, J. J.; May, P. S., Near Infrared-to-Near Infrared Upconversion Nanocrystals for Latent Fingerprint Development. *ACS Applied Nano Materials, 2(7), 4518-4527,* **2019**. DOI: 10.1021/acsanm.9b00890, https://pubs.acs.org/doi/full/10.1021/acsanm.9b00890
2. Dennis Kovarik and Mengyu Qiao, “Automatic Sweat Pore Extraction Using Convolutional Neural Networks”, MICS 2020, April 3, 2020, https://www.youtube.com/watch?v=SxnEgzi0Fhw&list=PLdG9tWxbeSAS7tMrlCBV2ZiO3rstq3-Vp&index=17
3. Dennis Kovarik and Mengyu Qiao, “Improved Minutiae Search in Latent Fingerprint”, MICS 2020, April 3, 2020, https://www.youtube.com/watch?v=mpvqgZdEE00&list=PLdG9tWxbeSAS7tMrlCBV2ZiO3rstq3-Vp&index=12
4. Hannah Weppner, Sierra Rasmussen, Jon Kellar, and William Cross, “Analysis of Upconverting Nanoparticles for Latent Fingerprint Detection”, American Academy of Forensic Sciences (AAFS) Young Investigators Poster Session, AAFS Annual Meeting, Baltimore, MD, February 2019.
5. W.M. Cross, P.S. May, A. Baride, J.J. Kellar, D. Kovarik, M. Daniell, S. Rasmussen, J.D. Hillard, A. Chowdhury, L. DeVeaux, and M. Qiao, “Security Crystals: NIR-to-NIR Upconverting Nanoparticles for Fingerprint Identification and DNA Extraction”, NIJ Poster Session, Pittcon, Philadelphia, PA, February 2019.

6. John Hillard, Aravind Baride, Jon Kellar, William Cross, Stanley May, "Reader Device for NIR-to-NIR Upconverting Nanoparticles in Fingerprint Development", Pacifichem 2020, Honolulu, HA, December, 2020.
7. W. Cross, J. Kellar, M. Qiao, S. Rasmussen, D. Kovarik, B. Ramseyer, P. May, A. Baride, A. Chowdhury, L. DeVeaux, C. Esparza, "Upconverting Security Nanocrystals: DNA Collection and Reader System Development", Presented in the NIJ Poster Session at the Virtual American Academy for Forensic Science Annual Meeting, February 3-7, 2021.
8. W. Cross, J. Kellar, M. Qiao, B. Ramseyer, D. Kovarik, P. May, A. Baride, L. DeVeaux, "Fingerprint Identification System using NIR-To-NIR Upconverting Nanoparticles", Presented in the NIJ Poster Session at Virtual Pittcon, March 11, 2021.

Data sets generated

No data sets were generated in this work.

Dissemination activities

General Public Dissemination

In May, 2018, Dr. William M. Cross and Ph. D. student Sierra Rasmussen discussed research related to this grant on local TV station KOTA-TV. The link given next has a brief outline of the story and the story video. https://www.kotatv.com/content/news/Dusting-up-on-fingerprints--481700831.html

Dr. P. Stanley May (co-PI) appeared on the Credit Hour Podcast in September 2018 and discussed some aspects of the research from this grant. A link to the podcast is given below. This link also contains a link to the podcast itself. https://www.usd.edu/the-south-dakotan/stanley-may-discusses-counterfeiting-detection-on-credit-hour

National Institute of Justice

2017-IJ-CX-0026 Summary Report Appendix

COVER PAGE

Agency	**National Institute of Justice**
Award Number	**2017-IJ-CX-0026**
Project Title	**Security Crystals: NIR-To-NIR Upconverting Nanoparticles for Fingerprint Identification and DNA Extraction**
PI Name, Title and Contact Information	**Dr. William M. Cross, Ph.D.** **Professor, Materials and Metallurgical Engineering Department** **South Dakota School of Mines and Technology** **Rapid City, SD, 57701-3995** **Tel: (605) 394-2485; Fax: (605) 394-3369** **E-mail: William.Cross@sdsmt.edu**
Name of Submitting Official, Title, and Contact Information (Director/PI)	**Dr. William M. Cross, Ph.D.** **Professor, Materials and Metallurgical Engineering Department** **South Dakota School of Mines and Technology** **Rapid City, SD, 57701-3995** **Tel: (605) 394-2485; Fax: (605) 394-3369** **E-mail: William.Cross@sdsmt.edu**
Submission Date	**5/19/2022**
DUNS and EIN Numbers	**DUNS: 929928018; EIN: N/A**
Recipient Organization	**South Dakota School of Mines and Technology** **501 East St. Joseph Street** **Rapid City, SD 57701**
Recipient Identifying Number or Account Number, if any	**N/A**
Project/Grant Period	**January 1, 2018 – December 31, 2021**
Reporting Period End Date	**December 31, 2021**
Report Term or Frequency	**Final**

Signature of Submitting Official

William M. Cross

Table of Contents

Executive Summary

The goal of this research was to develop a safe, portable field *system* for sensitive, interference-free latent fingerprint identification. The system will be based on near infrared (NIR)-to-NIR upconversion luminescence from optimized upconverting nanoparticles (UCNP) and be capable of capturing highly resolved fingerprint images under full ambient lighting, even on highly fluorescent surfaces. In addition, the nanoparticles will be used to extract DNA from fingerprints.

Two systems were developed, one utilizing a laser to excite the upconverting nanoparticles (UCNPs) and a modified cellular phone as a camera to read the upconversion. The UCNPs were tested and worked well on a wide variety of substrates, including fluorescent surfaces and under room lighting. A platform for interpreting the fingerprint minutiae and matching fingerprints was also developed. A second light emitting diode (LED)-based system was also developed to read the upconversion from the UCNPs on fingerprints. This utilized a 100 Watt, 980 nm emitting LED and a modified camera to collect the upconversion light. The LED system also included a water-cooling setup to keep the LED emitting light for longer.

Finally, UCNPs were modified to be more attractive to DNA molecules. Acetic acid was used to modify the surface of the UCNPs. Acetic acid modification allowed the UCNPs to pick up DNA at low pH and to shed this DNA when the pH was raised sufficiently. This resulted in the recovery of 15-20% of the DNA. In addition, at low DNA concentrations, polymerase chain reaction (PCR) of the DNA seemed to be inhibited by the presence of UCNPs or contaminants from the UCNPs that are present when UCNPs are used.

Accomplishments

1. What are the major goals and objectives of the project?

The goal of the proposed research is to develop a safe, cost-effective portable field *system* for sensitive, interference-free latent fingerprint identification. The system will be based on near infrared (NIR)-to-NIR upconversion luminescence from optimized upconverting nanoparticles (UCNP) and be capable of capturing highly resolved fingerprint images under full ambient lighting, even on highly fluorescent surfaces. In addition, the nanoparticles will be used to extract DNA from fingerprints. These goals will be accomplished by an interdisciplinary team with a confluence of expertise in photodynamics, nanoparticle synthesis, particle surface modification (for selective adhesion), interfacial phenomenon, and image analysis. The project builds upon significant prior team success in using upconverting nanoparticles for security printing applications.

The overall goal was met by achieving the following objectives: *a)* optimize UCNP synthesis, scale-up and particle-surface modification for NIR-to-NIR fingerprint imaging and DNA extraction, *b)* develop UCNP transfer procedures to minimize the airborne transport of nanoparticles, *c)* use statistical methods to evaluate UCNP fingerprints against standard procedures, and *d)* develop an optical-capture/image-processing device for implementation of a complete field system.

Figure 1 displays the revised timeline for this project after no-cost extension. All milestones have been met, and are described in the body of this report.

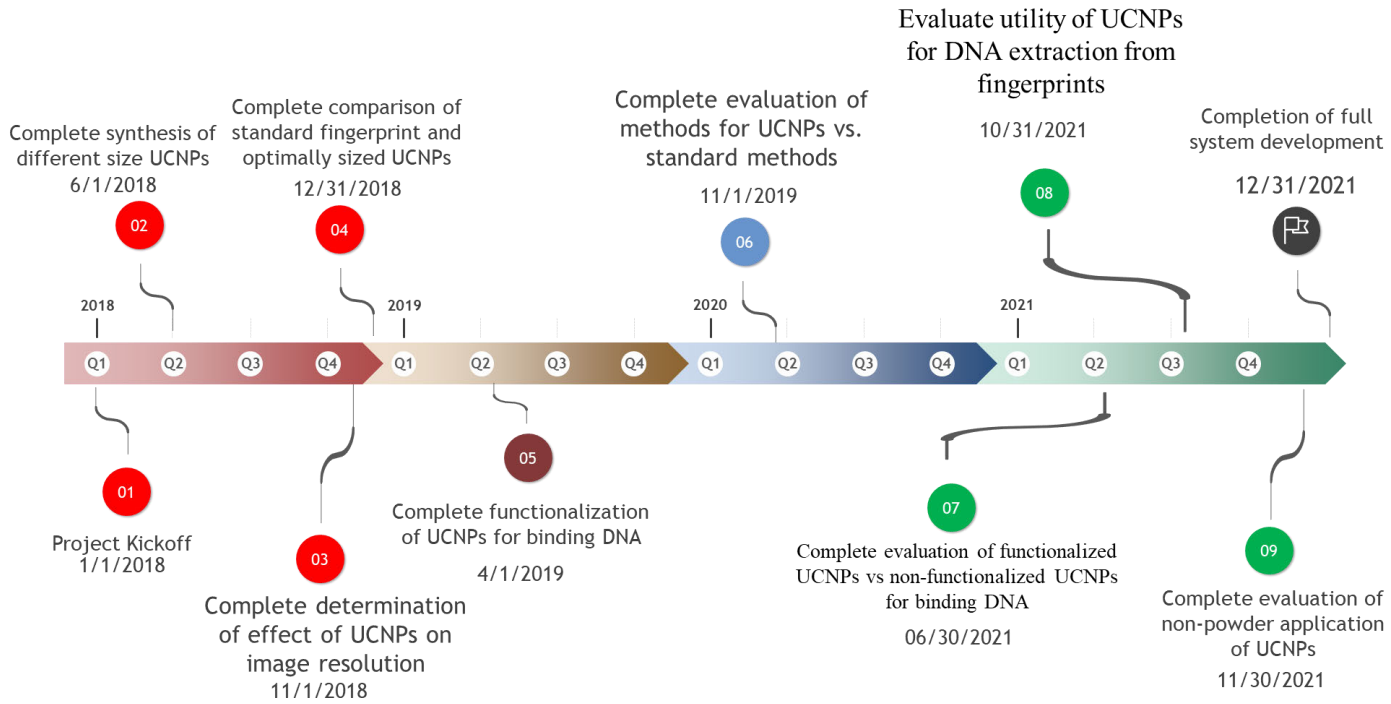

Figure 1. Revised project timeline.

2. What was accomplished under these goals?

The research performed for each of the identified tasks and is described under each Task Identifier along with the more specific purpose of the task, and the overall task outcome survey. Overall, we developed a system that can

develop and obtain fingerprints on a variety of substrates using doped-$NaYF_4$ upconverting nanoparticles (UCNPs). Recovery of DNA from fingerprints using doped-UCNPs was possible, although the polymerase chain reaction (PCR) proved difficult with this system.

Task 1: Kickoff Meeting

Purpose: The purpose of this meeting was to get the team together, introduce the team members that did not know each other and to begin to develop an initial team-based strategy.

Task Summary: A kickoff meeting was held via our Access Grid node to discuss the grant and develop a strategy for the upcoming research. This meeting was held the week of January 3-10, 2018. In addition, meetings were held approximately weekly via the Access Grid node and then Zoom after the campuses were partially closed due to Covid-19 (spring 2020). In these weekly meetings research results were shared and the current and future directions for the research were discussed by all participants.

Task 2: Complete Synthesis of a Range of UCNP Sizes

Purpose: Achieving the proper size of upconverting nanoparticles (UCNPs) was critical to the success of this research grant. Several competing factors interplay to create an optimal size for UCNPs. In particular, as the UCNP size increases, the emission of upconverted light increases. However, as UCNP size increases there will come a point at which fingerprint detail, including minutiae, will be lost. The first step in this process was to manufacture a range of UCNP sizes.

Research: With respect to this task, UCNP sizes of approximately 48, 70, 150 and 220 nm were synthesized. **Figure 2** shows micrographs of the UCNPs synthesized.

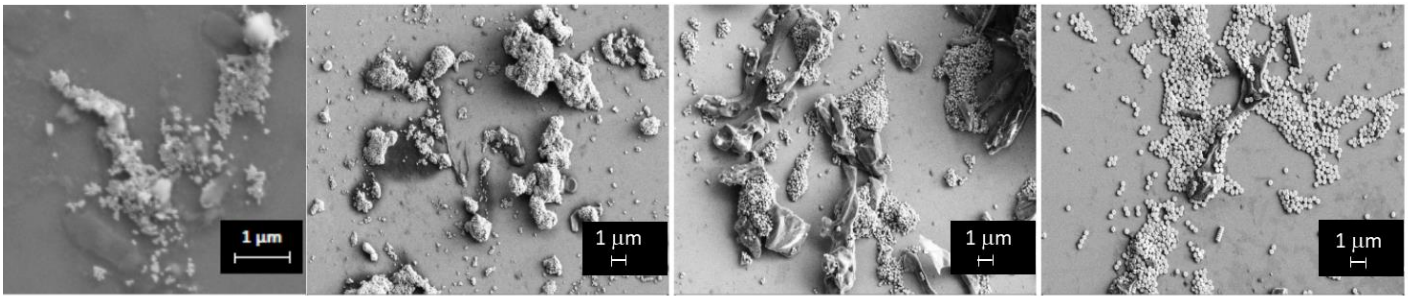

a) 48 nm b) 70 nm c) 140 nm d) 220 nm

Figure 2. SEM micrographs of the UCNPs manufactured for this research. The UCNP sizes are given below each figure.

Task Research Summary: Four different sizes of doped-$NaYF_4$ upconverting nanoparticles were manufactured and were tested as described in Task 3.

Task 3: Effect of UCNP Size/Surface Characteristics on Image Quality

Purpose: With the UCNPs manufactured in Task 1, the optimum UCNP size between the sizes manufactured was determined.

Research: Understanding the trade-offs in choosing the optimal particle size for fingerprint development is especially important for upconversion nanomaterials. The intrinsic quantum yields of UCNPs are known to fall rapidly as particle size drops below ~100 nm due to surface quenching effects. Surface quenching is particularly deleterious in UCNPs, because of the non-linear nature of the excitation mechanism. Therefore, from a

'brightness' point of view, the larger the particles the better. However, it has also been shown that UCNPs produce higher-resolution fingerprint images compared to micron-sized powders of the same material. An optimal size of the nanoparticles was determined based on three criteria: image intensity, resolution and contrast.

Four sizes of the fingerprint development particles were used: 70 nm, 140 nm, 220 nm and a micron-sized upconversion powder. To reduce the number of variables in the fingerprint itself, four pre-cut pieces of silicon wafer were arranged as shown in **Figure 3** (left) and a single fingerprint was stamped over all the four sections of the silicon wafer. Each section of the silicon wafer, containing a partial fingerprint, was developed using one of the four UC powder sizes under study. Two sets of fingerprint samples were prepared, in which, the first set was developed using a soft feather brush and the second set was developed by sprinkling the powder and removing the excess powder by tapping the substrate. The prepared fingerprint samples were used for the scanning electron microscope (SEM) imaging followed by optical imaging.

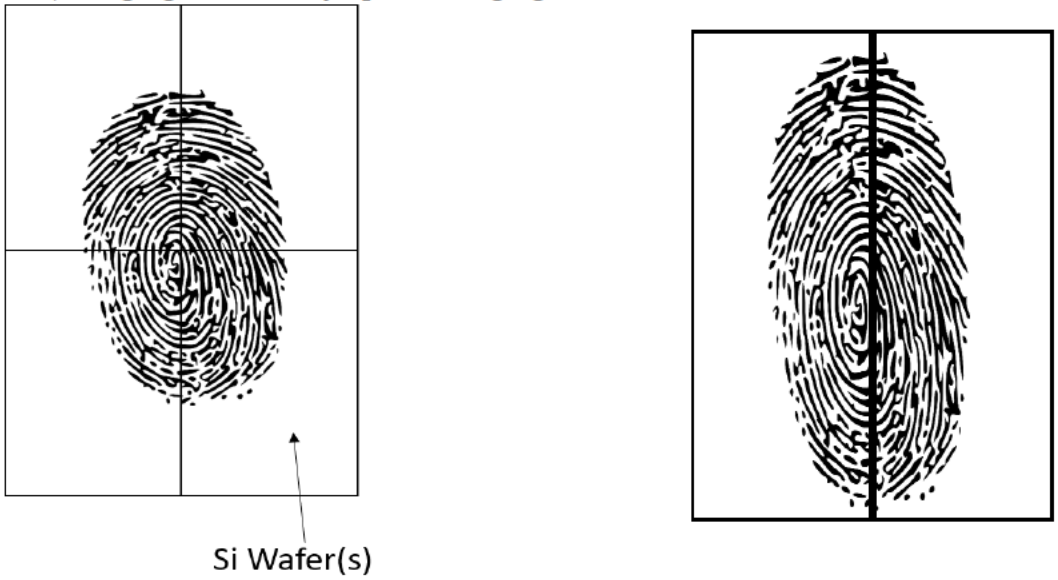

Figure 3. Techniques used for the fingerprint deposition and analysis. To enable SEM analysis of the powder deposition, a Si (conductive) substrate was divided into four sections (left). The real-life (non-Si) substrates were prepared by dividing into two sections (right).

In addition to the analysis on the conductive Si wafers, which enabled SEM characterization, three sizes of the UCNP particles were used for the analysis of fingerprint development on "real-life" substrates: 70 nm, 140 nm and 220 nm. The preparation of fingerprint sample on the non-Si substrates such as plastic cards, glass and a Coca-Cola label, is represented by schematic diagram in **Figure 3** (right). Two sections of the substrates with a partial fingerprint were developed using two different sizes of the nanoparticles at a time. In the first step, each section of the fingerprint samples was developed with one of 70 nm and 140 nm powders. In second step, two sections of the fingerprint samples were developed with one of 140 nm and 220 nm powders. The developed fingerprint samples were studied by optical imaging.

SEM was used to characterize the distribution of particles on the fingerprint residues on Si. The SEM images in **Figure 4** show that the nanoparticles are well distributed along the oil residues defining the fingerprint ridges. The 220 nm size powder is distributed more uniformly than the other powders under study. Whereas, in the fingerprint sample prepared with micron size powder (not shown here), the distribution of particles along the oils is not uniform.

This resource was prepared by the author(s) using Federal funds provided by the U.S. Department of Justice. Opinions or points of view expressed are those of the author(s) and do not necessarily reflect the official position or policies of the U.S. Department of Justice.

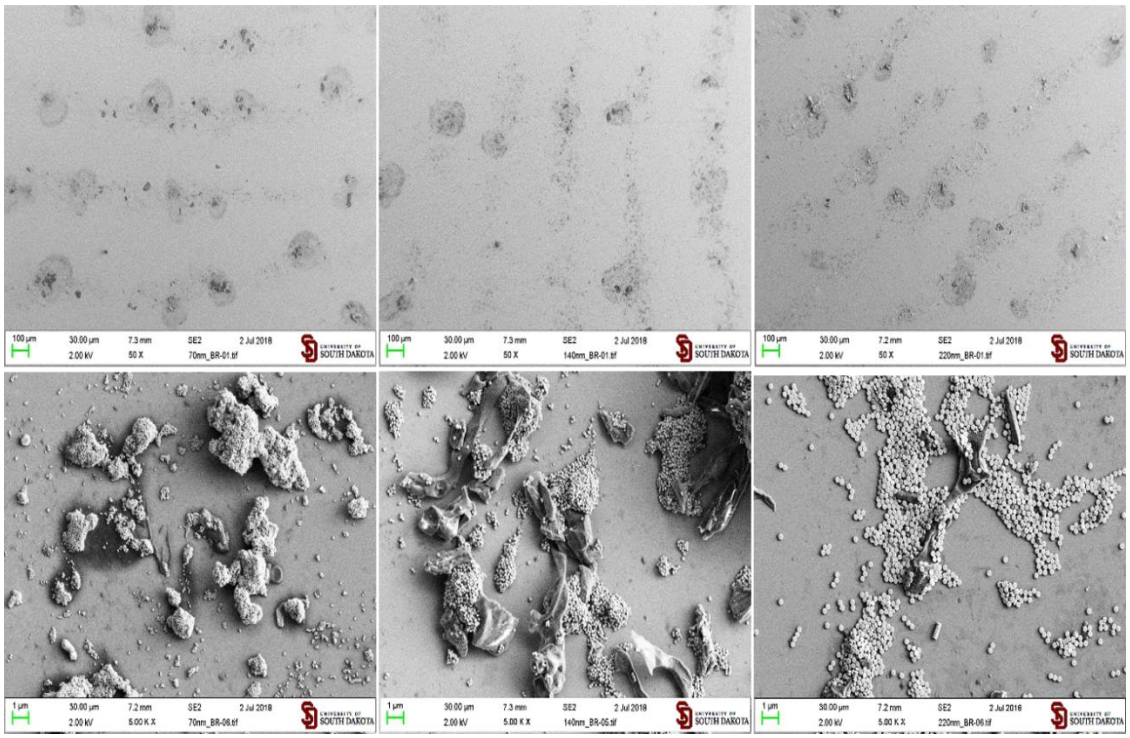

Figure 4. SEM images of the fingerprint developed using different sized UCNP using a brush technique. The left panels correspond to 70 nm UCNP, the center panels to 140 nm (center panel), and the right panels to 220 nm UCNP. The first-row images are at 50× magnification. The second-row images are at 5,000× magnification.

Comparison of optical images of the fingerprint samples on the silicon wafer showed that sprinkling produced brighter than those developed with the brush. However, the resolution and contrast of the fingerprint was better when developed using the brush (**Figure 5**). For the brush technique, it was consistently observed that the 220 nm UCNP produced by far the brightest images with no notable loss of resolution or contrast relative to the smaller particles.

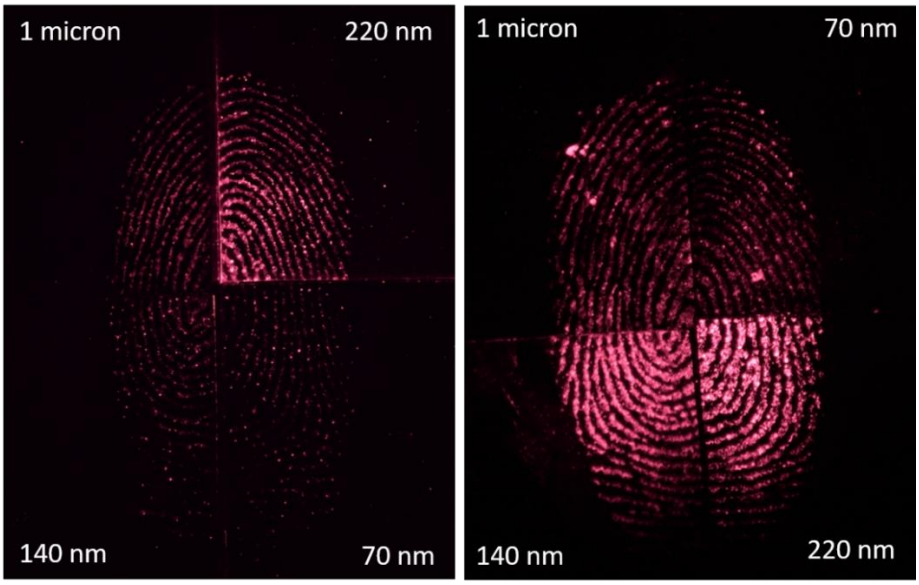

Figure 5. Images of fingerprints developed on silicon wafers using brush (left) and sprinkling (right) powder application for four different sized particles. The power density used for the fingerprint developed using the brush was 650 mW/cm^2 and for the fingerprint developed by sprinkling was 100 mW/cm^2.

An optical imaging study was done using several substrates such as a printing paper with complex background patterns, a plastic card, a Coca-Cola plastic label and a glass slide. In this study, a comparison between the fingerprints was performed in two steps. In the first step, fingerprints developed by 70 nm and 140 nm sized UC powders were evaluated for intensity, resolution and contrast. **Figure 6** is the fingerprint image developed on printing paper with a complex background. The complex background in **Figure 6a** was printed on normal printing paper using an Epson thermal ink-jet printer. The powders were applied by sprinkling and excess was dusted off from the substrates by tapping. The actual image (**Figure 6b**) was converted into a negative (**Figure 6c**) and grayscale images (**Figures 6c** and **6d** using ImageJ software. The loss in contrast in some areas of the actual image was improved by converting to the negative image and producing its grayscale image. The fingerprint developed with 140 nm powder was expected to be brighter than the fingerprint image developed with 70 nm powder. However, surprisingly, there were no significant differences in the fingerprint images regarding intensity, indicating that more 70 nm material adhered better to the fingerprint residue relative to that of the 140 nm material. There was no marked difference in resolution and contrast of the images produced using the 70 nm and 140 nm UCNP.

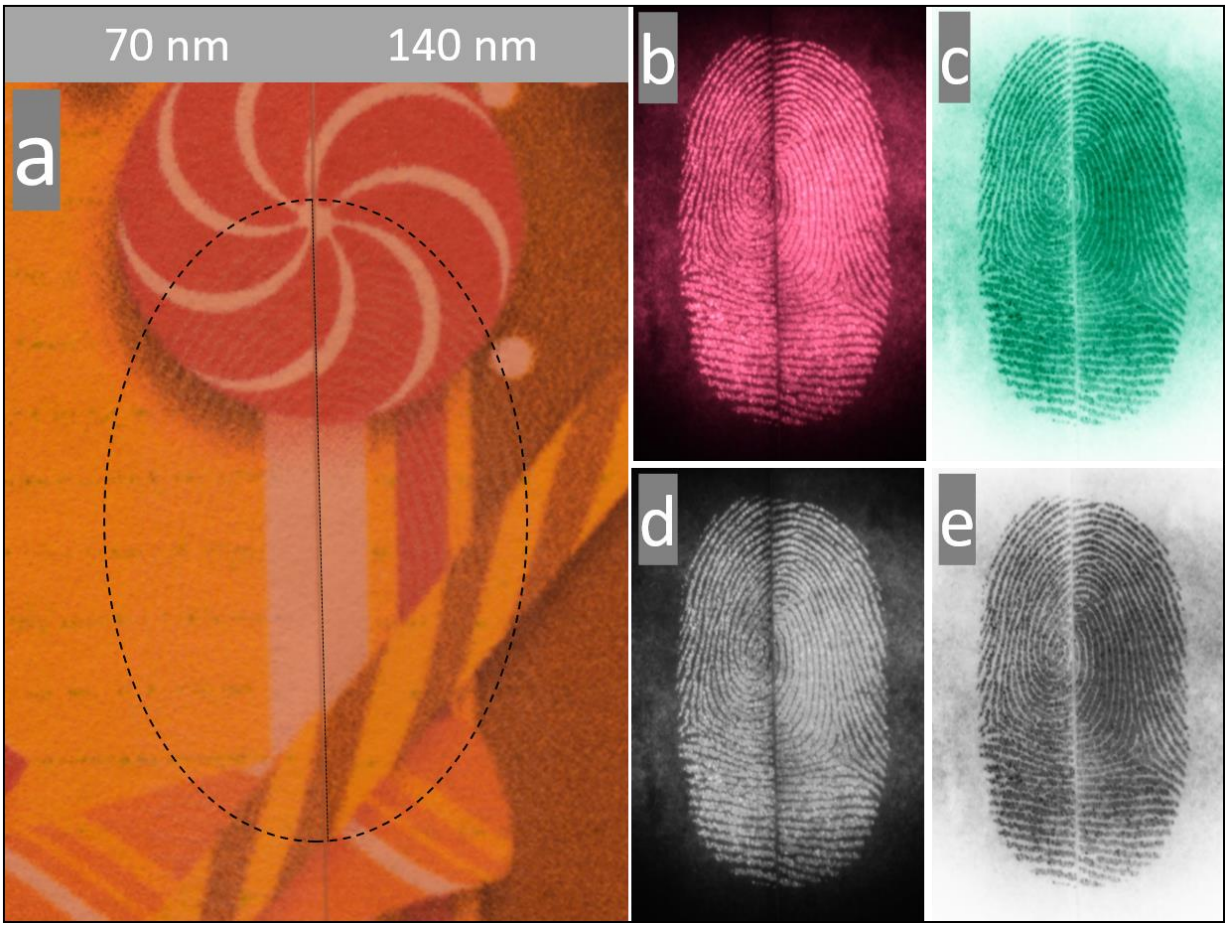

Figure 6. Fingerprints developed on printing paper with a complex pattern produced by an Epson thermal inkjet printer. a) Room-light image of the substrate showing fingermark inside dashed line. Left half of image was developed using 70 nm powder and the right half was developed using 140 nm powder. b) image captured at 100 mW/cm^2 laser power, c) inverted (negative) image created of (b). (d) and (e) are grayscale images of (b) and (c) respectively. The negative and grayscale images were obtained with the help of the ImageJ software.

Similar results were obtained when the fingerprints were developed on the plastic card and the glass slide regarding intensity, resolution, and contrast (**Figure 7**).

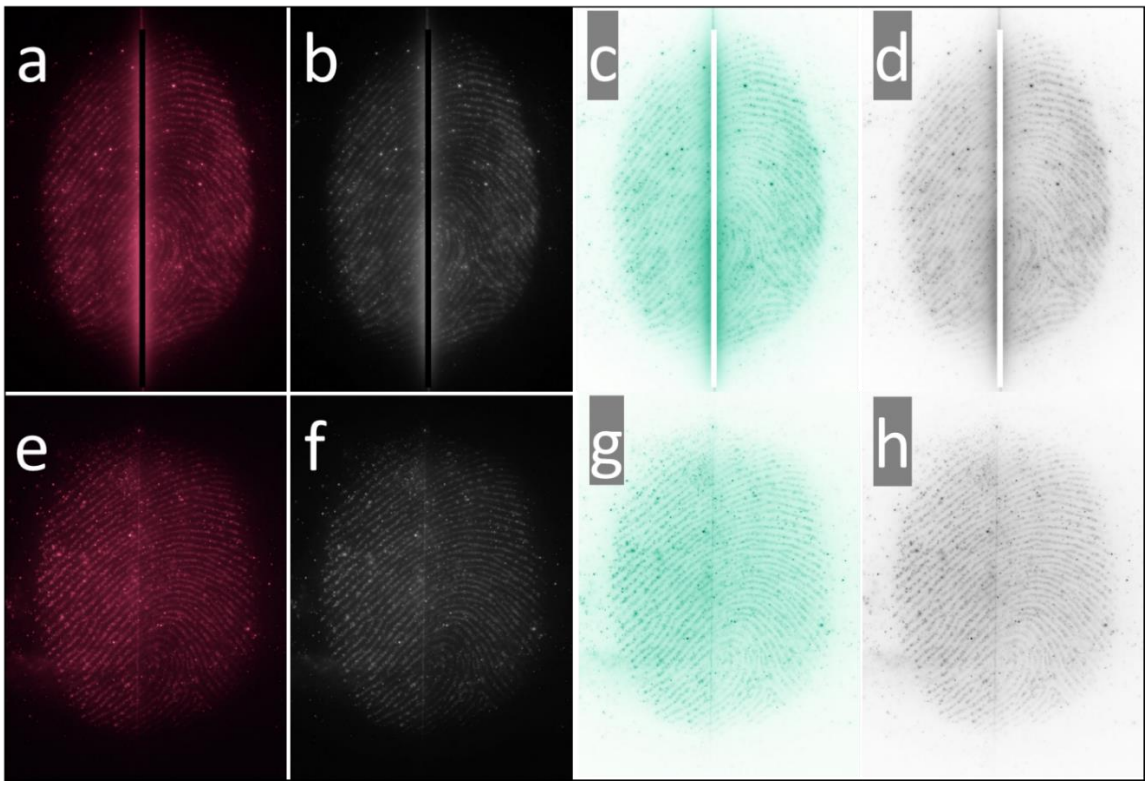

Figure 7. Fingerprint images developed on a plastic card (first row) and glass slide (second row). (a, e) are images captured using a 975 nm laser source at 150 mW/cm^2 and 300 mW/cm^2 respectively. (b, f) are grayscale images of (a, e); (c, g) are inverted images of (a, e); (d, h) are grayscale images of (c, g) respectively. The left half of each image was developed by 70 nm powder and right half of each image was developed by 140 nm powder. The negative and grayscale images were obtained with use of ImageJ software.

In the second step, fingerprints developed by 140 nm and 220 nm sized powders were evaluated for resolution and contrast. Both the 70 nm and 140 nm powders have 48% ytterbium and 2% thulium, whereas, the 220 nm powder has 98% ytterbium and 2% thulium. **Figure 8** is the fingerprint image developed on a Coca-Cola label and a glass slide. It was observed that the part of fingerprint developed by 220 nm powder was brighter compared to the other half of the fingerprint developed by 140 nm powder.

The powder with higher Yb^{3+} doping concentration is expected to produce a brighter image based on a previous report in the literature. Comparing the relative intensities and resulting resolution and contrast of the fingerprints developed with the NIR powders having two different doping concentrations at the same excitation laser power density could be misleading. To overcome this problem, another study was done by comparing the fingerprints at different exposure times, keeping the power density equal. The image in **Figure 9** is the fingerprint image developed on glass slides and captured at two different exposure times. This shows two halves of the fingerprint developed by 220 nm and 140 nm powders. The fingerprint sections, **Figure 9a'** and **Figure 9b**, exhibit comparable resolution and contrast. The two sections are from two different images captured at two different exposure times. The fingerprint images are captured at two different exposure times to obtain the images of each of the fingerprint sections with comparable brightness.

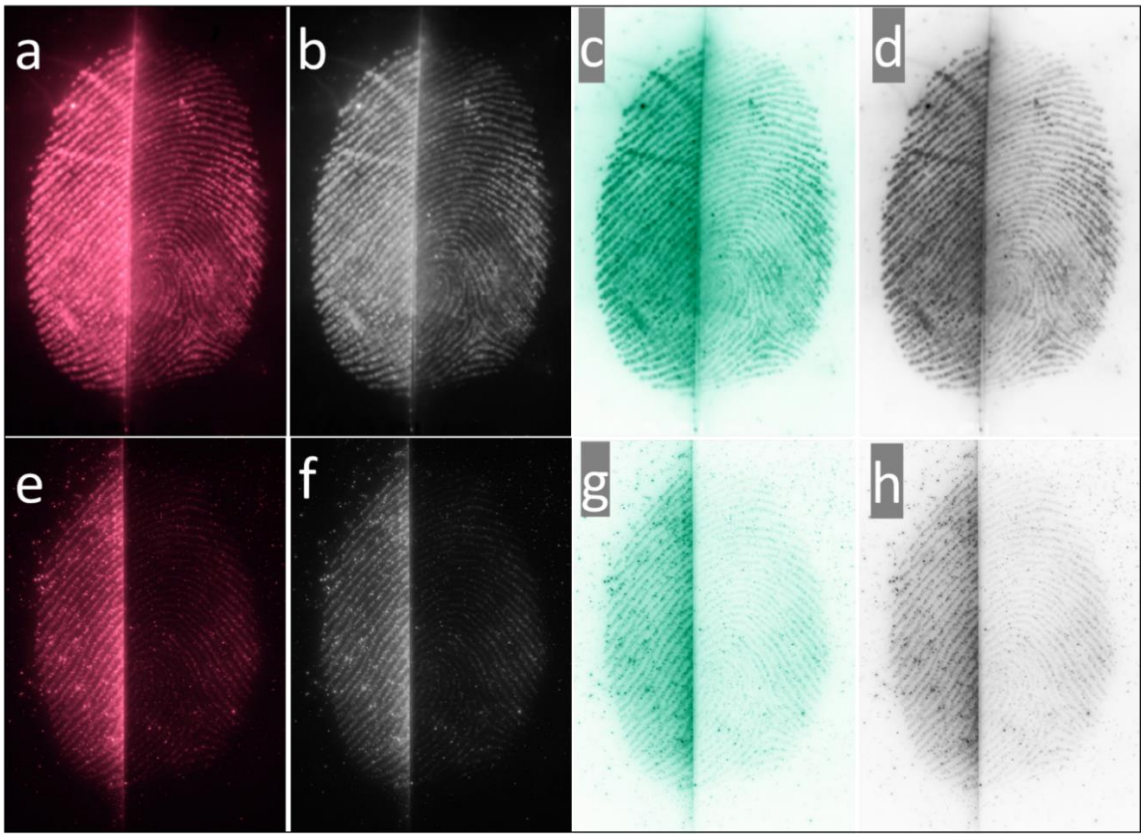

Figure 8. Fingerprint images developed on a Coca-Cola label (first row) and a glass slide (second row). (a, e) are images captured using a 975 nm laser source at 150 mW/cm^2 and 200 mW/cm^2 respectively. (b, f) are grayscale images of (a, e); (c, g) are inverted images of (a, e); (d, h) are grayscale images of (c, g) respectively. Left half of each image was developed by 220 nm powder and right half of each image was developed by 140 nm powder. The negative and grayscale images were obtained with the help of the ImageJ software.

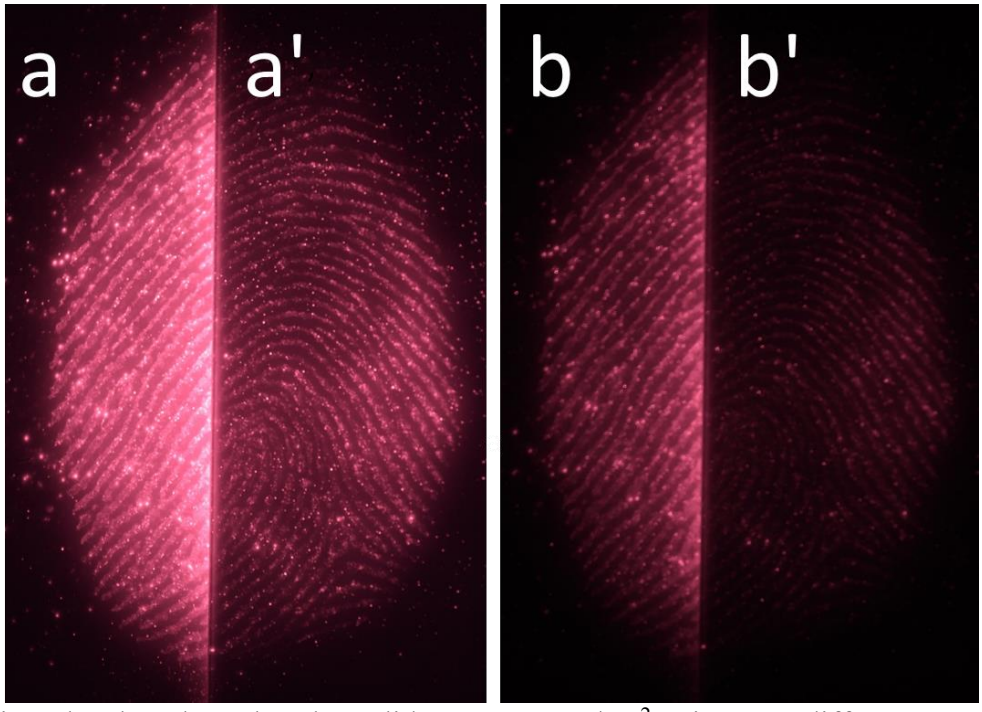

Figure 9. Fingerprints developed on the glass slide at 250 mW/cm^2 using two different exposure times. The exposure time was 1/2 s and 1/10 s for the left image (a,a') and the right image (b,b') respectively. The left half of each image (a,b) was developed using 220 nm powder and the right half of each image (a',b') was developed using 140 nm powder.

Similarly, the fingerprint developed on the Coca-Cola label using 220 nm and 140 nm powders are shown in **Figure 10**. The fingerprint sections, **Figure 10a'** and **Figure 10b**, exhibit comparable resolution and contrast. The two sections are from the two different images captured at two different exposure times. It is concluded that there is no noticeable difference in the resolution and the contrast of the fingerprint images developed with the 220 nm and 140 nm sized powders. However, the fingerprint images are taken at two different exposure times to obtain the images of each of the fingerprint sections with comparable brightness.

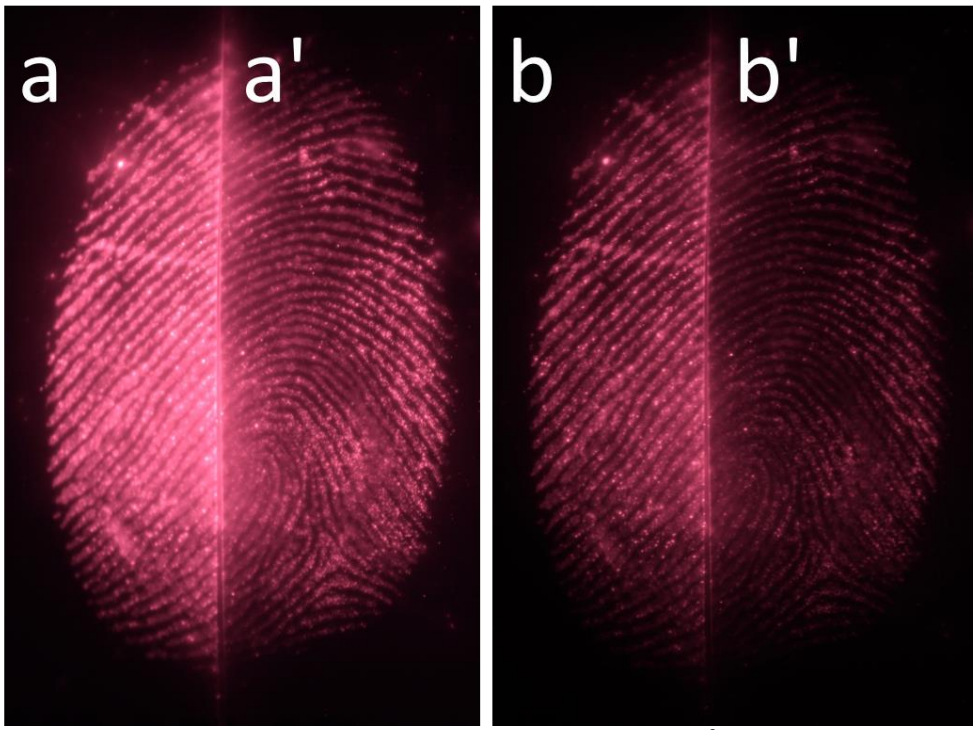

Figure 10. Fingerprints developed on the Coca-Cola label at 200 mW/cm^2 using two different exposure times. The exposure time was 1/4 s and 1/15 s for the left image (a,a') and the right image (b,b') respectively. The left part of each image (a,b) was developed using the 220 nm powder and the right part of each image (a',b') was developed using the 140 nm powder.

Task Research Summary: In summary, our study showed no noticeable difference in the resolution and the contrast of the fingerprint images for the different UCNP sizes manufactured. However, the 220 nm UCNP produce by far the brightest images under a given set of exposure conditions, making these UCNP the optimal materials for fingerprint development.

Task 4: Comparison: Optimal UCNP System versus Standard Procedures

Purpose: This task utilized dry powder processing of fingerprints developed with UCNPs and compared with standard powders on a variety of substrates

Research: The optimal UCNP size using both green and near infrared (NIR) upconverting powders has been examined on soft drink cans, soft drink plastic labels, and substrates with complex color patterns, which are often difficult to examine using conventional powders.

To facilitate SEM imaging, latent fingerprints were impressed on smooth silicon substrates. The latent fingerprints were then developed using UCNPs taken from the various stages of processing: crushing with mortar and pestle, then vortex agitation, followed by pressing between weighing papers.

The top row of SEM images in **Figure 11** show raw, undeveloped fingerprints at magnifications of 50×, 500×, and 2500×. The ridges of the prints are visible due mainly to oils deposited on the substrate. Small crystals of NaCl(s), which presumably form during sweat evaporation, are also observed in the high-magnification image.

The second row of SEM images in **Figure 11** shows fingerprints developed with UCNP powder crushed with a mortar and pestle, at magnifications of 50×, 500×, and 2500×. The 'particles' on the substrate are clearly large, jagged aggregates of nanoparticles on the order of microns in dimension, such that the potential resolution advantage of the nanoparticles is lost.

The third row of SEM images in **Figure 11** shows fingerprints developed with UCNP powder crushed with a mortar and pestle, then agitated with a vortex mixer. The vortex mixing has effectively increased the size of the aggregates observed after mortar and pestle grinding, but the aggregate particles are rounder and much less jagged. In fact, as discussed below, the UCNP within these aggregate particles are very loosely bound together and the aggregates are easily destroyed by gentle pressing of the powder between weighing papers.

The fourth row of SEM images in **Figure 11** shows fingerprints developed with UCNP powder crushed with a mortar and pestle, then agitated with a vortex mixer, and, finally, pressed between weighing papers. The large spherical aggregates observed following vortex mixing have been effectively broken down, and the oil residues of the fingerprints are covered mainly by monolayers of individual UCNPs. In a larger reproduction of image 'l', the smooth coating of the oil residues with non-aggregated UCNP can be seen. Note also that the UCNP are highly selective for the oil residues, with low densities of particles seen on the clean surfaces of the substrate.

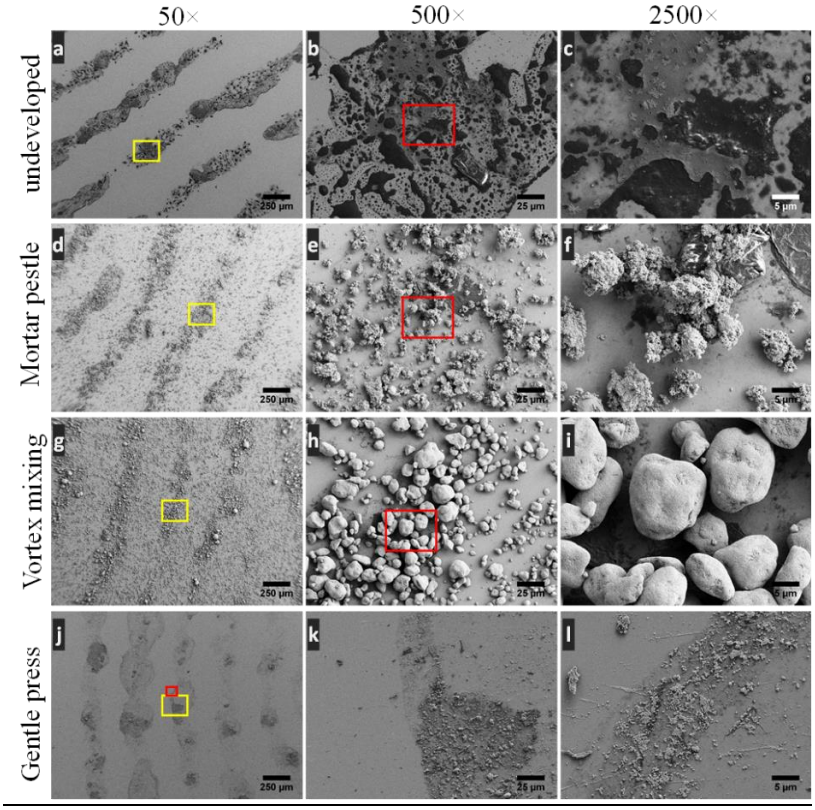

Figure 11. SEM images of latent and UCNP-developed fingerprints on silicon. The top row of images represent an undeveloped latent fingerprint. Each subsequent row of images represents fingerprints developed with UCNP powders obtained at different stages of the processing shown in **Figure 10**. Each column represents a different level of magnification (left-to-right: 50×, 500×, 2500×). Top row (images a-c): undeveloped fingerprint. Second row (images d-f): as-cleaned UCNP powder crushed with mortar and pestle. Third row (images g-i): the powder agitated with a vortex mixer. The fourth row (images j-l): the agitated powder pressed between weighing papers. The yellow box in the first column corresponds to the area that is further magnified in the second column. The red box corresponds to the area that is further magnified in the third column.

Figure 12 shows a comparison of latent fingerprints on a soft-drink can developed with NIR-to-NIR (top row) and NIR-to-visible (bottom row) UCNP using two different levels of excitation irradiance. The first image in each row is a photograph of the fingerprint area in fluorescent room light. The second and third images in each row are photographs of the developed fingerprints at excitation irradiance levels of 400 $mW \cdot cm^{-2}$ and 600 $mW \cdot cm^{-2}$, respectively.

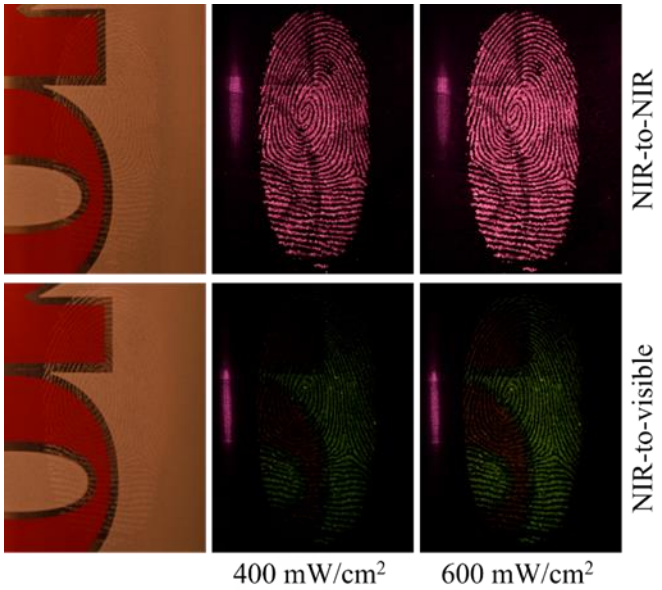

Figure 12. Latent fingerprints on a soft-drink can developed with NIR-to-NIR (top row) and NIR-to-visible (bottom row) UCNP. Left-to-right, the fingerprint area is shown a) in fluorescent room light, b) under 976 nm excitation at 400 $mW \cdot cm^{-2}$ irradiance, and c) under 976 nm excitation at 600 $mW \cdot cm^{-2}$ irradiance.

The NIR-to-NIR nanoparticles under 400 $mW \cdot cm^{-2}$ irradiance (top row, center panel) produce an image exhibiting excellent sensitivity, selectivity, and contrast. The contrast of the background pattern is greatly reduced in the NIR (800 nm) and does not interfere significantly with the fingerprint image. The contrast between the red fill within the lettering and white base color of the beverage can is almost completely eliminated.

In contrast, the NIR-to-visible nanoparticles under 400 $mW \cdot cm^{-2}$ irradiance (bottom row, center panel) fail to yield a readable image of the print. If the irradiance is increased to 600 $mW \cdot cm^{-2}$, (bottom row, right panel) the portion of the print over the white background becomes visible, but the interference from the lettering on the can obscures the remainder of the image.

Figure 13 shows a comparison of latent fingerprints on a plastic label developed with NIR-to-NIR (top row) and NIR-to-visible (bottom row) UCNP using two different levels of excitation irradiance. The first image in each row is a photograph of the fingerprint area in room light. The second and third images in each row are photographs of the developed fingerprints at excitation irradiance levels of 200 $mW \cdot cm^{-2}$ and 600 $mW \cdot cm^{-2}$, respectively.

Even at the low irradiance of 200 $mW \cdot cm^{-2}$, the NIR-to-NIR developed print is well imaged, with essentially no interference from the substrate background (top row, center panel); the print image shows uniform brightness over the entire print area. In contrast, an irradiance of 200 $mW \cdot cm^{-2}$ produces no readable image for the NIR-to-visible UCNP. At 600 $mW \cdot cm^{-2}$, the NIR-to-visible print image becomes apparent, but contrast is poor over the colored portions of the background, and there is a large variation in intensity over the print area. The brightness of the NIR-to-NIR fingerprint image obtained at 600 $mW \cdot cm^{-2}$ is shown for comparison (top right panel). The loss in contrast relative to that obtained under 200 $mW \cdot cm^{-2}$ irradiance (top center panel) is due to camera saturation; contrast at 600 $mW \cdot cm^{-2}$ is restored by reducing the exposure.

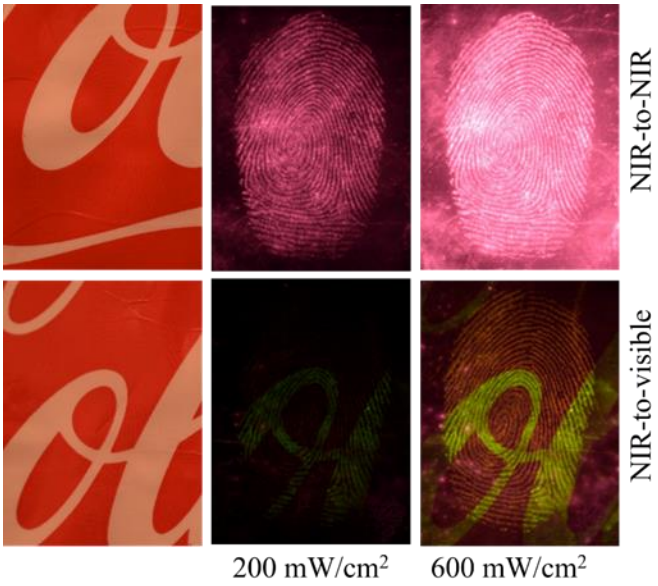

Figure 13. Latent fingerprints on the plastic label of a soft-drink bottle developed with NIR-to-NIR (top row) and NIR-to-visible (bottom row) UCNP. Left-to-right, the fingerprint area is shown a) in room light, b) under 976 nm excitation at 200 $mW \cdot cm^{-2}$ irradiance, and c) under 976 nm excitation at 600 $mW \cdot cm^{-2}$ irradiance.

The suppression of background color when imaging in the NIR is due primarily to the fact that many inks used in printing have little or no absorbance in the NIR. (This is not true, however, for pigments containing carbon black, for example.) **Figure 14** shows the NIR-to-NIR print images developed on several different substrates with complex color patterns: a polymer banknote, a paper banknote, and a business card. The upper row of panels are normal photographs of the areas to be imaged, and the lower row of panels are the corresponding NIR-to-NIR fingerprint images. For the most part, the background images are suppressed or significantly reduced.

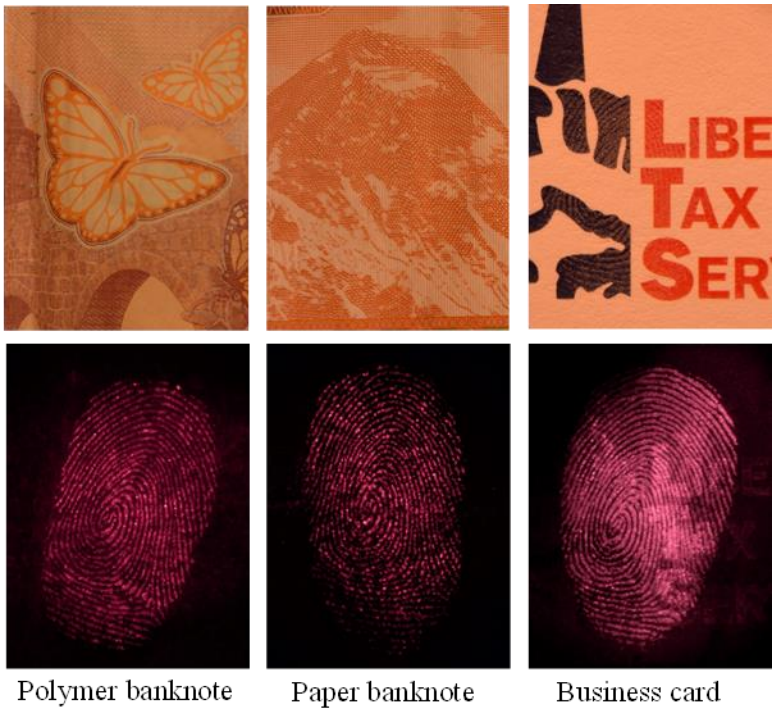

Figure 14. Fingerprints developed with NIR-to-NIR UCNP on substrates with complex color patterns (high value substrates). The upper row of panels are normal photographs of the areas to be imaged, and the lower row of panels are the corresponding NIR-to-NIR fingerprint images.

Figure 15 shows a comparison of 'dark' and room-light imaging of fingerprints using the NIR-to-NIR and the NIR-to-visible nanoparticles. **Figure 15a** indicates the area of the substrate to be imaged. **Figures 15c and 15d** show the fingerprint imaged using NIR-to-NIR nanoparticles in the dark and in fluorescent room light, respectively. Note that there is very little difference in the quality of the two images. Only a slight loss of contrast is observed in room-light conditions, which we attribute to imperfect filtering of the visible spectrum.

Figure 15b compares the output of two common types of room lighting (LED and fluorescent) with the upconversion emission spectra of our NIR-to-NIR and NIR-to-visible nanoparticles. Both the LED and fluorescent sources show significant overlap with the upconversion spectrum of the NIR-to-visible UCNP. This is particularly true for the fluorescent light source, for which the strong Tb^{3+} emission at 540 nm almost perfectly overlaps the NIR-to-green emission of the UCNP. Obviously, room lighting will significantly reduce the contrast and sensitivity of fingerprint development using the NIR-to-visible nanoparticles.

However, for purposes of efficiency, the output of modern artificial lighting is confined to the visible spectrum. As shown in **Figure 15b** there is virtually no overlap between the 800 nm upconversion band of the NIR-to-NIR UCNP and the emission output of the LED and fluorescent sources. The configuration of the camera used for NIR imaging captures only the NIR portion of the light spectrum outlined in the upper right panel of **Figure 16** by a black dotted-line box. Therefore, fingerprint images can be captured in full fluorescent or LED room light with little loss of contrast or sensitivity.

Figures 15e and 15f show the fingerprint imaged using NIR-to-visible nanoparticles in the dark and in fluorescent room light, respectively. Only the portion of the light spectrum centered on the green upconversion at 540 nm, indicated by the box drawn in **Figure 15b**, was captured by the camera. In this case, there is a complete loss of sensitivity of the upconversion image in room light, because the upconversion luminescence intensity is overwhelmed by the green output of the fluorescent lighting. The only visible indication of the print is due to the contrast in the reflected room light.

Figure 16 shows an example of fingerprint development using NIR-to-NIR UCNP that simultaneously highlights two of the main advantages of these materials: background pattern suppression and high-sensitivity imaging in room light. The substrate (**Fig. 16a**) is a complex, black pattern printed on normal paper using an Epson thermal ink-jet printer. **Figures 15b and 15c** show the luminescent NIR image of the developed fingerprint captured in the dark and in room light, respectively. Again, only a slight loss of contrast is observed in moving from in-dark to room-light conditions. **Figure 16d** is an optimized reproduction of **Figure 16c**. The image optimization was performed using IrfanView 4.44 software (Auto Adjust Colors -> convert to Gray Scale -> invert imaging, all channels).

The developed fingerprint images in **Figures 12 and 13** were examined for minutiae by one of the PIs (Cross) who is trained in fingerprint identification. The fingerprint images were enlarged to simulate the magnification that is typically used to examine fingerprints for minutiae. **Figure 17** compares some of the minutiae identified for fingerprints on a beverage can which have been developed using NIR-to-NIR and NIR-to-visible UCNP. These images correspond to those shown in the middle column of **Figure 12**. The NIR-to-NIR image in **Figure 17** (left image) is an unenhanced raw image, whereas the brightness and contrast of the NIR-to-visible image (right image) has been enhanced in order to assist minutiae identification. The minutiae are very clear for the NIR-to-NIR imaged fingerprints over the entire image. However, even for the optimized NIR-to-visible image in **Figure 17**, many of the minutiae falling within the red-paint background of the substrate are obscured and unidentifiable.

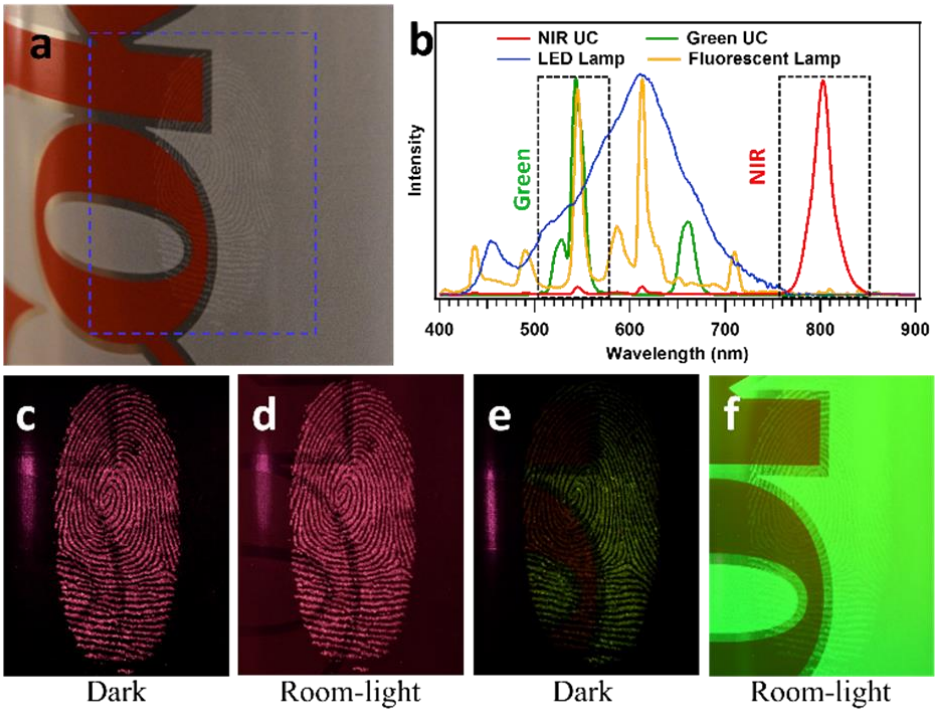

Figure 15. Comparison of dark and fluorescent room-light imaging of fingerprints using NIR-to-NIR and NIR-to-visible UCNP. a) Substrate area to be imaged; b) Comparison of spectral output of fluorescent and LED lamps with the upconversion luminescence spectra of NIR-to-NIR and NIR-to-visible UCNP. Boxes indicate the spectra regions imaged for NIR-to-NIR and NIR-to-visible, which are centered at 800 nm and 540 nm, respectively; c) and d) NIR upconversion images captured in dark and fluorescent room light, respectively; e) and f) visible upconversion images captured in dark and fluorescent room light, respectively.

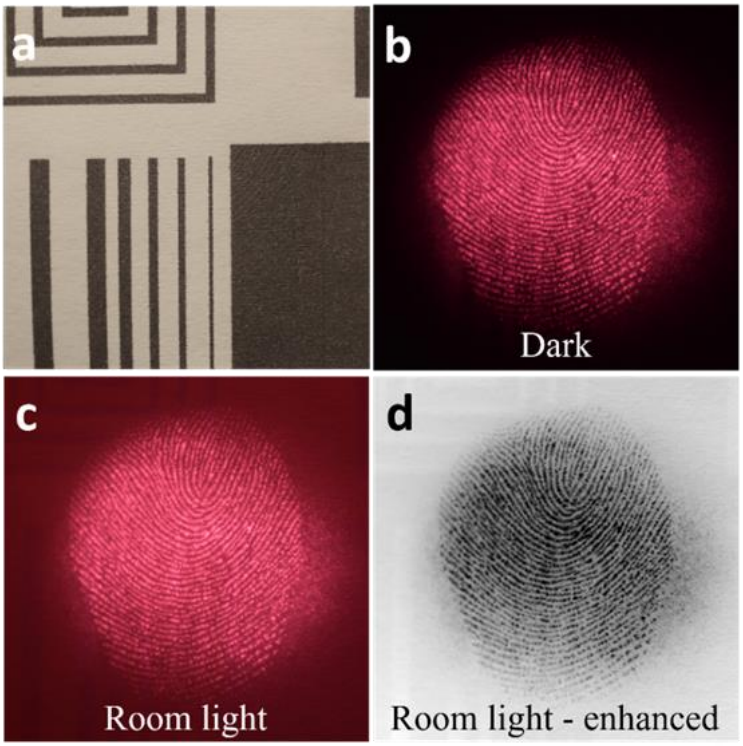

Figure 16. Demonstration of ability to capture high-quality fingerprint images in full room light (fluorescent) from a substrate with a complex background pattern using NIR-to-NIR UCNP. a) Patterned area to be imaged; b) NIR upconversion image captured in the dark and c) in full fluorescent room light. d) IrfanView 4.44 enhanced image of panel 'c' (Auto Adjust Colors –> convert to Gray Scale -> invert imaging, all channels).

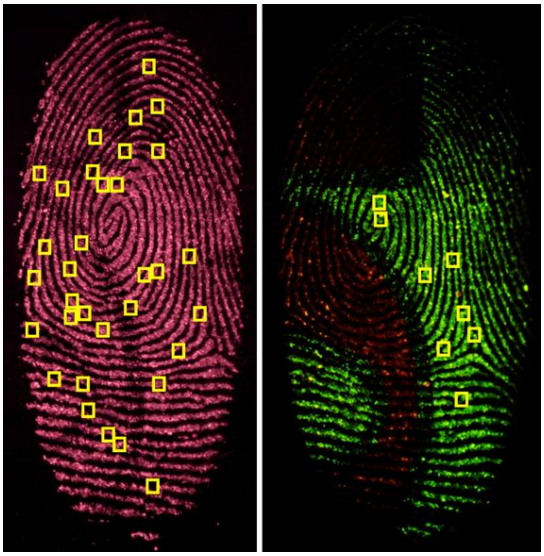

Figure 17. Comparison of the minutiae identified for fingerprints on a beverage can which have been developed using NIR-to-NIR and NIR-to-visible UCNP at an excitation irradiance of 400 $mW \cdot cm^{-2}$. These images correspond to those shown in the middle column of **Figure 12**. The NIR-to-NIR image in **Figure 17** (left image) is an unenhanced raw image, whereas the brightness and contrast of the NIR-to-visible image (right image) has been enhanced in brightness in order to assist with minutiae identification.

Figure 18 shows a comparison of two halves of a latent fingerprint, with one half developed using the core UCNP and the other with the core-shell UCNPs. Core-shell UCNPs (synthesized later in the project timeline) are a type of nanoparticle that provides much better brightness, by coating the manufactured core particle in a shell of the core material. The fingerprint is on a paper substrate containing a pattern produced using a thermal inkjet printer. The lefthand panel shows the pattern under room lighting conditions. The right-hand panel shows a comparison of the luminescent image obtained for the two halves of the developed print using a very low irradiance of 50 $mW \cdot cm^{-2}$. The half-print developed with core-shell nanocrystals produces an excellent reproduction of the print, whereas, at this level of irradiance, the half-print developed using the core nanocrystals produces an insufficiently bright image for critical analysis. Note that the printed background on the substrate has been effectively suppressed in the luminescent image.

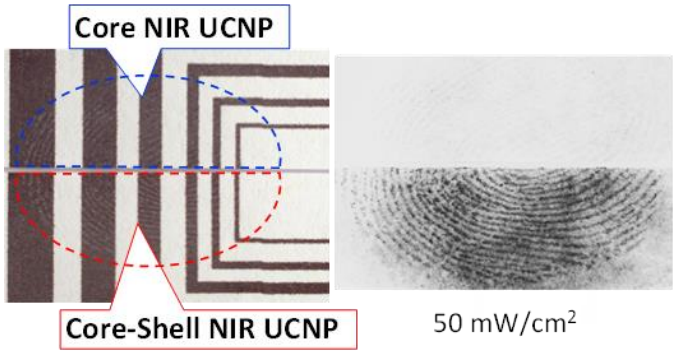

Figure 18. Comparison of two halves of a latent fingerprint developed using the core NIR-to-NIR UCNP and the core-shell UCNP, respectively. The fingerprint is on a paper substrate containing a pattern produced using a thermal inkjet printer. The right-hand panel shows the 800 nm luminescent image obtained for the two halves of the developed print using a very low irradiance of 50 $mW \cdot cm^{-2}$. The luminescent image has been converted to gray scale and inverted.

Task Research Summary: The optimal sized UCNPs found by imaging analysis were tested on a variety of substrates including several high-value substrates, a variety of lighting conditions, and laser excitation irradiances.

In all cases NIR-to-NIR UCNPs worked better than visible light producing UCNPs. The NIR-to-NIR UCNPs worked under all conditions tested.

Task 5: Functionalization of UCNPs for Targeted Binding to DNA

Purpose: This purpose of this task is to determine what modifications, if any, to the particle surface are necessary to extract DNA from fingerprints using our UCNPs. The goal was to optimize DNA extraction from treated fingerprints, to ensure that nanoparticles do not interfere with DNA recovery. In addition, we investigated the effect of nanoparticle presence on the amplification of short tandem repeat (STR) loci. Two different approaches were used. Approach one, direct polymerase chain reaction (PCR), has the advantage of minimal loss of material, but amplification may be inhibited by the presence of debris or the nanoparticles themselves. Approach two, extraction will remove impurities, but may result in some loss of material. The initial functionalization to be tested is the oleate (currently prepared UCNPs).

This task contained three main areas. First, identifying the participant DNA shedder status; second, extracting DNA from fingerprints using UCNPs; and, third, optimizing the recovery of DNA from fingerprints using UCNPs.

Research: This task was broken into three subtasks related to the three main areas identified in the Purpose section.

Participant DNA Shedder Status DNA transfer during direct contact between skin and a substrate defines the shedder status of the person touching an object. Some donors have a higher propensity to transfer their DNA than other donors (so-called shedders). The goal of this portion of the research was to determine the best shedder among our donors and begin with the best donor to separate DNA from the fingerprint. The method for this determination involved applying a fluorescent DNA staining dye to the latent print. The dye binds to the DNA within the nucleus of cells present in the fingerprint. The cells are then visible as bright spots in a fluorescent microscope image, which, in turn can be counted using appropriate image analysis software.

Glass slides were used as the substrate for determining shedding status. The slides were cleaned with 3% bleach, followed by wiping with absolute ethanol to ensure no DNA was present prior to fingerprint deposition. Control samples were collected from areas of the glass prior to any deposition of a fingerprint. The donors made contact with the clean, DNA-free glass slides with their fingers for 30 seconds with medium pressure. The slides were stained with staining solution prepared by 1:1 ratio of ethanol solution (50%) to the stock solution. The stock solution is a 10,000 times dilution of Diamond™ Nucleic Acid Dye (Promega, Madison, WI, USA) in water. The Diamond Dye (DD) is not fluorescent in its free form (non bound), but becomes fluorescent when bound to DNA. **Figure 19** shows the excitation and emission spectrum of the Diamond Dye solution when DNA is present. The peak emission of the DD is around 550 nm.

A Dino-Lite fluorescent digital microscope (**Figure 20**, AnMo Electronics Corporation, New Taipei City, Taiwan) equipped with a blue LED excitation light source (480 nm) was used to visualize the presence of dyed material, referred to as cellular material hereafter.

Figure 21 shows different areas of the luminescent image of a fingerprint. The bright spots indicate intact cells, whereas the diffuse emission is probably attributable to extracellular DNA. The ridge structure of the print is clearly visible. The ImageJ software package was then used to count the cells per area within each fluorescent fingerprint image. ImageJ has several useful tools to approach the problem. The ‘‘Threshold . . .’’ command can separate the background from the particles of interest, which can then be counted by the ‘‘Analyze Particles . . .’’ command. Before counting, the image represented in Figure 6 was converted to grayscale (See **Figure 22**), and the threshold intensity value was found. The ImageJ analysis algorithm was then be applied to count all spots of a particular shape and size (see **Figure 23**). We set a cutoff for all particles with an area less than 100 pixels

(noise) but did not impose any restrictions on shape because of the tendency of cells to coalesce at higher concentrations; thus, in this case the software would at least detect the aggregate, although only as one particle.

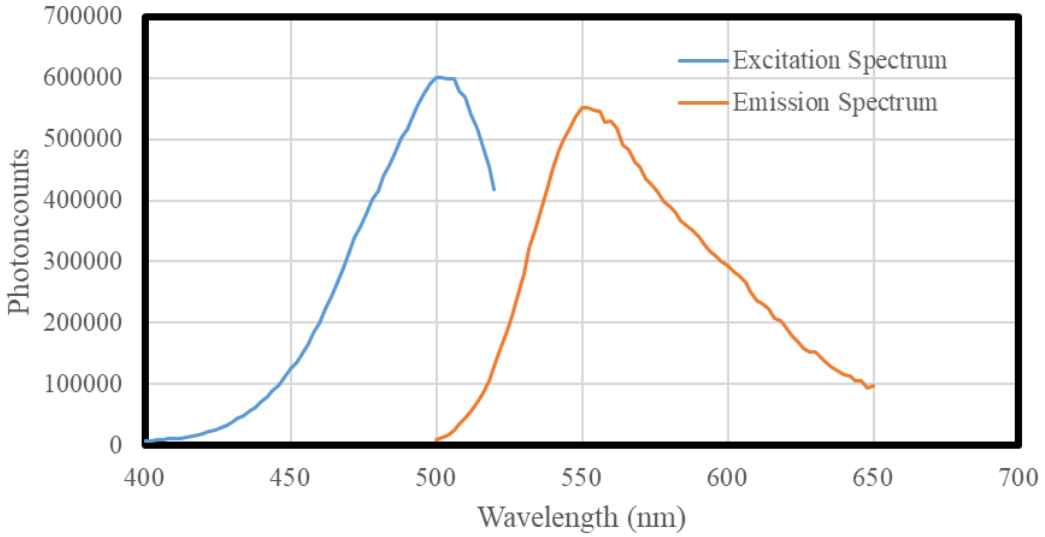

Figure 19. Excitation and emission spectra of Diamond™ Nucleic Acid Dye using Fluoromax-4.

Figure 20. Dino-Lite fluorescent digital microscope equipped with an emission of filter of 510 nm and a blue LED excitation light source (480 nm) was used to visualize the presence of dyed material.

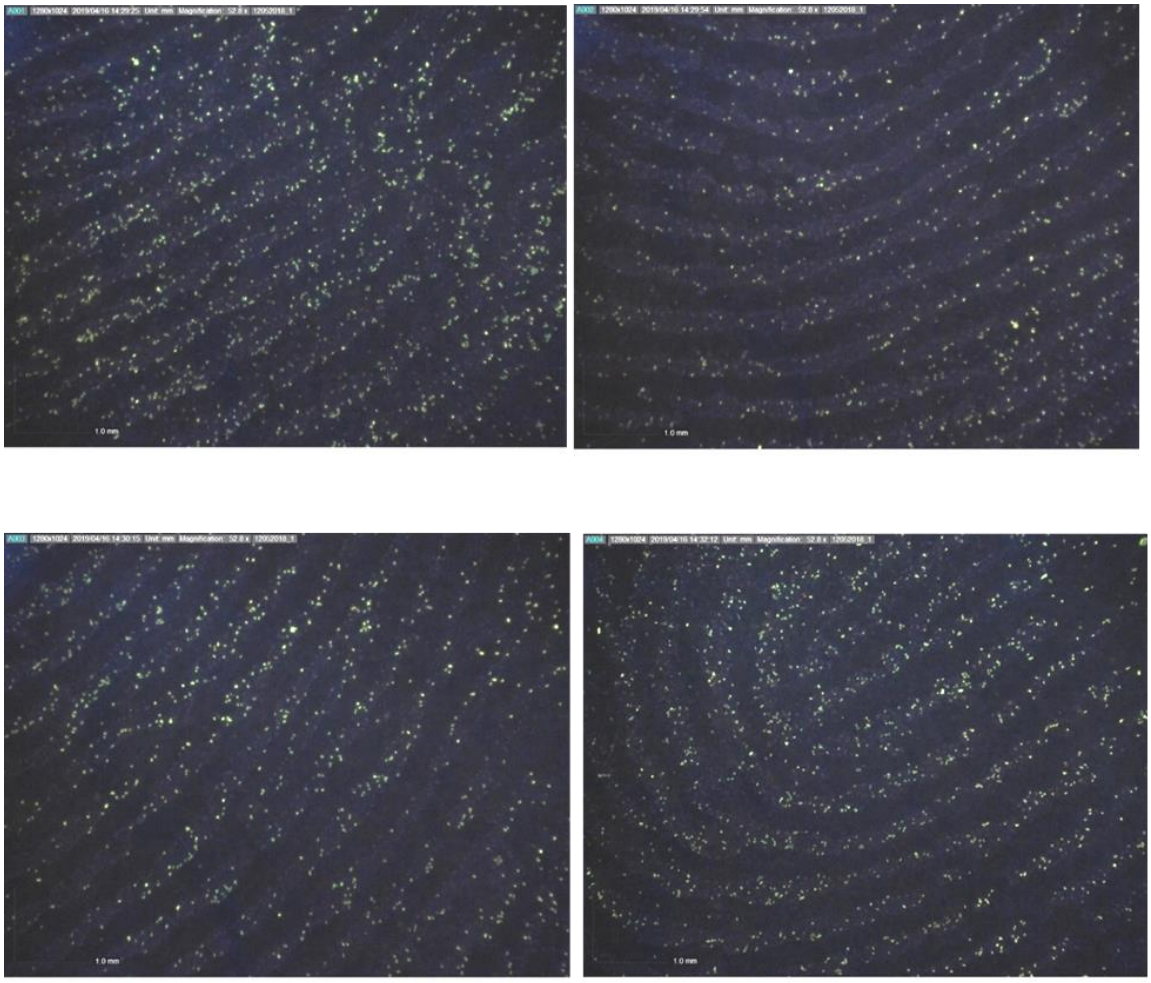

Figure 21. Dino-Lite fluorescent digital microscope images of different areas of index fingerprint of a donor. The bright spots indicate intact cells, whereas the diffuse emission is probably attributable to extracellular DNA.

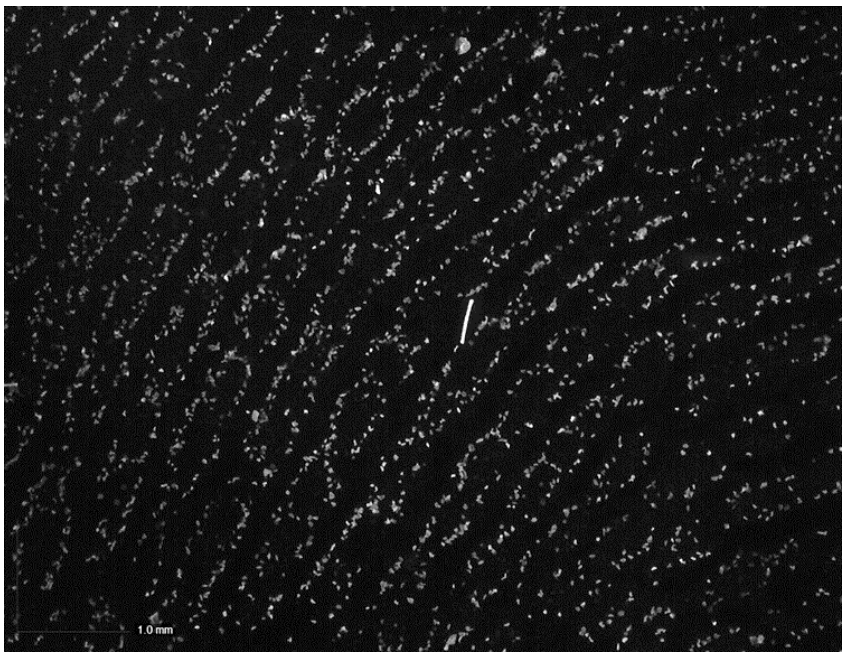

Figure 22. The image of fingerprint processed to grayscale.

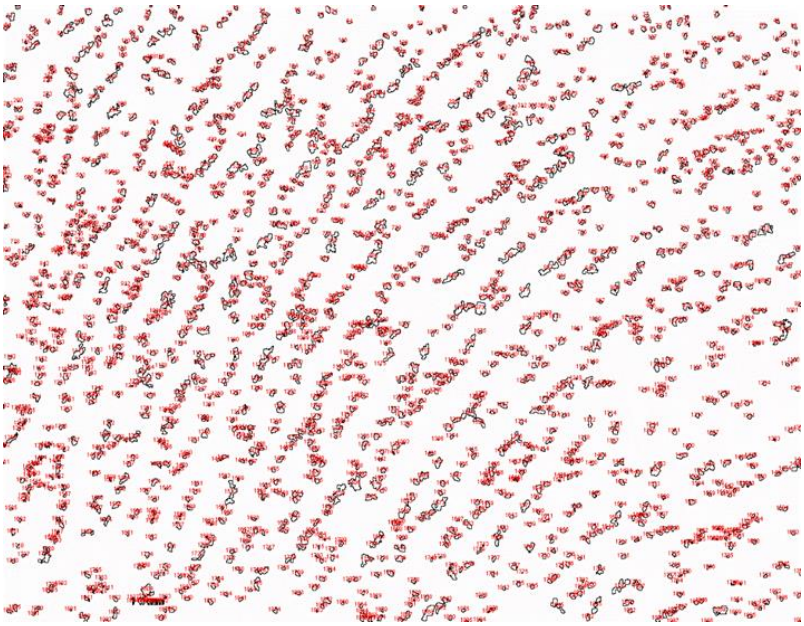

Figure 23. The resultant image after the ImageJ analysis algorithm applied to count the relevant fluorescent spots in **Figure 22**.

One issue that arose during this research was that fingerprint samples for DNA analysis needed to be shipped to the New Mexico Institute of Mining and Technology (NMT) as the team used fingerprint samples from the University of South Dakota, as those were provided by a known shedder. Since these fingerprints were shipped from South Dakota, by definition they were not freshly applied. To identify a shedder donor in New Mexico, several potential donors were screened by visualizing their fingerprints on clean glass slides stained with Diamond^{TM} dye under UV light, as previously described. A potential shedder donor was identified through this method (**Figure 24**).

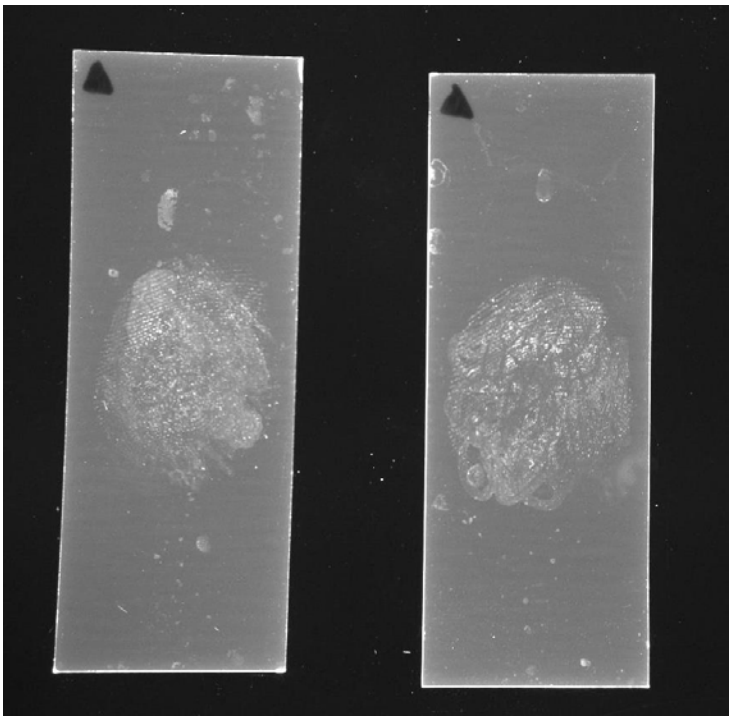

Figure 24. Potential DNA shedder fingerprints stained with Diamond^{TM} dye. Fingerprints were deposited as described previously, with medium pressure for 30 seconds. Left slide is the left thumbprint and the right slide is the right thumbprint of the same individual.

DNA Extraction via Magnetic Particles The possibility of using the magnetic properties of our nanoparticles to extract DNA from fingerprint residues was explored. To establish a baseline for the efficacy of this method, we attempted to use a commercial magnetic DNA purification kit (AbraMag® Genomic DNA Magnetic Purification Kit) to extract DNA from latent fingerprints. The kit is designed to purify genomic DNA from mammalian tissues and bacteria using a procedure shown in **Figure 25**. Magnetic beads with uniform particle size efficiently bind DNA, resulting in high yields of DNA with minimal RNA, proteins, nucleases, and other cellular contaminants. The kit is intended for manual purifications using a magnetic separator.

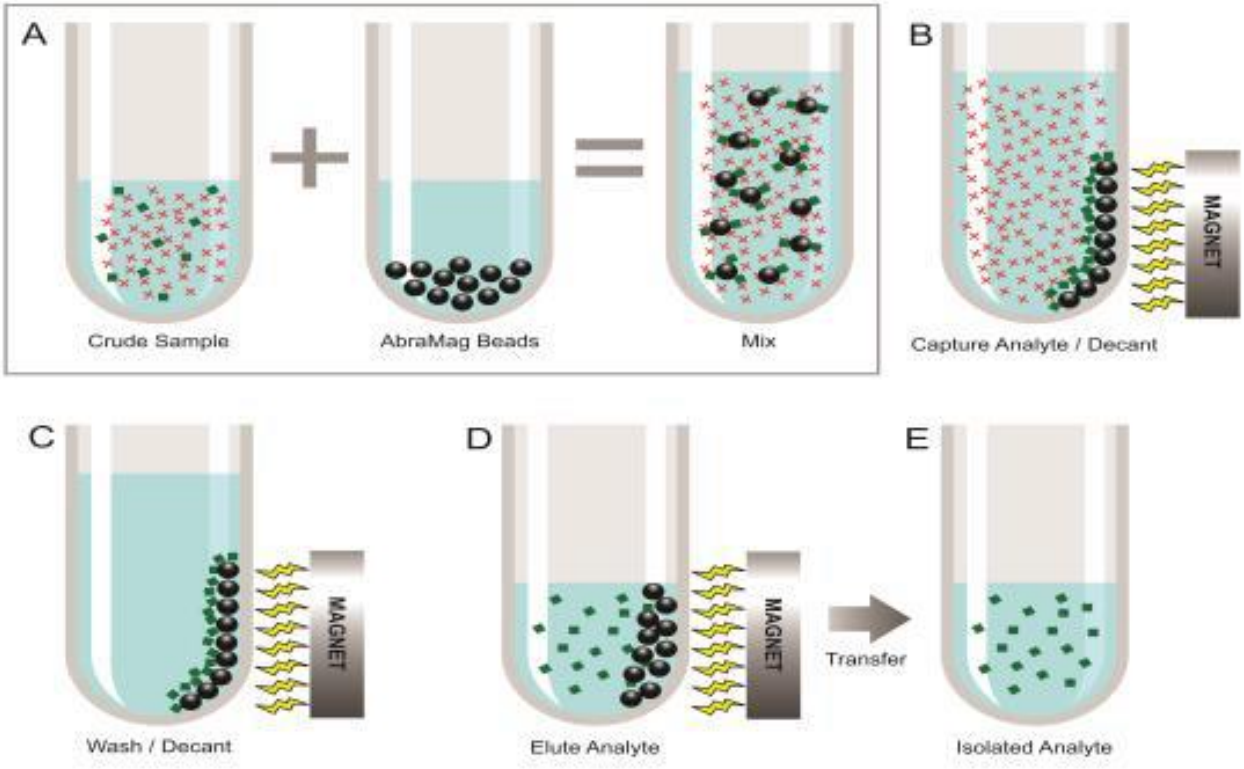

Figure 25. Schematic of AbraMag® Genomic DNA Magnetic Purification Kit process.

With respect to UCNPs, an attempt was made to magnetize the UCNPs by dysprosium (III) doping. The hypothesis is, Dy(III) doped NIR-to-NIR UCNP enables extraction of DNA from cellular remnants by magnetic field, similar to the method used by the magnetic beads. The NIR-to-NIR UC helps in imaging the fingerprint.[3] $NaDyF_4$ is iso-structural to the $NaYF_4$ but exhibits paramagnetic properties. In order to study the magnetic interaction, pure $NaDyF_4$ NPs were synthesized following a method identical to UCNP synthesis except using Dy_2O_3 as a precursor instead of Y_2O_3.[4] The Dy_2O_3 powder and the granules of $NaDyF_4$ respond to the magnetic field but the NPs in toluene did not, see **Figure 26**.

Due to the absence of magnetic response of $NaDyF_4$ dispersion, DNA purification by magnetization method was not pursued further.

This resource was prepared by the author(s) using Federal funds provided by the U.S. Department of Justice. Opinions or points of view expressed are those of the author(s) and do not necessarily reflect the official position or policies of the U.S. Department of Justice.

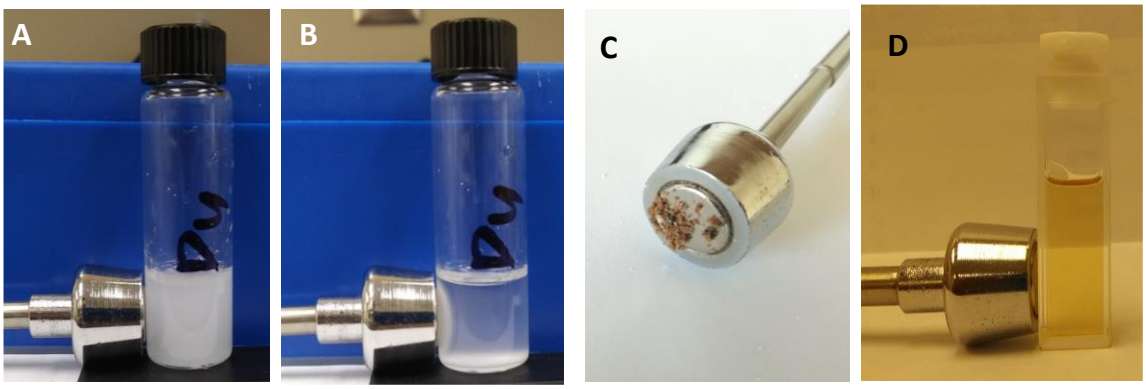

Figure 26. A study of magnetic response of $NaDyF_4$ NPs compare to Dy_2O_3 precursor used in the synthesis. Dy_2O_3 dust dispersed in water (A) was attracted by the magnet and collected along the wall of the vial (B) within 10 minutes. Note that large chunks of $NaDYF_4$ NPs were attracted to the magnet (C) but when dispersed in toluene the $NaDyF_4$ NP did not collect along the wall of the container.

Surface Functionalization A second method was utilized in addition to the magnetic particles. The surface of the UCNPs was functionalized so that the UCNPs would be coated with a surfactant that was more amenable to interaction with the DNA than the oleic acid coating that is formed in the standard method of manufacturing the UCNPs.

As a first step, a DNA separation technique was conducted on chicken flesh following the manufacturer's instructions below.

- Collect 15 mg meat into a 1.5 mL microcentrifuge tube pre-filled with DNA Lysis Solution.
- Add Proteinase K Solution to the DNA Lysis Solution/sample tube and incubate the sample at 55 °C for 30 minutes. Add DNA Binding solution to the sample lysate and vortex well.
- Transfer the sample lysate to the ethanol/bead mix.
- Place the tube on the magnetic separator, remove and discard the supernatant using a pipette, without disturbing the beads that have collected at the magnet.
- Remove the tube from the magnetic separator and add DNA Wash Solution 1, return the tube to the magnetic separator, remove and discard the supernatant using a pipette, without disturbing the beads that have collected at the magnet and repeat the wash with DNA Wash Solution 2.
- Remove the tube from the magnetic separator and add DNA Elution Solution. Incubate the sample at 65 °C for 10 minutes and return the tube to the magnetic separator for two minutes.
- Leave the tube on the separator, transfer the eluate to a new 1.5 mL tube using a pipette.

The presence of separated DNA was then detected using the same DD solution described earlier. The eluate contains the purified genomic DNA which we can observe from emission spectrum of eluate solution into diamond nucleic acid dye using a Fluoromax-4 fluorimeter.

Figure 27 shows the emission spectrum of the chicken-meat eluate resulting for the magnetic bead distraction. One spectrum (Meat) was obtained from a meat sample that was processed directly. The "Meat Swabbed" sample was processed by first spreading a thin layer of the pureed meat sample on a glass slide, and then collecting the sample using the same swab technique used to acquire fingerprint samples.

This resource was prepared by the author(s) using Federal funds provided by the U.S. Department of Justice. Opinions or points of view expressed are those of the author(s) and do not necessarily reflect the official position or policies of the U.S. Department of Justice.

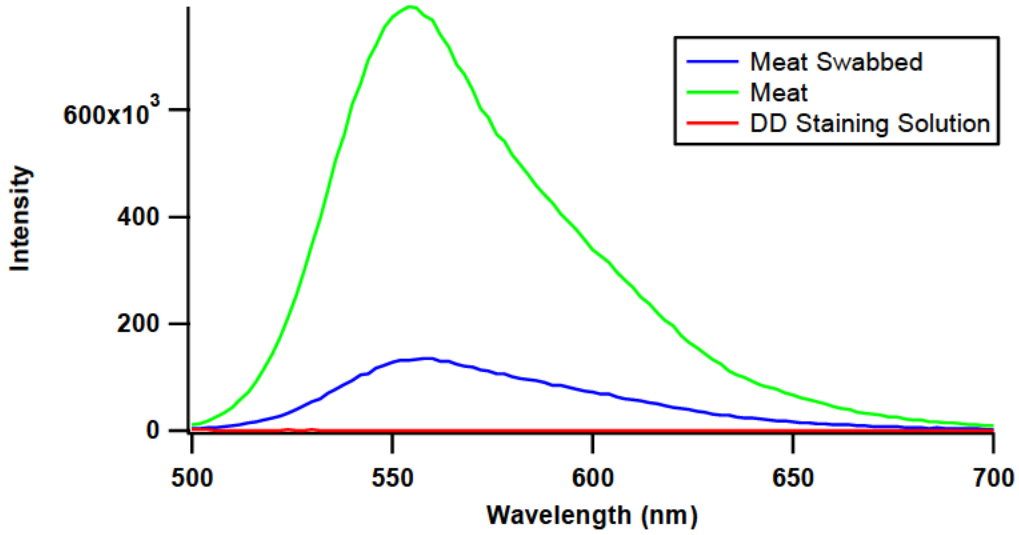

Figure 27. Emission spectrum of diamond dye solution (red); separated DNA from meat into diamond dye solution (green) and separated DNA from swab (swabbed meat) into diamond dye solution (blue).

A Diamond™ dye based spectroscopic method was developed to quantify the DNA present in the samples. The Diamond™ dye fluoresces in the presence of small (a few nanograms) of DNA (**Figure 28**). In order to quantify the DNA present in the fingerprints a standard calibration curve was developed by measuring Diamond™ dye fluorescence in the presence of known concentrations of calf thymus DNA. DNA concentration versus fluorescence signal is plotted in the **Figure 29**.

Spectroscopy was performed on the swab samples collected from latent fingerprints (un-developed) by double swab technique[1] showed presence of 8 ppb of DNA in a fingerprint on average. Spectroscopy was also performed on the swab samples collected from the fingerprints developed with oleate capped UCNP (OA-UCNP). The swab head when soaked in water released the DNA into the medium leaving UCNP adhere to the swab head. The DNA released into the solution was quantified by fluorescent spectroscopy. The quantity of DNA collected from the UCNP developed fingerprints was measured to be 7.6 ± 2.2 ppb. There is no significant difference in fluorescent intensity of Diamond™ dye DNA solution for DNA collected from fingerprints with and without UCNP. This implies DNA extraction from UCNP developed fingerprint was achieved without compromise in the DNA quality.

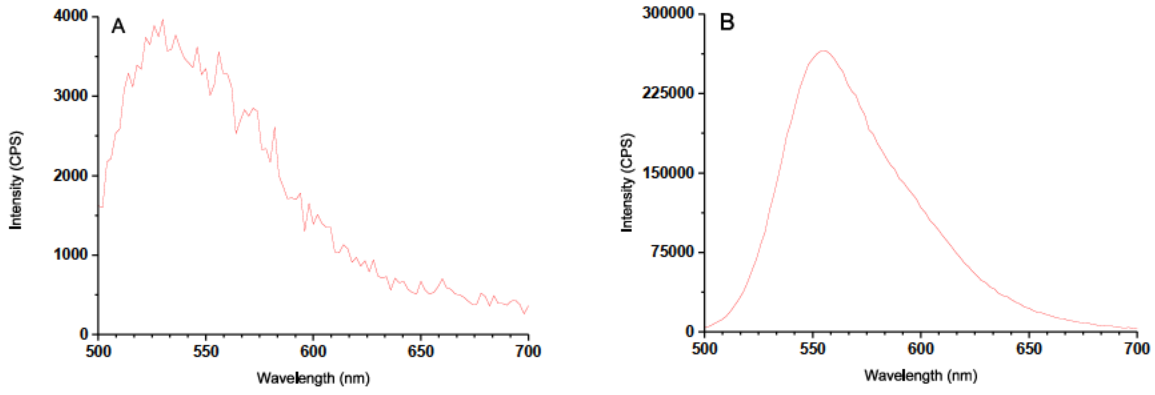

Figure 28: Fluorescence spectra of Diamond™ dye solution without DNA (A) and with DNA (B) were collected after exciting with 480 nm light. A strong emission signal from the Diamond Dye is observed in the presence of DNA.

This resource was prepared by the author(s) using Federal funds provided by the U.S. Department of Justice. Opinions or points of view expressed are those of the author(s) and do not necessarily reflect the official position or policies of the U.S. Department of Justice.

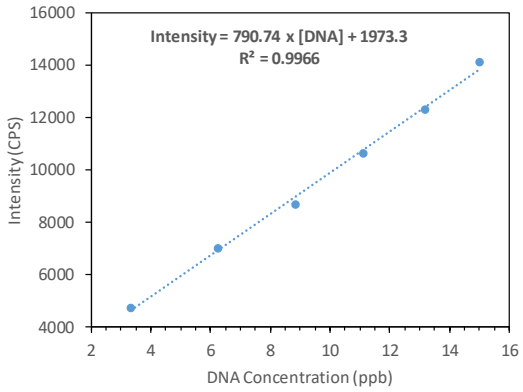

Figure 29. A calibration curve was acquired for Diamond™ Dye emission intensity vs DNA concertation. The calibration curve for DNA quantification showing linear relationship between the concentration (ppb) of DNA and fluorescence emission intensity.

The above results suggest that the use of UCNPs for fingerprint development did not interfere with DNA extraction and UCNPs adhere to the swab head helped to separate the DNA and fingerprint. The direct extraction of DNA from swab heads without interference of the UCNPs is an added advantage. However, an investigation was carried to purify the DNA using UCNP to enhance the performance of the DNA. The goal is to purify the DNA from fingerprint constituent that may interfere with DNA amplification in PCR.

Following the calibration of the test method, UCNPs were functionalized to selectively attract DNA to purify DNA from other fingerprint constituents. Phosphate ions have high affinity for $NaYF_4$.[5-6] The hypothesis is to selectively bind the DNA onto UCNP by taking the advantage of phosphates terminal of the DNA backbone. DNA bound UCNPs can be isolated from other fingerprint constituents by centrifugation or other suitable methods. The pure DNA from UCNP can be separated by adjustment of pH and centrifugation.

Latent fingerprints were developed and the DNA collected from the fingerprints was quantified by the method detailed previously. The DNA quantified from UCNP developed fingerprint is comparable to the DNA quantified from the fingerprint without UCNP. The absence of DNA interaction with the UCNP might be due to presence of steric coating of oleic acid around UCNP. In order to facilitate DNA binding to the UCNP, oleate ligand present on the UCNP was removed with acetic acid treatment. The removal of oleate was confirmed by Fourier transform infrared (FTIR) spectroscopy (**Figure 30A**). The decrease in the intensity of C-H stretching band at 2960 cm^{-1} and the C=O stretching band at 1570 cm^{-1} of acetate capped UCNP (AAUCNP) suggests significant portions of oleate was removed by acetic acid treatment. The effect of acetic acid treatment on UCNP morphology was evaluated with scanning electron microscopy (SEM). The SEM images of OAUCNP and AAUCNPs suggest no change in the morphology of the UCNPs upon acetic acid treatment, see **Figure 30B** and **30C**. The AAUCNP are less greasy, therefore, the surface ligand composition of AAUCNP can be altered by adjusting the pH of the medium.

This resource was prepared by the author(s) using Federal funds provided by the U.S. Department of Justice. Opinions or points of view expressed are those of the author(s) and do not necessarily reflect the official position or policies of the U.S. Department of Justice.

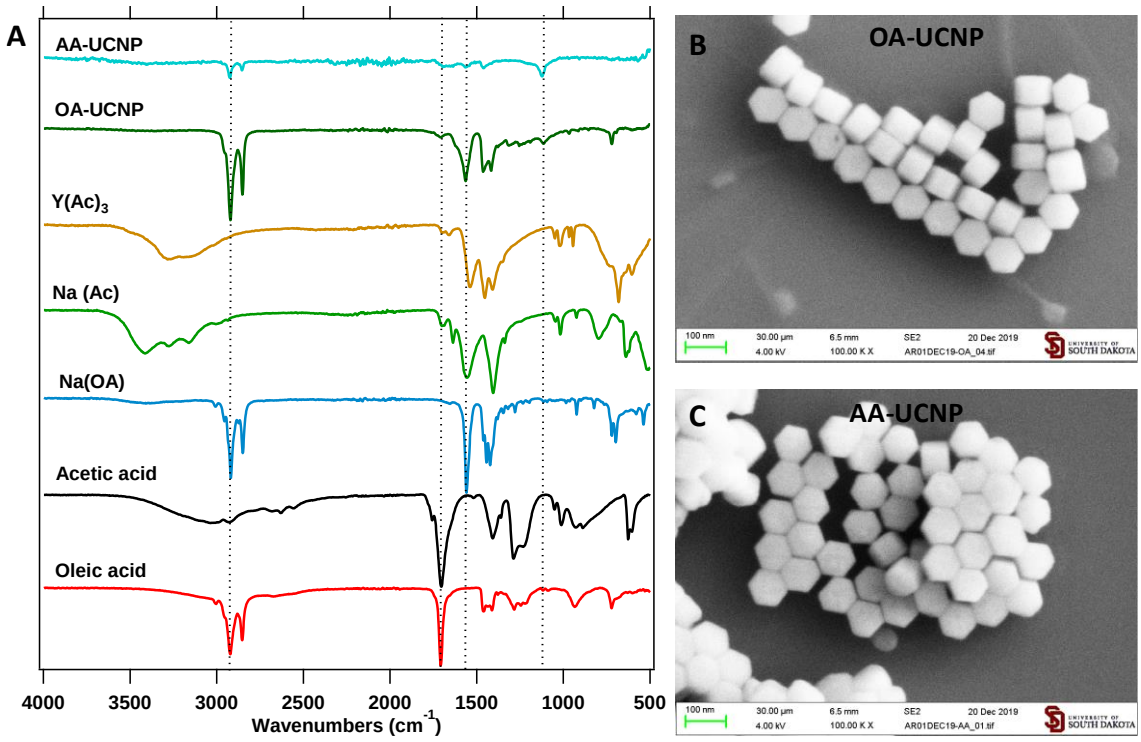

Figure 30. (A) FTIR spectra of acetate-capped UCNP (AA-UCNP) compared to oleate-capped UCNP (OA-UCNP), yttrium acetate ($Y(Ac)_3$)), sodium acetate (Na(Ac)), sodium oleate (Na(OA)), acetic acid, and oleic acid. The decreased in intensity of C-H stretch at 2960 cm^{-1} and C=O stretch at 1570 cm^{-1} suggests significant removal of oleic acid capping. Scanning electron micrograph (SEM) of (B) OAUCNP and (C) AAUCNP suggests no change is the morphology of UCNP upon functionalization.

The objective of this subtask is to extract DNA from fingerprints using AAUCNPs. Phosphate groups have high affinity towards UCNPs. Our hypothesis is that low steric loading on AAUCNP facilitate phosphate groups of DNA conjugating with UCNP. We quantified DNA in fingerprints by fluorescence spectroscopy using Diamond Dye as a DNA tagging. The Diamond Dye-DNA fluorescence response is highly pH sensitive. In the presence of AA-UCNP the pH was altered and yielded unreliable fluorescence response of Diamond Dye-DNA complex. The AAUCNP interaction with DNA and quantification in *tris*-buffer would be an alternate solution to negate the pH effect. However, experiments were not pursued further in this direction due to advent of COVID-19 restrictions (spring 2020).

Phosphate groups are known for strong binding with lanthanide ions. Considering the potential of irreversible binding of DNA with AAUCNP, an alternate method for DNA extraction has been investigated. Dimercapto succinic acid (DMSA) offers pH responsive binding of DNA to the carboxylate group of DMSA. The AAUCNP were further functionalized with dimercapto succinic acid ligand (DMSA) by ligand exchange protocol. The UCNP functionalization with DMSA was confirmed by FTIR spectroscopy (**Figure 13**). The DMSA-UCNP interaction with DNA is under investigation.

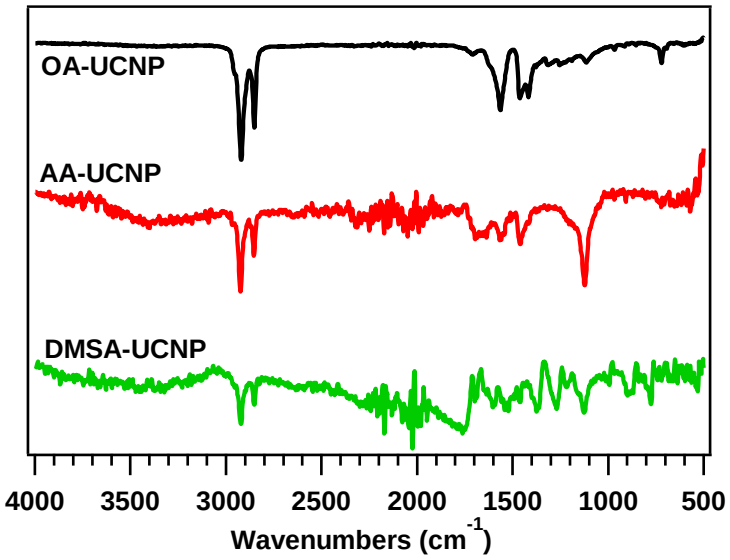

Figure 31: FTIR response pure oleic acid capped UCNP (OAUCNP), acetic acid capped UCNP (AAUCNP), and DMSA capped UCNP (DMSA-UCNP). OAUCNP were first treated with acetic acid to form AAUCNP followed by DMSA treatment to produce DMSA-UCNP.

Optimizing the Recovery of DNA from Fingerprints with UCNPs Initial work was focused on optimizing amplification from dilute samples, by exploring a variety of DNA concentration techniques and PCR optimization. We explored the Invitrogen™ ChargeSwitch™ Forensic DNA Purification Kit and MagnaRack™ Magnetic Separation Rack as an alternative to ethanol precipitation.

Fingerprints obtained from the shedder from the previous period were used in an initial test of the Invitrogen™ ChargeSwitch™ Forensic DNA Purification Kit and MagnaRack™ Magnetic Separation Rack**.** Prints from both thumbs were obtained by the donor applying medium pressure for 30 seconds to cleaned glass slides. The fingerprints were dried in the chemical fume hood for 30 minutes prior to recovery. Each print was swabbed twice (double-swab technique) by swabs that had been soaked in sterile water. The swab heads were placed into a microfuge tube containing 200 µL of sterile water, and vortexed for 30 seconds to remove attached DNA.

This sample was used in the DNA Purification Kit according to the manufacturer's directions. 1 mL of lysis buffer and 10 µL of Proteinase K solution was added to the sample and gently mixed. The mixture was incubated at 55 ℃ for 30 minutes. The supernatant was removed to a fresh tube, and 200 µL of Purification buffer was added. The magnetic bead suspension (20 µL) was added to the sample and gently pipetted to mix.

The MagnaRack™ Magnetic Separation Rack was used to separate and concentrate the DNA recovered according to the manufacturer's directions. Briefly, the sample was incubated for 1 minute at room temperature to allow the DNA to bind to the magnetic beads. Then, the sample tubes were placed in the separation rack for 1 minute, until the beads formed a visible pellet. The supernatant was removed and discarded. Wash buffer (500 µL) was added to the tubes and mixed gently. The tubes were once again placed in the separation rack for 1 minute, and the supernatant removed. This washing step was repeated. Finally, the DNA was eluted by adding 150 µL of elution buffer to the tubes, mixing gently, and incubating at room temperature for 5 minutes. The tubes were placed in the separation rack once again for 1 minute, after which the supernatant, containing the eluted DNA, was removed to a fresh tube.

The DNA samples were used in the standard PCR reactions, using 2 µL of DNA as the template and RenA4 primers. The gel for this experiment showed amplification only for the known DNA control, but not for the

fingerprint DNA. The PCR reaction was repeated using 6 µL (maximum) of template DNA, but there was still no amplification, suggesting that either the template was in insufficient quantity or quality.

Because the recovery from fingerprints using the Invitrogen™ ChargeSwitch™ Forensic DNA Purification Kit and MagnaRack™ Magnetic Separation Rack was insufficient, we investigated the recovery from human buccal cells to determine the expected yield.

Buccal cells from a volunteer were obtained by rinsing the mouth with sterile 0.9% saline. The rinse was centrifuged in a clinical centrifuge to pellet the cells. The pelleted cells were treated in two ways: 1) 400 µL of pelleted cells were subjected to cell lysis using Chelex resin and 60 °C incubation, according to standard protocol, prior to use in the isolation kit and 2) 400 µL of pelleted cells were used directly in the isolation kit.

Following PCR and electrophoresis, the band corresponding to the amplified product was visible in all lanes expected (**Figure 32**). This demonstrated that the isolation kit was successful in lysing human cells and extracting DNA without diminishing quality, when cells were in sufficient quantity.

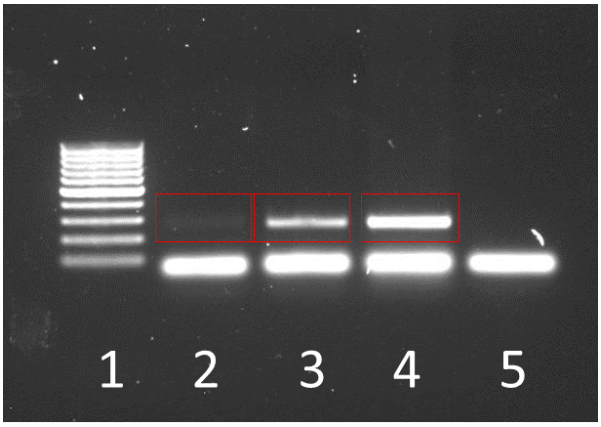

Figure 32: Amplification of DNA from buccal cells by magnetic bead kit. Lane 1: 100 bp ladder; Lane 2: Buccal cell DNA isolated with Chelex, then magnetic beads; Lane 3: Buccal cell DNA isolated with magnetic bead kit; Lane 4: Known DNA positive control; Lane 5: No template control. All reactions used previously reported optimized PCR conditions and RenA4 primers.

The previous experiment demonstrated that magnetic bead recovery of DNA from isolate buccal cells was efficient and provided template DNA with no PCR inhibitors. To enhance recovery from fingerprints, several adjustments were made to the protocol. Rather than a water bath for the 55°C incubation, a metal bead bath was used, and the time was increased to 45 minutes. Binding time onto magnetic beads was increased from 5 minutes to 10 minutes. Elution time from magnets was increased from 1 minute to 10 minutes.

These adjustments were made on fresh fingerprints, using the double swab technique to recovery cellular material. For the PCR reactions, 2 µL of template DNA and RenA4 primers were used. This adjustment resulted in no amplification for any of the experimental samples, again indicating insufficient recovery of DNA from the fingerprints.

Effect of UCNPs on DNA Amplification The first step towards optimizing the extraction of DNA from fingerprints with UCNPs was to determine the effect (positive or negative) of nanoparticles on downstream DNA amplification from developed fingerprints, we obtained primer pairs for the following loci: FesFep, D21S11, D1S80 and RenA4. The primers are listed in **Table 1**.

Gradient PCR using Taq polymerase and human DNA template obtained from an anonymous volunteer revealed the optimum temperature for annealing of these four sets of templates listed in **Table 1**. Reaction conditions were

as follows: 2' at 94 °C; 30 cycles of 30" at 94 °C, 30" at gradient of temperatures, 30" at 72 °C. Final extension 2' at 72 °C. Hold at 4 °C.

Table 1. Primers used in this research.

Primer	Sequence	Optimum annealing temperature
Fes Fep F	GCTTGTTAATTCATGTAGGGAAGGC	59 °C
Fes Fep R	GTAGTCCCAGCTACTTGGCTACTC	
D21S80 F	GTGAGTCAATTCCCCAAG	54 °C
D21S80 R	GTTGTATTAGTCAATGTTCTCC	
D1S80 F	GAAACTGGCCTCCAAACACTGCCCGCCG	60 °C
D1S80 R	GTCTTGTTGGAGATGCACGTGCCCCTTGC	
RENA4 F	AGAGTACCTTCCCTCCTCTACTCA	54 °C
RENA4 R	CTCTATGGAGCTGGTAGAACCTGA	

Next, we performed PCR in the presence of nanoparticles (NP). In the initial experiment a suspension of nanoparticles was prepared in sterile water. This suspension was used in place of water in a standard PCR reaction using RenA4 primers, control human DNA (ThermoFisher), Taq polymerase, dNTPs, Mg^{2+} and 10X reaction buffer, with vigorous vortexing prior to pipetting to resuspend the particles. Approximately 170 µg of nanoparticles were determined to be present in each reaction (**Figure 33**).

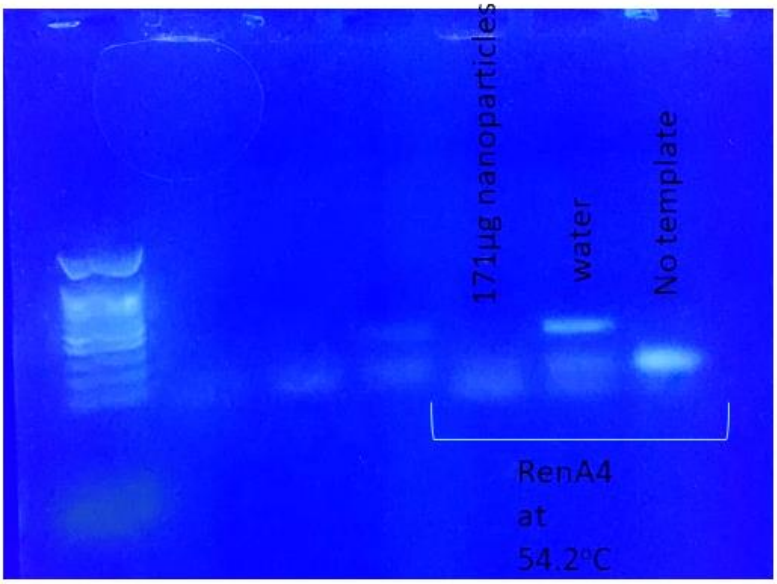

Figure 33. Effect of nanoparticles on amplification of the RenA4 locus by PCR. First lane is a DNA size standard. Presence of nanoparticles prevents amplification seen in the water control lane, where a band of the appropriate size (approximately 300 bp) is present. The "no template" control shows no amplification, as the human DNA template is not present; the prominent lower band is composed of unbound primers (absent in the NP lane, as there is template for binding, but no amplification took place).

The lack of amplification as well as unbound primers indicates that the nanoparticles interfere with extension by the polymerase and not with annealing of the primers. To further define the extent of this interference, a series of NP suspensions were used in PCR reactions with primers to two different loci, using DNA isolated from anonymous volunteer buccal cells. Three loci were used in this experiment: RenA4, which should amplify a band of approximately 300 bp; FesFep, which should also amplify a band of approximately 300 bp; and D1S80, which should amplify a band of approximately 500 bp, using the primers listed in **Table 1**. Two-fold serial

dilutions of an NP suspension were used in place of water in a series of PCR reactions. In these experiment the enzyme was GoTaq (ThermoFisher), which is provided with buffer, Mg^{2+} and dNTPs in a single 2X reaction mix. The results of three sets of PCR reactions using the same template, three different primer pairs, and serial dilutions of nanoparticles is shown in **Figure 34**.

Based on these results, the nanoparticles themselves are inhibitory but only at higher concentrations. It remains to be determined what weight of nanoparticles are expected to carry over from developed fingerprints during DNA extraction. It may also be possible to remove the nanoparticles prior to amplification, if necessary, either by centrifugation or by altering their surface chemistry. Such changes may also mitigate the inhibitory effect, and may be used to aid in DNA recovery.

Initial attempts to use swabbing techniques for direct PCR from fingerprints resulted in no amplification. This will be the focus of the next reporting period, along with determining the amount of nanoparticle carryover during routine DNA extraction from fingerprints.

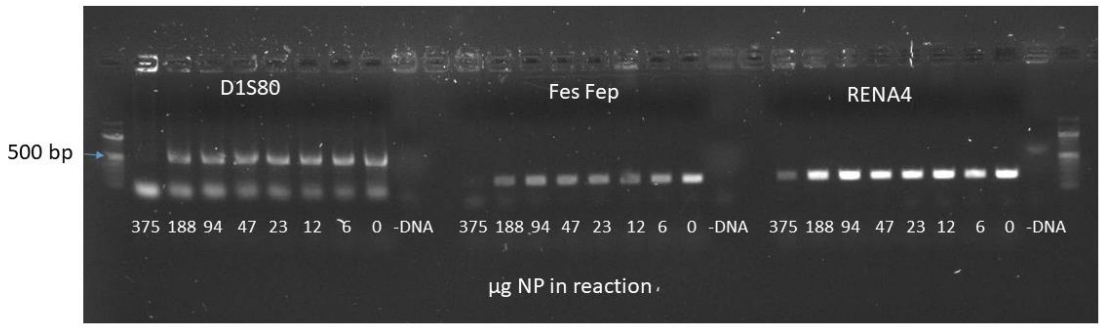

Figure 34. Effect of decreasing nanoparticle concentration on amplification in standard PCR reactions. Three primer pairs were used. Only the highest concentration of nanoparticles inhibited the reactions.

Work to date has been performed using Promega GoTaq™ DNA polymerase, provided in a 2X master mix containing dNTPs and buffer (Fisher Scientific) for PCR amplification. In order to optimize amplification from low DNA template concentrations, we compared the GoTaq polymerase to another commercially available polymerase, Applied Biosystems™ AmpliTaq Gold™ 360, also provided in a 2X Master Mix. In addition, AmpliTaq Gold can be used with a GC enhancer. For these comparisons, reactions were carried out using commercially obtained human DNA as the template, and the RenA4 primers described previously.

All reactions contained:

- 2.5 µL of 2X Master Mix (containing polymerase, buffer, and nucleotides)
- 2 µL of template DNA (or water for negative control)
- 0.5 µL Forward primer (stock concentration 25 mM)
- 0.5 µL Reverse primer (stock concentration 25 mM)
- 9.5 µL µL nuclease-free molecular grade water
- In addition, for reactions with AmpliTaq Gold GC enhancer, 2 µL of enhancer

Reactions were carried out in one of three BioRad T100™ thermocyclers under the following conditions: Initial denaturation at 94 °C for 2'; 35 cycles of denaturation at 94 °C for 30", annealing for 30"(experiment-specific temperature), extension at 72 °C for 30"; final extension at 72 °C for 5'; then 12 °C for an infinite hold.

All reactions were subsequently combined with 6x DNA gel loading dye (Fisher Scientific) and loaded onto a 1% agarose gel in TAE (40 mM Tris-20 mM acetic acid-1 mM EDTA) buffer. A 100 bp DNA ladder (Fisher Scientific) was also loaded onto the gel (3 µL). Gels were run at 120V for approximately 30 minutes to separate the amplified band (PCR product) from the unincorporated nucleotides and free primer DNA. Gels were prepared

using Invitrogen™ SYBR™ Safe Stain (Fisher Scientific), and visualized under UV using a gel documentation system.

In the experiment shown in **Figure 35**, decreasing amounts of commercially prepared human genomic DNA (158 ng to 2 ng) were used as the template in reactions using either GoTaq (top panel), AmpliTaq Gold 360 (middle panel), or AmpliTaq Gold 360 plus enhancer (bottom panel). The positive control (+) contained buccal cell DNA from a volunteer donor as the template, and the negative control (-) contained no template DNA.

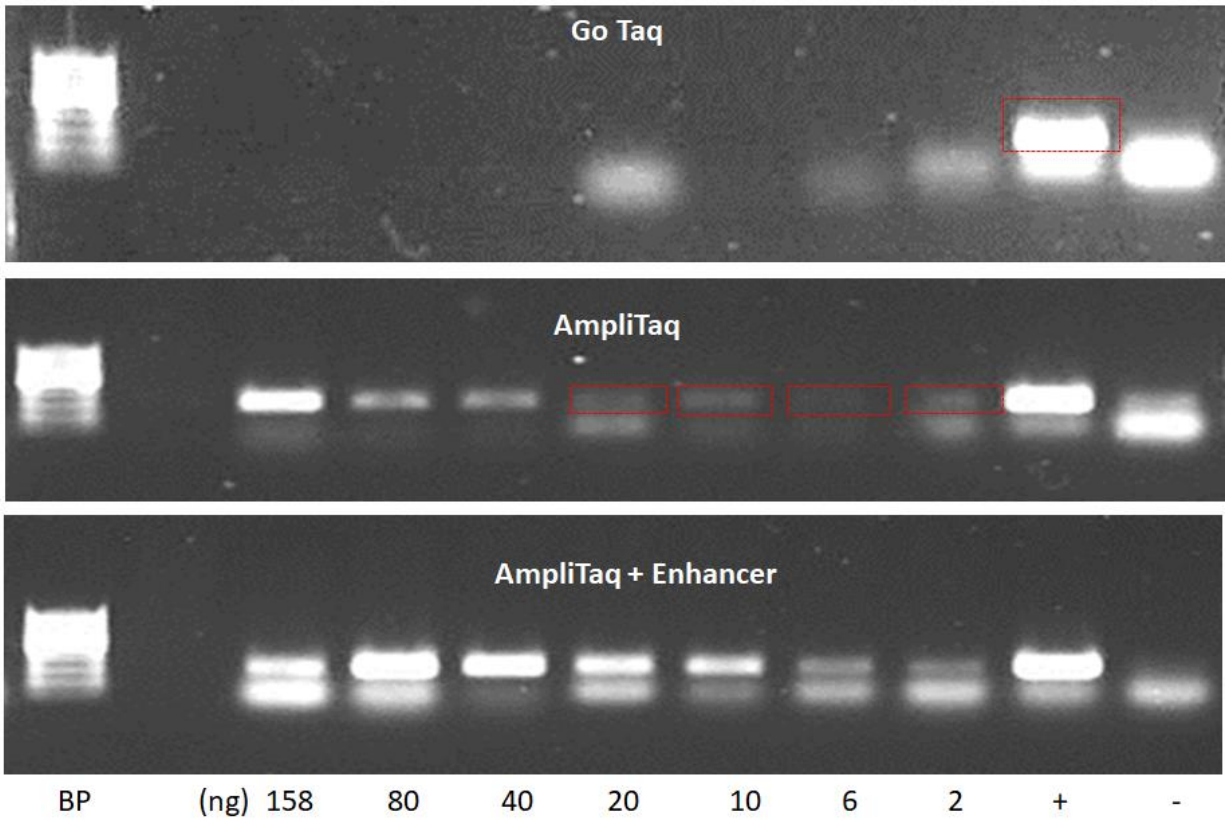

Figure 35. Comparison of Taq polymerase efficiencies. Reactions were carried out using decreasing amounts of human DNA as template for PCR reactions. Primers were RenA4 forward and reverse. Annealing temperature was 58 °C.

The results demonstrate the superiority of AmpliTaq Gold 360 + GC enhancer for amplification of the 300 bp PCR product.

Since initial attempts to use swabbing techniques for direct PCR from fingerprints resulted in no amplification, we focused on ways to concentrate template DNA in fingerprint samples in order to increase the concentration of template. One standard method for concentrating DNA is precipitation using ethanol. To each 200 µl solution, 20 µL 3 **M** sodium acetate and 400 µL absolute ethanol were added, the solution mixed, and placed at -20 °C for at least 1 hour. The tubes were centrifuged at 13,000 rpm for 10 minutes, the liquid was removed and the DNA pellet allowed to dry prior to resuspension in nuclease-free water.

The double swab technique was used to obtain a dilute crude sample of DNA from fingerprints or dried human DNA, on glass slides. In the experiment shown in **Figure 36**, each sample was concentrated 10x by ethanol precipitation prior to being used as template in PCR reactions with each of the three Taq polymerase conditions described above.

This resource was prepared by the author(s) using Federal funds provided by the U.S. Department of Justice. Opinions or points of view expressed are those of the author(s) and do not necessarily reflect the official position or policies of the U.S. Department of Justice.

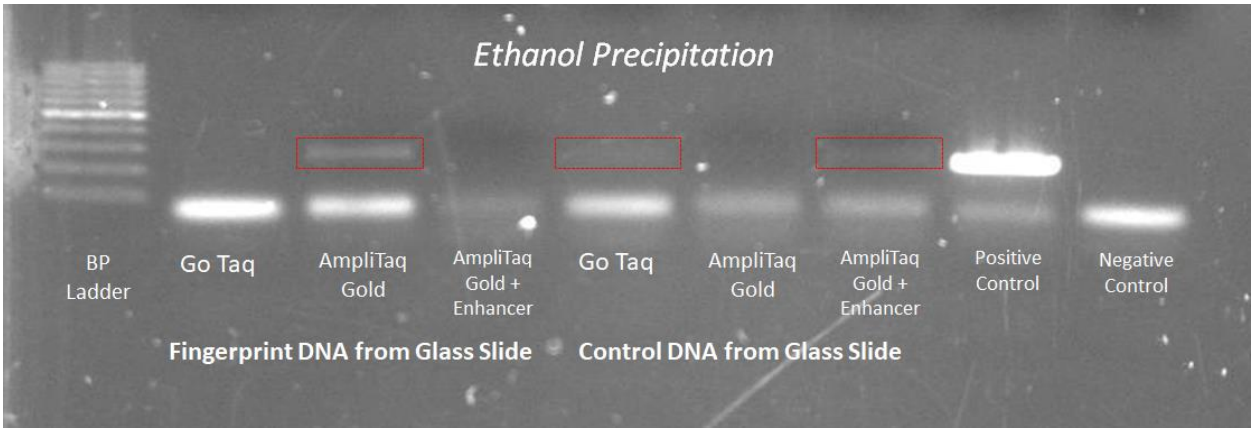

Figure 36. Effect of concentrating DNA by ethanol precipitation. DNA was obtained by double-swab technique from a fingerprint and dried buccal DNA on glass slides, both contributed by the same donor. Following swabbing into 200 ul water, the DNA was precipitated and subsequently resuspended in 20 ul of water prior to being used in a PCR reaction, as described above, using either GoTaq, AmpliTaq Gold 360, or AmpliTaq Gold 360 + GC Enhancer. Primers used were RenA4 forward and reverse. Annealing temperature was 58 °C. Amplified product was visible in three experimental lanes (red boxes), as well as in the positive control, at 300 bp.

Although difficult to see in the photograph, there was amplification of the appropriately sized product using the concentrated DNA (red boxes outline the bands).

Once amplification was established with concentrated DNA, we tested the effect of the presence of nanoparticles in developed fingerprints on DNA recovery and amplification. We obtained white cards and glass slides from USD, each containing fingerprints from their shedder donor. Some of the fingerprints were developed with nanoparticles; the NMT team was not told which fingerprints had been developed until after the amplification results were obtained. Each fingerprint was double-swabbed, and the solution precipitated with ethanol and resuspended, then used as template in PCR reaction.

As shown in **Figure 37**, amplification, although faint, was achieved in 5 out of the 8 samples; these included both undeveloped as well as developed fingerprints.

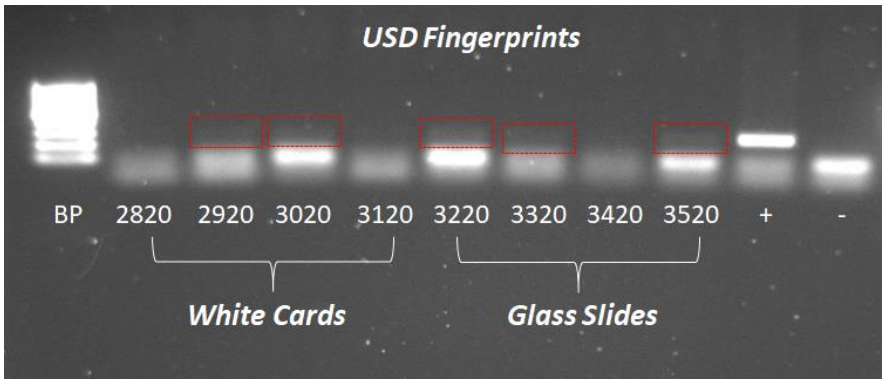

Figure 37. Effect of nanoparticle development on amplification of fingerprint DNA. Fingerprints from a single shedder donor, either index finger or thumb, were placed on white plastic cards or glass slides, and either developed or not. The double-swab technique was used to obtain DNA, which was subsequently concentrated by ethanol precipitation prior to being used in PCR reactions with the RenA4 primers and AmpliTaq Gold 360 + Enhancer. Annealing temperature was 58 °C. The samples are: 2820 - Left Index Developed; 2920 - Left Thumb Developed; 3020 - Left Index Undeveloped; 3120 - Left Thumb Undeveloped; 3220 - Left Index Developed;

3320 - Left Index Undeveloped; 3420 - Right Thumb Developed; 3520 - Right Thumb Undeveloped. Red boxes indicated presence of amplified product at 300 bp.

NMT used three BioRad T100 thermocyclers interchangeably during these experiments. In order to rule out inconsistencies in amplification between thermocyclers, we directly compared the three machines using identical master mixes.

In the experiment shown in **Figure 38**, each thermocycler was set to produce a gradient of annealing temperatures, ranging from 55 °C to 70 °C. This was to ensure that the optimal temperature used was identical between the machines. All four primer pairs reported in the last report were used. The template DNA was buccal cell DNA from a volunteer donor, and AmpliTaq Gold 360 + GC enhancer was used in all reactions.

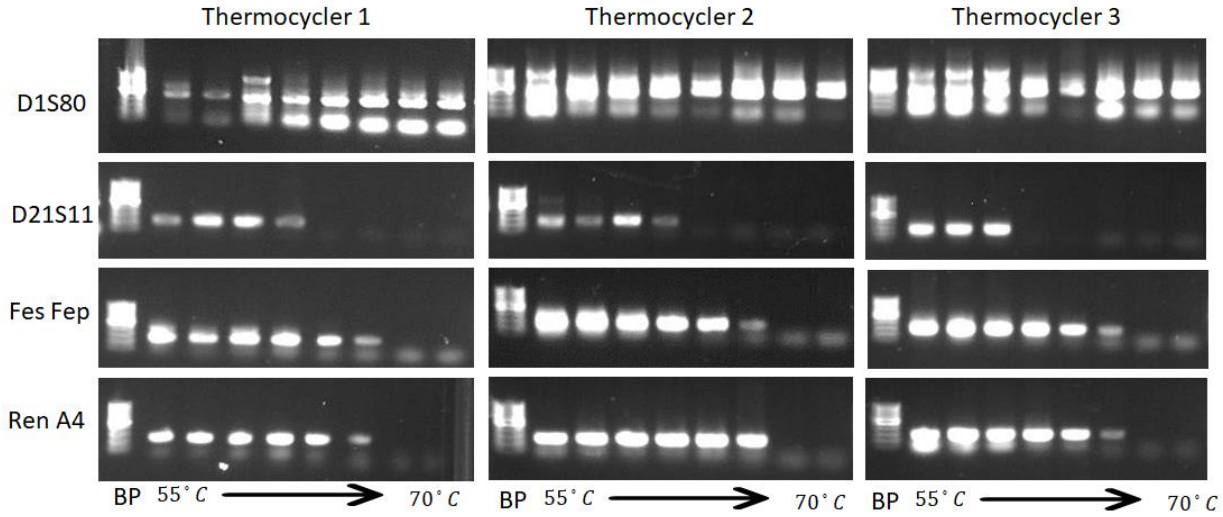

Figure 38. Comparison of three thermocyclers. Three BioRad T100 thermocyclers were set to the same reaction conditions using a gradient of annealing temperatures from 55 °C to 70 °C. Polymerase was AmpliTaq Gold 360 + GC Enhancer. Primers are listed on the left. Buccal DNA from a volunteer donor was used as template.

This comparison confirmed that 58 °C is the optimal annealing temperature for all four primer pairs on all three machines, and that they can be used interchangeably.

Efforts during this period focused on the use of acetic acid-capped nanoparticles (AAUCNP) in the recovery of DNA from fingerprints. As reported last period, work was halted by the closure of New Mexico Tech on March 13, 2020 due to the COVID-19 pandemic, and did not resume until September 2020. Social distancing requirements in the laboratory and stringent check in/check out measures for potential contact tracing limited laboratory time for experiments.

We have previously shown that oleic acid-capped nanoparticles (OAUCNP) are not inhibitory to standard PCR reactions in low concentration, but inhibit at high concentrations. In order to assess the effect of acetic acid-capped nanoparticles (AAUCNP) on the ability to amplify DNA, a comparison test was conducted. In addition, since AAUCNP have been shown by researchers at the University of South Dakota to bind DNA (see **Task 7**), the ability of DNA bound to AAUCNP to be amplified was also tested.

For each test, 300 µg of UCNP (OAUCNP or AAUCNP) were suspended in 25 µl of DNA (approximately 2.5 µg) in water. Two buccal cell DNA sample were used; one was freshly prepared and the other had been isolated prior to the March shutdown. Standard PCR reactions using 2 µL of DNA as the template and RenA4 primers were conducted.

The first PCR reactions were conducted using the UCNP/DNA suspension. Next, the suspension was centrifuged, and the supernatant (containing DNA that had not bound the nanoparticles) was removed to be used in a PCR reaction. Finally, the pellet, containing UCNP and any bound DNA, was resuspended in water, and used in a PCR reaction as in the first step. The gel for this experiment is shown in **Figure 39**.

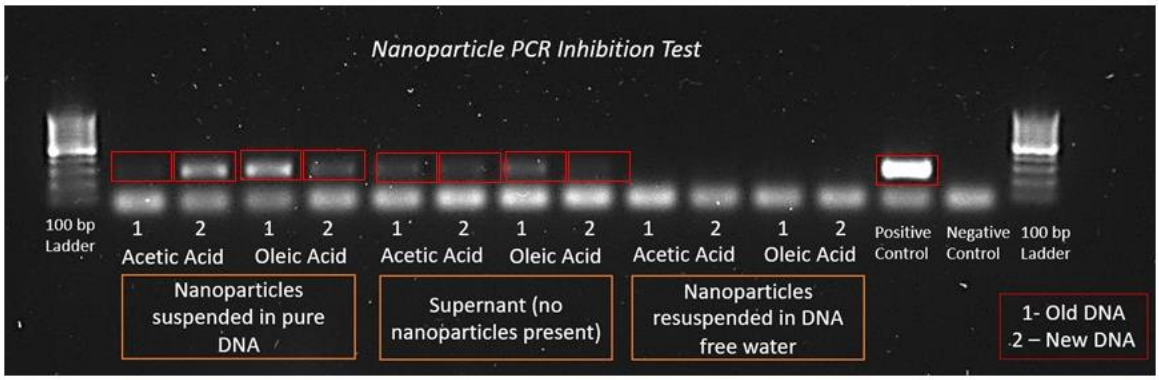

Figure 39. Effect of UCNP on PCR reaction. Red boxes indicate the amplification product.

Neither OAUCNP nor AAUCNP inhibited the amplification of DNA in suspension (first four lanes; nanoparticles suspended in pure DNA). For both types of UCNP, the UCNP-free supernatant contained amplifiable DNA (second four lanes; Supernatant, no nanoparticles present), but the UCNP pellet did not (last four lanes; nanoparticles resuspended in DNA-free water). This suggests that either the DNA is not bound to either type of UCNP, or that bound DNA is not able to be amplified.

Because amplification of DNA bound to AAUCNP was unsuccessful, the pH of the buffer solution was altered to either promote or discourage DNA binding to AAUCNP at various steps of the previous process. The previous experiment was repeated using AAUCNP, but three separate conditions were used, as outlined in **Figure 40**. PCR reactions were performed at each step, as indicated in **Figure 40**. The results are shown in **Figure 41**.

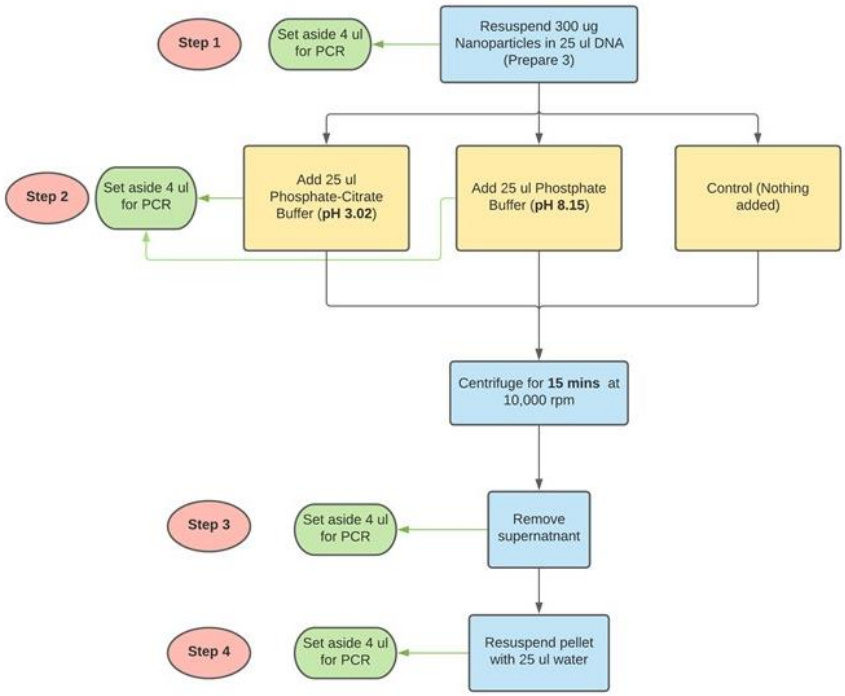

Figure 40. Flowchart of pH dependence experiment. The experiment was repeated, with the addition of pH changes in the binding step (Step 2).

This resource was prepared by the author(s) using Federal funds provided by the U.S. Department of Justice. Opinions or points of view expressed are those of the author(s) and do not necessarily reflect the official position or policies of the U.S. Department of Justice.

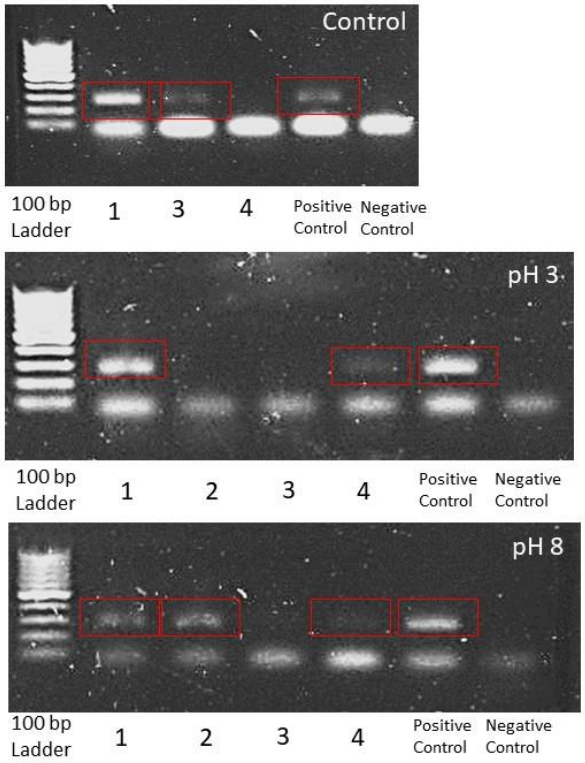

Figure 41. Effect of pH on binding and amplification of DNA in the presence of AAUCNP. Amplified product is indicated by the red boxes. Top panel: Control reactions (no change in pH); Middle panel: acidified conditions (pH 3); Bottom panel: basic conditions (pH 8). Lane numbers refer to steps in the **Figure 40** procedure.

These results indicate that at neutral (unbuffered) pH (**Figure 41**, top panel), the DNA not bound to AAUCNP was amplifiable (Lane 3), but if DNA was bound to AAUCNP, it was not amplifiable (Lane 4), confirming the results in **Figure 39**. At acidic pH, no amplification of combined DNA/UCNP was obtained (**Figure 41** middle panel, Lane 2), presumably because the acidic pH was inhibitory to the enzyme. No amplification occurred in the supernatant (Lane 3) presumably because all DNA was bound to the AAUCNP. However, amplification of DNA did occur from AAUCNP-bound DNA, in Lane 4. This result is in contrast to the experiment shown in **Figure 39** and the control shown in **Figure 41**, where amplification of AAUCNP-bound DNA at neutral (unbuffered) conditions did not occur. Under basic conditions (**Figure 41**, bottom panel), Step 2 yielded amplification (Lane 2), presumably because the pH 8 is close to the optimal pH of the enzyme and is not inhibitory. No amplification occurred from the supernatant (Lane 3), but it did occur from the resuspended nanoparticles (Lane 4). This result supports those of the University of South Dakota researchers, who found that a pH above 8 was necessary for release of the DNA from the nanoparticles. For the next experiment, a pH of 10 will be used to release the DNA from the nanoparticles prior to PCR.

Because amplification of DNA bound to AAUCNP was unsuccessful, the pH of the buffer solution was altered to either promote or discourage DNA binding to AAUCNP at various steps. Based on the previously described University of South Dakota results, the acidifying buffer was potassium hydrogen phthalate (pH 4.2) and the buffer for basification was sodium borate. Also, this pH was raised to 8.8 to improve release of DNA. The experimental design is presented as a flowchart in **Figure 42**.

PCR reactions were performed at the steps indicated in **Figure 42**. The results are shown in **Figure 43**.

This resource was prepared by the author(s) using Federal funds provided by the U.S. Department of Justice. Opinions or points of view expressed are those of the author(s) and do not necessarily reflect the official position or policies of the U.S. Department of Justice.

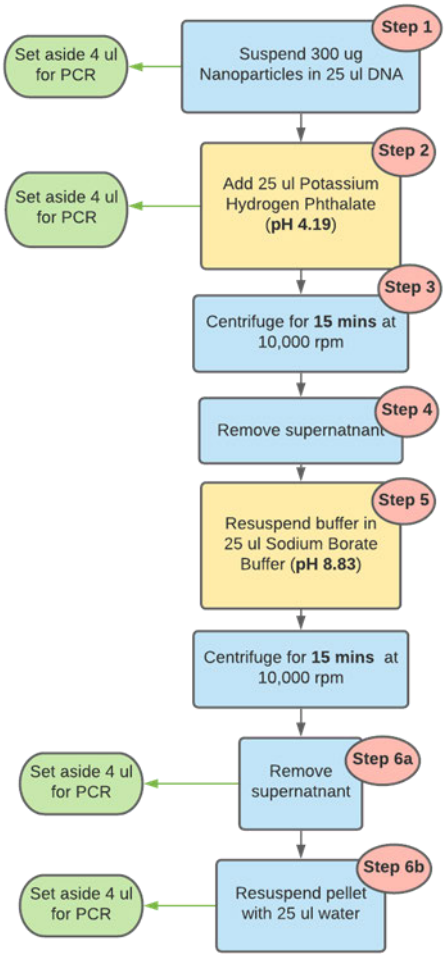

Figure 42. Flowchart of pH dependence experiment.

DNA bound to nanoparticles in water showed little/no amplification by PCR (Lane 1; Suspension). Acidification further reduced amplification (Lane 2; Acidify). This was to be expected, as the PCR reaction requires specific pH conditions, and we have previously shown that bound DNA is not amplifiable by PCR. The acidified nanoparticles were put into pellets and the acidic buffer removed (Steps 3 and 4), then the nanoparticles were resuspended in basic buffer (Step 5). At this point, we expected the nanoparticles to release all bound DNA into the buffer. The nanoparticles were once again pelleted by centrifugation, and the supernatant buffer was tested for amplifiable DNA (Lane 6a; basify supernatant). The remaining pellets were also resuspended in water and tested for amplification (Lane 6b; basify pellet). Only the supernatant amplified, indicating that the nanoparticles had released the DNA into solution, making it available for amplification.

The next step was to use the pH dependence of binding and release to optimize recovery of DNA from developed fingerprints. While awaiting developed fingerprints from South Dakota, we revisited the double-swab technique of DNA recovery, testing multiple primer sets from the CODIS database. This method is summarized below.

- Submerge one swab in a tube filled with Molecular biology grade water.
- Remove DNA from the slide by swab ten times vertically and ten times horizontally over the fingerprint. Make sure to get up as much water as possible.
    - The swab should not be dry anywhere.
- Place a swab in a sterile falcon tube.
- Repeat previous steps with another swab.

- Add in 200 ul of fresh molecular biology grade water to the swabs.
- Centrifuge falcon tube for 5 minutes at the fastest speed.
- Once done, remove the swabs from the tube. Spin down for 30 seconds to ensure no liquid is left on the sides of the tube.
- Remove 200 ul of liquid and place in a new microcentrifuge tube.

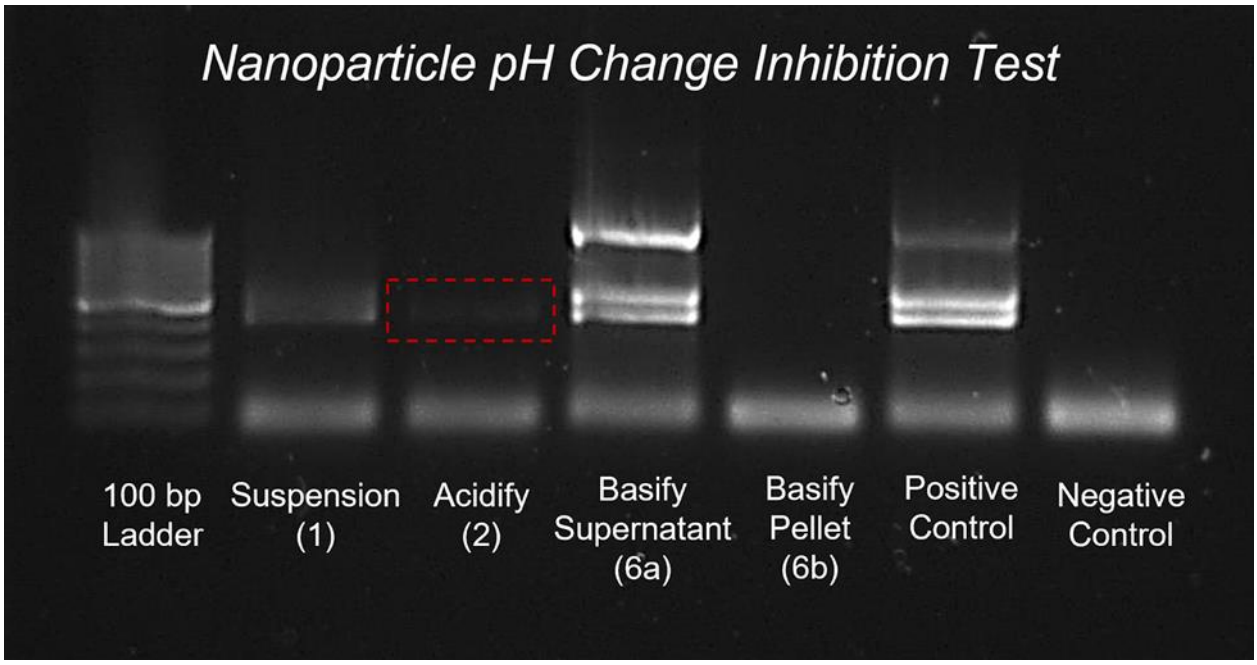

Figure 43. Effect of pH on binding and amplification of DNA in the presence of AAUCNP1. Bands present in the Positive control lane but not in the negative control lane are amplified product. Lane numbers refer to steps in the **Figure 42** procedure.

Fingerprints from the right (R) and left (L) hands of four individuals were tested (RC car, No, Cat and ST690). Isolated DNA was analyzed using the Nanodrop spectrophotometer and concentrations determined (**Table 2**).

Table 2. Concentration of recovered fingerprint DNA.

	DNA concentration (ng/µL)	
Individual	Right	Left
RC Car	5.5	6.1
No	2.6	4.3
Cat	4.2	3.5
ST690	3.6	3.9

These recoveries were less than expected. Three primer sets were used to amplify the DNA: D1S80, Fesfep, and RenA4, using known DNA as control. The results are shown in **Figure 44**.

Although not visible in **Figure 44**, there was amplification of D1S80 from RC Car (R), No (L) and ST690 (R). Neither of the other two primer sets amplified this DNA.

Task 6: Comparison: Optimal UCNP System vs Standard Procedures on High-Value Substrates

High-value substrates were examined as part of Task 4. The UCNPs worked well on these type of substrates including polymer banknotes, paper banknotes, and business cards. Proving their utility on high-value substrates.

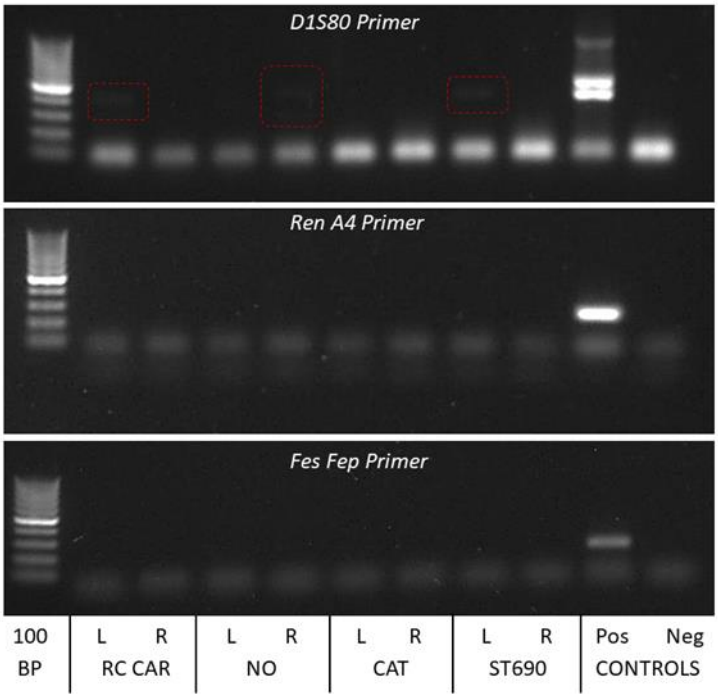

Figure 44. Amplification of DNA isolated from fingerprints using double-swab technique.

Task 7: Comparison: Non-functionalized versus Functionalized UCNP for Imaging DNA

Purpose: Examining how UCNPs capture DNA was the primary focus of this task.

Research: The non-functionalized and functionalized UCNPs were tested in Task 5, with the AAUCNPs found to work best for DNA extraction. Further study of the acetic acid-capped UCNPs was performed.

The experimental procedures for this task are as follows:

DNA Stock Solution (DSS): 120 µL of DNA solution (10 mg/mL) diluted to 1.5 mL **-> 0.6 mg/mL**

NPs Stock Solution (NSS): 20 mg of AAUCNP (AA-AR29JUL20) dispersed in 10 mL water **-> 2 mg/mL**

Three sets of specimens were made for three different concentrations of DNA. The first set is the 'Test' the second set is the '+ve control' and the third set is the '-ve control'. The Test specimen has DNA and UCNP, the '+ve control' has only DNA and no UCNP and the '-ve control' has only UCNP and no DNA.

Figure 45 shows the test specimen used. In three 1.5 mL centrifuge tubes 1.0 mL of NSS was added followed by 0.02 mL, 0.1 mL and 0.3 mL of DSS in each of the tubes. The final volume was set to 1.5 mL by addition of 0.28 mL, 0.2 mL, and 0 mL of water, respectively. The final quantity of the DNA low, moderate, and high concertation solutions is, 12 µg, 60 µg, and 180 µg, respectively, per 2 mg of UCNP. The solutions were kept aside for 10 minutes to let the DNA bind the UCNP. The UCNP are isolated by centrifugation at 5000 rpm for 5 minutes. The supernatant is used to quantify the un-bound DNA. The precipitated was re-dispersed in the supernatant for zeta potential measurement.

+ve control: The procedure is identical as the 'Test' except 1.0 mL of water was added instead of NSS.

-ve control: In three 1.5 mL centrifuge tubes 1.0 mL of NSS was added followed centrifugation at 5000 rpm for 5 minutes. A supernatant is collected and 0.02 mL, 0.1 mL and 0.3 mL of DSS was added to each of the tubes.

The rest of the procedure is identical to the 'Test' except the precipitated was re-dispersed in the water for zeta potential measurement.

Low concentration (12 µg) of DNA	Moderate concentration (60µg) of DNA	High concentration (180 µg) of DNA
1.0 mL UCNP dispersion + 0.02 mL DNA Stock sol. + 0.28 mL water **->centrifuged<-**	1.0 mL UCNP dispersion + 0.1 mL DNA Stock sol. + 0.2 mL water **->centrifuged<-**	1.0 mL UCNP dispersion + 0.3 mL DNA Stock sol. **->centrifuged<-**
1.0 mL UCNP dispersion **->centrifuged<-** Supernatant + 0.02 mL DNA Stock sol. + 0.28 mL water	1.0 mL UCNP dispersion **->centrifuged<-** Supernatant + 0.1 mL DNA Stock sol. + 0.2 mL water	1.0 mL UCNP dispersion **->centrifuged<-** Supernatant + 0.3 mL DNA Stock sol.
1.28 mL water + 0.02 mL DNA Stock sol. **->centrifuged<-**	1.20 mL water + 0.1 mL DNA Stock sol. **->centrifuged<-**	1.0 mL water + 0.3 mL DNA Stock sol. **->centrifuged<-**

Figure 45. Description of test specimen.

Spectroscopy procedure: 10 mL aliquots are added to 3 mL of Diamond-dye solution 10,000x dilution.

Emission Scan Parameters: Range: 495 – 650 nm; Step size: 2 nm; Integration time: 0.2 sec; excitation: 480 nm; Slit entrance: 0.5 mm; and Slit exit: 1.0 mm. No correction. No blank subtraction.

The emission intensities of the supernatant of low, moderate, and high concentration DNA loaded UCNPs (see **Figure 46**) were collected and compared to the respective +ve control and -ve control samples. In the low concentration samples, the intensity of the -ve control, i.e., UCNP supernatant +DNA, intensity lower than the +ve control suggests that the supernatant is contributing to the decrease in the emission intensity, see **Figure 46**. Indeed, in the low, moderate, and high concentration samples the intensity is 80%, 19%, and 3% lower than the respective +ve control specimen. Since the quenching is not proportional to the DNA concertation, but remains constant for all the three concentration solutions, it can be interpreted that the fixed volume addition of the specimen could be the reason for the quenching. The addition of the specimen might have attributed to the change in the chemical environment of the dye medium thereby quenching the dye intensity.

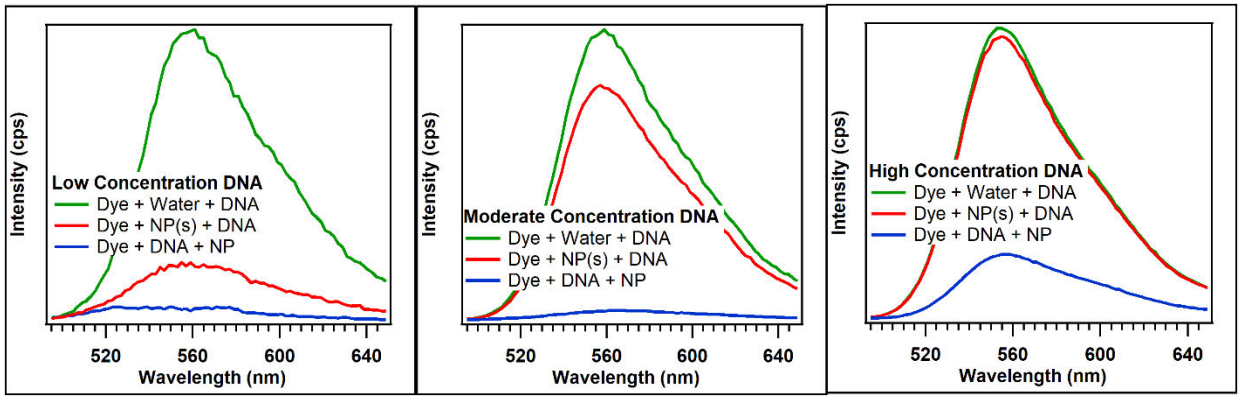

Figure 46. Evaluation of DNA emission intensities.

However, in all three concentration specimens of the Test sample, i.e., UCNP+DNA supernatant, the intensity is significantly lower than the -ve control specimen suggests that the DNA is binging to the AAUCNP. The solvent induced quenching is very insignificant for low concentration samples. Therefore, the intensity of the moderate and high concentration test specimens is corrected, using Equations 1 and 2, for the solvent induced quenching to calculate the amount of the DNA bound to the UCNP.

This resource was prepared by the author(s) using Federal funds provided by the U.S. Department of Justice. Opinions or points of view expressed are those of the author(s) and do not necessarily reflect the official position or policies of the U.S. Department of Justice.

$$DNA_{conc} = \frac{(I-c)}{S}; I = intensity; c = y - interceipt; S = slope \quad (1)$$

$$\%\, DNA_{bound} = \frac{(DNA_{-ve} - DNA_{test})}{DNA_{+ve}} \times 100 \quad (2)$$

The amount of the DNA bound to the UCNP is calculated to be approximately 73%, i.e., 103 and 343 µg/mg of UCNP for moderate and high concentration DNA, respectively.

In order to further confirm the binding of the DNA to the UCNP, zeta potential measurements of the low, mid, and high concentration DNA samples were collected and compared to the AAUCNP without DNA, see **Figure 47**.

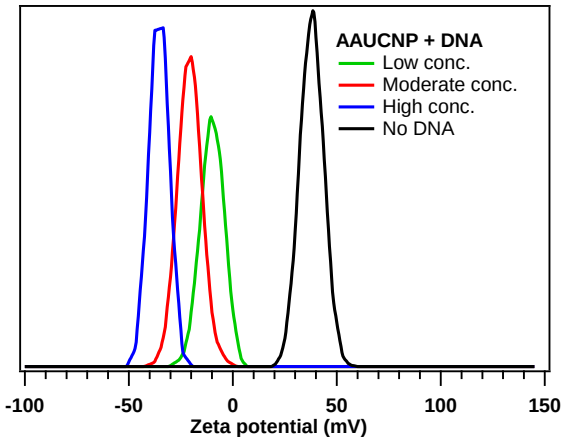

Figure 47. Zeta potential measurement for acetic acid-capped nanoparticles with and without DNA.

The AAUCNP without DNA has positive zeta potential of 39±7 mV and the zeta potential became negative for DNA loaded UCNPs. The zeta potential became -9.5±7 mV, -21±6 mV, and -35±5 mV for low, moderate, and high DNA loaded UCNP, respectively. This is an indication that DNA may be binding to the AAUCNPs

Task Research Summary: The spectroscopy helped to characterize the amount of the DNA bound to the UCNP and the zeta potential helped characterize the surface nature of the DNA bound UCNP. Spectroscopic studies and zeta potential measurements both compliment and strongly suggests that increase in the DNA concentration resulted in more DNA binding to the UCNPs.

Task 8: Evaluate Utility of UCNPs for DNA Extraction from Fingerprints

Purpose: This task was aimed at determining how well functionalized (acetic acid capped) and non-functionalized (oleic acid capped) UCNPs extract DNA from fingerprints.

Research: DNA binding and fingerprint interactions of AAUCNP and OAUCNP was studied. The results showed that the AAUCNP have poor adherence to the latent fingerprint (LFP) compared to the OAUCNP. The DNA-UCNP interaction with AAUCNP and OAUCNP was inconclusive due to the low DNA concentration in the LFP.

In order to study the effect of the pH on the DNA-AAUCNP interaction four pH buffer solutions, pH 4, pH 6, pH 8, and pH10, were used for this study. pH 4 is a phthalate buffer, the pH 6 and pH 8 are phosphate buffers and the pH 10 is carbonate buffer. Three specimen (DNA (+ve control), UCNPs (-ve control), DNA+UCNPs (test sample) were prepared in all four buffer solutions. The test, +ve control and –ve control were treated identically.

For the DNA solution, 75 µL of 10 mg/mL DNA was added to each buffer and diluted to a volume of 3.0 mL. For the upconverting nanoparticle dispersion, 10 mg of AAUCNP were dispersed in 2 mL of DI water by

sonication. For the test solution, 1.35 mL of DNA solution was added to 0.15 mL of UCNP dispersion. The DNA specimen was made with 1.35 ml of DNA solution with the pH buffer. The UCNP specimen used 1.35 ml of the relevant pH buffer without DNA was added to 0.15 nl of the UCNP dispersion.

The final concentration of DNA and UCNP are 225 µg/mL and 500 µg/mL, respectively. Zeta potential of the dispersions were acquired for all specimen within 30 minutes of the specimen preparation and after 24 hours. The dispersion was centrifuged and the precipitates were dried in vacuum at 65°C for FTIR studies.

Zeta potential measurements: At pH 4, the zeta potential of the test specimen (DNA+UCNP) is -39±10 mV, whereas, the zeta potential of the UCNP control is 0±12 mV, as shown in **Figure 48**. The -39 mV zeta potential of the test specimen agrees with the other results. However, the zeta potential of the UCNPs in the pH 4 buffer is significantly lower than the AAUCNP zeta potential measured in water reported previously. This imlies that the composition of the pH buffer has a major role in the zeta potential besides the DNA coating onto the UCNP. Below is the summary of the zeta potentials of test, DNA control, and UCNP control specimen for four different pH values (pH 4, pH 6, pH 8, and pH 10), collected within 30 minutes and after 24 hours, as shown in **Table 3**.

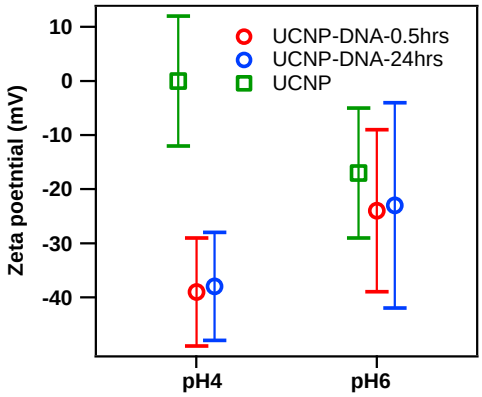

Figure 48. Zeta potential measurement for acetic acid-capped nanoparticles with and without DNA.

Table 3. Zeta potential measurement for acetic acid-capped nanoparticles with and without DNA.

Zeta Potential (mV)	pH4	pH 6	pH 8	pH 10
UCNP	0±12	-17±12	-32	-35
UCNP+DNA	**-39±10**	**-24±15**	**-35**	**-34**
DNA	-16±16	-20±15	-8	-17
UCNP+DNA 24hrs	-38±10	-23±19	-29	-34

The zeta potential of the DNA control is very broad with high standard deviation and low intensity. Since the standard deviation is higher than the zeta potential itself for DNA specimen, a meaningful zeta potential cannot be determined. Therefore, zeta potential of DNA specimen is excluded from the further discussion.

The zeta potential of the bare UCNP control is zero at pH 4 and gradually decreased to –17 mV with the increase to pH 6. The zeta potential decreased further to -32 mV at pH 8 and -35 mV at pH 10. Whereas the test specimen zeta potential is -39 mV at pH 4 and increased to -24 mV at pH 6. The test specimen zeta potential decreased to -35 mV at pH8 and remained in that region at pH 10.

It is important to note that the zeta potential of the test specimen and the UCNP control has no significant difference at pH 8 and pH 10. In order to assess the surface nature of the UCNP and the role of the pH, the

specimen were centrifuged and the precipitate was dried at 65°C to remove water remnants for FTIR measurements.

The FTIR spectra of pH 6 and pH 8 specimen for the test specimen and UCNP (-ve control) are identical suggests that the UCNP surface is totally altered by the buffering agent. The test and UCNP control specimen FTIR spectra for pH 4 and pH 10 are significantly different. To identify the contribution of the buffering agents; phthalate in pH 4 buffer, phosphate in pH 6 and pH 8 buffer, carbonate in the pH 10 buffer. FTIR spectra of potassium hydrogen phthalate, dibasic potassium phosphate, and sodium carbonate were acquired and compared to the respective test and UCNP (–ve control) specimen, see **Figure 49**.

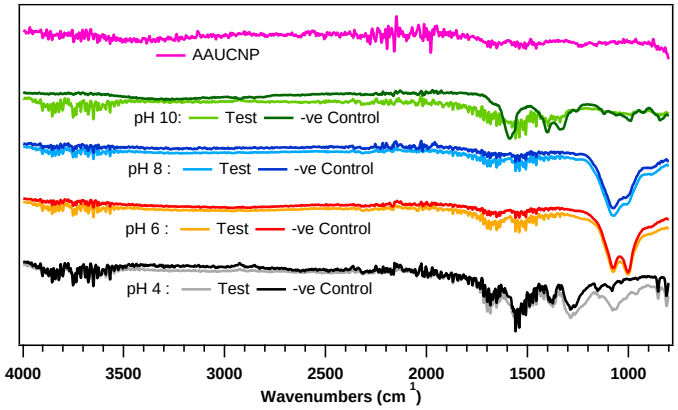

Figure 49. FTIR spectra of UCNPs at various pH values. Test indicates that there is DNA present, -ve control indicates no DNA.

The features observed in the FTIR response of the test and the UCNPs (–ve control) specimen resemble to the respective buffering salts except for the feature at 1050-1080 cm^{-1}. More specifically, the pH 4, specimen has a strong broad feature at 1050 cm^{-1}, which corresponds to the phosphate stretch of the DNA. The broad peak is missing in the case of the pH 10 test specimen suggests that the DNA is not binding to the surface of the UCNP in the pH buffer. It is inconclusive about the DNA binding to UCNP in pH 6 and pH 8 buffers due to strong signal of the phosphates from the buffering agent, see **Figures 50 and 51**.

The DNA interaction with UCNP in four different buffer solutions, pH 4, pH 6, pH 8, and pH 10, was studied. Zeta potential values were measured for the DNA-UCNP in the original buffer solutions. The DNA-UCNP in pH 4 buffer has the negative zeta potential compared to the bare UCNP at pH 4. The FTIR of the DNA-UCNP prepared in pH 4 buffer also showed a unique feature at 1050 cm^{-1}, which may be related to the bound DNA. However, for pH 6, pH 8, and pH 10 buffers the zeta potential and FTIR results are inconclusive. Since the test and UCNP control specimen were used without further washing to remove buffer solution remnants, the buffering agents interfered with the FTIR and zeta potential measurements.

The effect of the pH buffer on DNA isolation: A total of five samples were prepared for comparison, +ve control, -ve control 1, -ve control 2, Test-1, and Test-2. The +ve control is DNA in water; the –ve control 1 is AAUCNPs in water; the –ve control 2 is AAUCNPs in pH8 buffer; the Test-1 is AAUCNP+DNA in water; and the Test-2 is AAUCNP+DNA in pH 8 buffer.

AAUCNP dispersion: In a 15 mL centrifuge tube, 50 mg of AAUCNP were taken and sonicated to form a homogenous dispersion. The dispersion was centrifuged at 4500 rpm for 5 minutes. The supernatant was decanted and the precipitate was re-dispersed in water. The washing process was repeated for one more time. Finally, one portion of 20 mg of the UCNP were dispersed in 10 mL of water and another portion of 20 mg of the UCNP was dispersed in 10 mL of pH 8 buffer to form 2 mg/mL dispersion. AAUCNPs were washed with water two times following this procedure.

This resource was prepared by the author(s) using Federal funds provided by the U.S. Department of Justice. Opinions or points of view expressed are those of the author(s) and do not necessarily reflect the official position or policies of the U.S. Department of Justice.

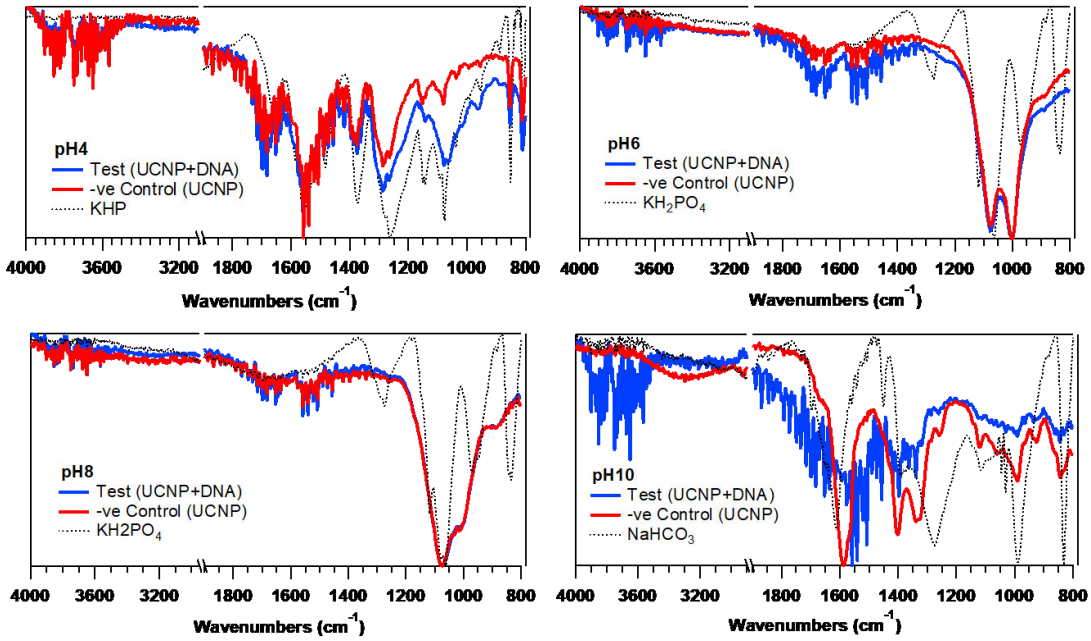

Figure 50. FTIR spectra of UCNPs, UCNPs with DNA, and buffer.

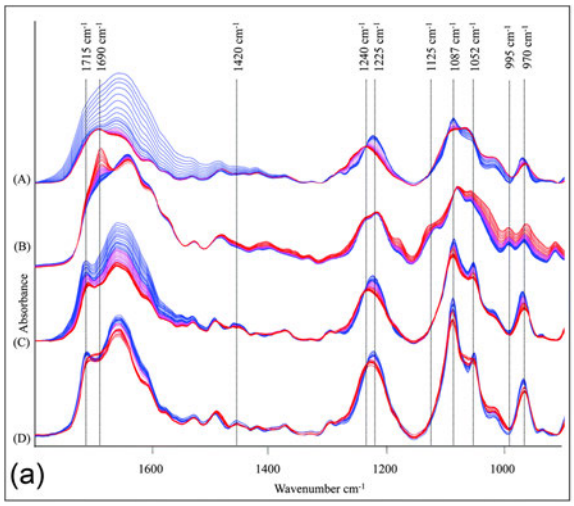

Figure 51. FTIR spectra of buffers with DNA.

Solution methodology: The aqueous solutions used in the work described were<u>DNA solution:</u> 10 mg/mL of the previously described solutions.

<u>Test-1:</u> To a 0.25 mL of aqueous AAUCNP dispersion, 0.075 mL DNA solution was added and diluted to 1.5 mL with water. The final concentration of the dispersion is, UCNP: 333 µg/mL and DNA: 500 µg/mL.

<u>Test-2:</u> Similar to Test-1 except pH 8 buffer AAUCNP dispersion was used and the pH 8 buffer was used for final dilution to 1.5 mL.

<u>-ve control 1:</u> Similar to Test-1 except 0.075 mL of water was added instead of DNA.

<u>-ve control 2:</u> Similar to Test-2 except 0.075 mL of water was added instead of DNA.

+ve control: Similar to Test-1 except 0.25 mL of water was added instead of AAUCNP dispersion.

All specimen, Test-1, Test-2, -ve Control-1, -ve Control-2, and +ve Control, were treated similarly. The specimen were mixed for 30 minutes using a vertical mixer. The UCNPs were separated by centrifugation at 4000 rpm for 5 minutes. The supernatant is collected in a separate vial for spectroscopy and the precipitates were washed with DI water and re-dispersed in 1.5 mL water for zeta potential measurement. The UCNP were precipitated again by centrifugation and dried in vacuum at 65°C for EDX measurement.

Spectroscopy: 20 µL aliquots of supernatant was added to 3 mL of Diamond Dye (10000x dilution). Emission Scan Parameters: Range: 495 – 650 nm; Step size: 2 nm; Integration time: 0.2 sec; excitation: 480 nm; Slit entrance: 0.5 mm; and Slit exit: 1.0 mm. No correction. No blank subtraction.

Since the spectroscopy measures the 'free' DNA in the supernatant, the intensity of Test-1 and Test-2 samples being less than the +ve Control suggests that the DNA is binding to the UCNPs. The DNA binding to the UCNPs appears greater in Test-1 specimen (in water) compared to the Test-2 specimen (in pH 8 buffer) suggests that the DNA-UCNP interaction is much stronger in water, see **Figure 52**.

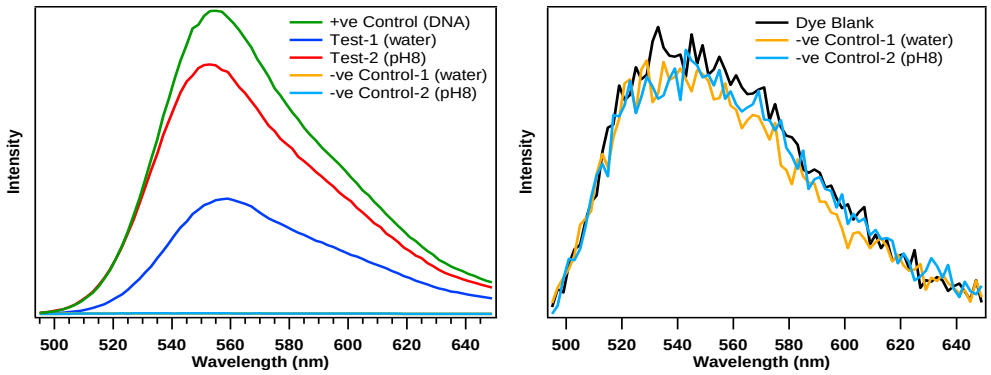

Figure 52. Fluorescence spectroscopy of DNA binding to AAUCNPs, left tests and controls; right, dye spectra.

Both of the –ve Control specimen, water and pH 8 buffer, did not alter the dye spectrum suggests that there is no significant effect of the solvents on the spectroscopy, see **Figure 52**.

Zeta potential: Zeta potential of the aqueous dispersion of the UCNP precipitate from the Test and –ve control specimen were collected. The –ve control-1 and –ve control-2 have the zeta potential of +38 ± 8mV and -5 ± 20mV, respectively. The negative zeta potential for –ve control-2 specimen, which was prepared in phosphate buffer and dispersed in water, strongly suggests that the phosphate group in the buffer attaches to the surface of the UCNP. The results agree with the strong negative zeta potential for the UCNP dispersed in the pH 6 and pH 8 phosphate buffers in the previous section, see **Figure 53**. The Test-1 and Test-2 specimen zeta potential becoming more negative agrees with previous observations.

SEM-EDX Analysis: The scanning electron micrographs (**Figure 54**) of the –ve Control and Test samples have no significant difference to report. To determine the DNA coating onto the UCNP, the –ve Control and the Test samples were subjected to energy dispersive X-ray (EDX) analysis (**Figure 55**).

The EDX spectra of all studied specimen look similar due to the large spectral contributions from Na-Kα at 1.04 keV, Yb-Mα at 1.53 keV, and F-Kα at 0.677 keV. However, significant difference in the intensity is observed for smaller O-Kα band at 0.525 keV and P-Kα band at 2.01 keV. Even though the P-Kα band overlaps with the Yb-$M\alpha_3$ band, the intensity of the peak at 2.01 keV is higher for –ve control-2 and test-2 specimen compares to the –ve control-1 and the test-1 specimen. The high intensity of the peak at 2.01 keV could be from the buffer phosphate ions. The presence of phosphates is further confirmed by the higher intensity of O-Kα at 5.25 keV for buffer-based specimen. No characteristic nitrogen Kα signals at 0.392 keV were found for both Test-1 and Test-2 specimen; this could be due to low DNA loading compared to the mass of the UCNP.

This resource was prepared by the author(s) using Federal funds provided by the U.S. Department of Justice. Opinions or points of view expressed are those of the author(s) and do not necessarily reflect the official position or policies of the U.S. Department of Justice.

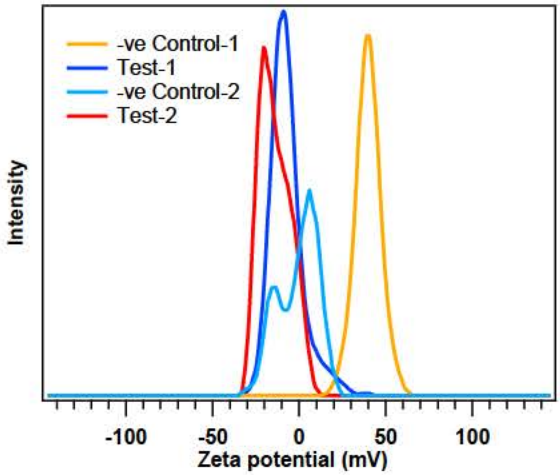

Figure 53. Zeta potential of AAUCNPs and DNA.

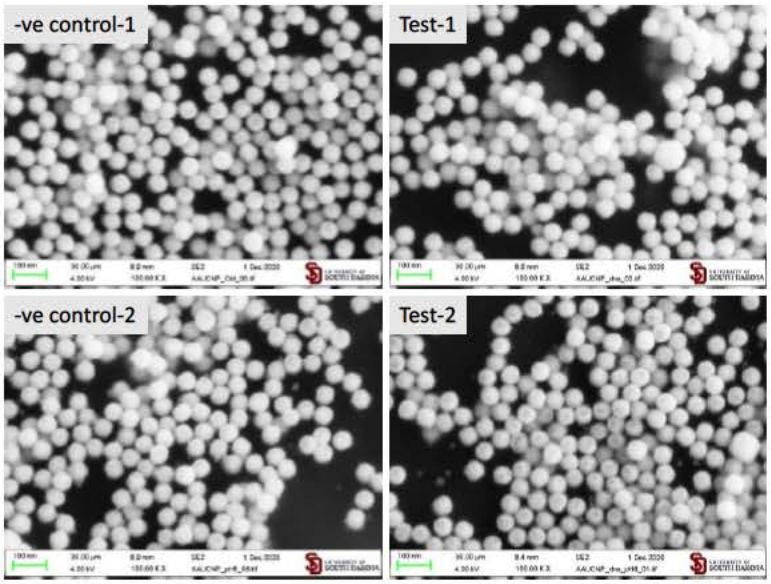

Figure 54. SEM micrographs of AAUCNPs after various treatments.

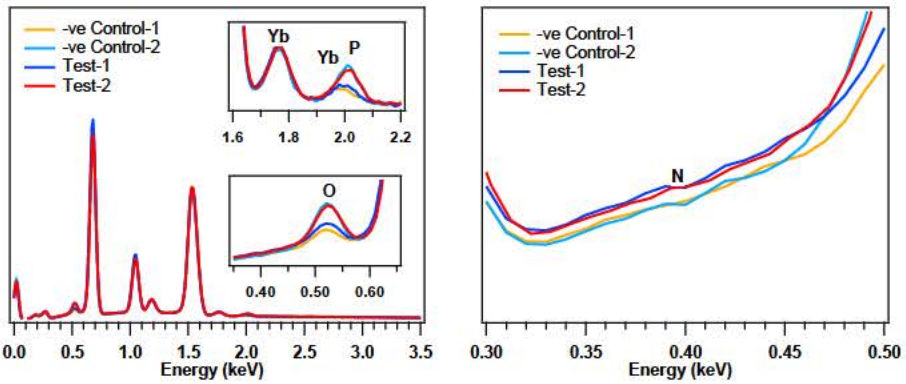

Figure 55. SEM-energy dispersive spectra (EDX) micrographs of AAUCNPs.

The DNA-UCNP interaction with and without pH 8 phosphate buffer was studied to understand the role of the phosphate group on the DNA binding to the UCNP. The spectroscopic studies suggests that the DNA has less affinity to bind to the UCNP in the presence of the phosphate buffer. The zeta potential and the EDX experiments confirmed that the phosphate groups in the buffer binds to the bare UCNP and thereby hinders the DNA interaction with the UCNP.

Since the DNA interaction with the UCNP is altered with the buffer medium, an experiment is designed to release the DNA from UCNP by introducing the UCNP to new buffer environment.

pH based DNA extraction using UCNPs:

To determine the effect of pH on the extraction of DNA by the upconverting nanoparticles, the samples listed in **Table 4** were used. The overall testing procedure is given in **Figure 56**.

Table 4. Sample descriptions usedfor testing the effect of pH on DNA extraction using UCNPs.

Sample ID	**Description**
Test-pH 4	75 µL of aq. **DNA (125 µg/mL) +** 75 µL of **UCNP (250 µg/mL)** in pH 4 buffer + 1.35 mL of **pH 4 buffer**
Test-W	75 µL of aq. **DNA (125 µg/mL) +** 75 µL of **UCNP (250 µg/mL)** in water + 1.35 mL of **water**
Test-pH 10	75 µL of aq. **DNA (125 µg/mL) +** 75 µL of **UCNP (250 µg/mL)** in pH10 buffer + 1.35 mL of **pH 10 buffer**
Blank-pH 4	75µL of water + 1.425 mL of **pH 4 buffer**; No DNA and No UCNP
+Ctrl-pH 4	75µL of aq. **DNA (125 µg/mL)** + 1.425 mL of **pH 4 buffer**
-Ctrl-pH 4	75µL of **UCNP (250 µg/mL)** in pH buffer **+** 75µL of water + 1.35 mL of **pH4 buffer**
Test-pH 4-s	**Supernatant** of the **Test-pH 4**
Test-pH 4-p	**Precipitate** of the **Test-pH 4** dispersed in water
Test-pH 4-pd	**Dried precipitate** of the **Test-pH 4-p**
Test-pH 4@pH 8	**Precipitate** of the **Test-pH 4-p** re-dispersed in **pH 8 buffer**
Test-pH 4@pH 8-s	**Supernatant** of the **Test-pH 4@pH 8**
Test-pH 4@pH 8-p	**Precipitate** of the **Test-pH 4@pH 8** in water for Zeta potential
Test-pH 4@pH 8-pd	**Precipitate** of the **Test-pH 4@pH 8-p**, dried
Test-pH 4@pH 10	**Precipitate** of the **Test-pH 4-p** re-dispersed in **pH 10 buffer**
Test-pH 4@pH 10-s	**Supernatant** of the **Test-pH 4@pH 10**
Test-pH 4@pH 10-p	**Precipitate** of the **Test-pH 4@pH 10** in water for Zeta potential
Test-pH 4@pH 10-pd	**Dried precipitate** of the **Test-pH 4@pH 10-p**

Spectroscopic Procedure: 20 µL aliquot of sample was added to 3 mL of 10000x dilute Diamond Dye solution.

Emission Scan Parameters: Range: 495 – 650 nm; Step size: 2 nm; Integration time: 0.2 sec; excitation: 480 nm; Slit entrance: 0.5 mm; and Slit exit: 1.0 mm. No correction. No blank subtraction.

The supernatant (s) collected from the blank, -Ctrl (UCNP), +Ctrl (DNA), and Test (DNA+UCNP) for in water (W), pH 4 buffer (pH 4), and pH 10 buffer (pH 10) was used for spectroscopic measurement. The blue curve in the below graphs corresponds to the response from DNA; the red and gray curves correspond to the response from Blank and UCNP; and the green curve corresponds to the response from the DNA-UCNP mixture for in various diluting solutions, see **Figure 57**.

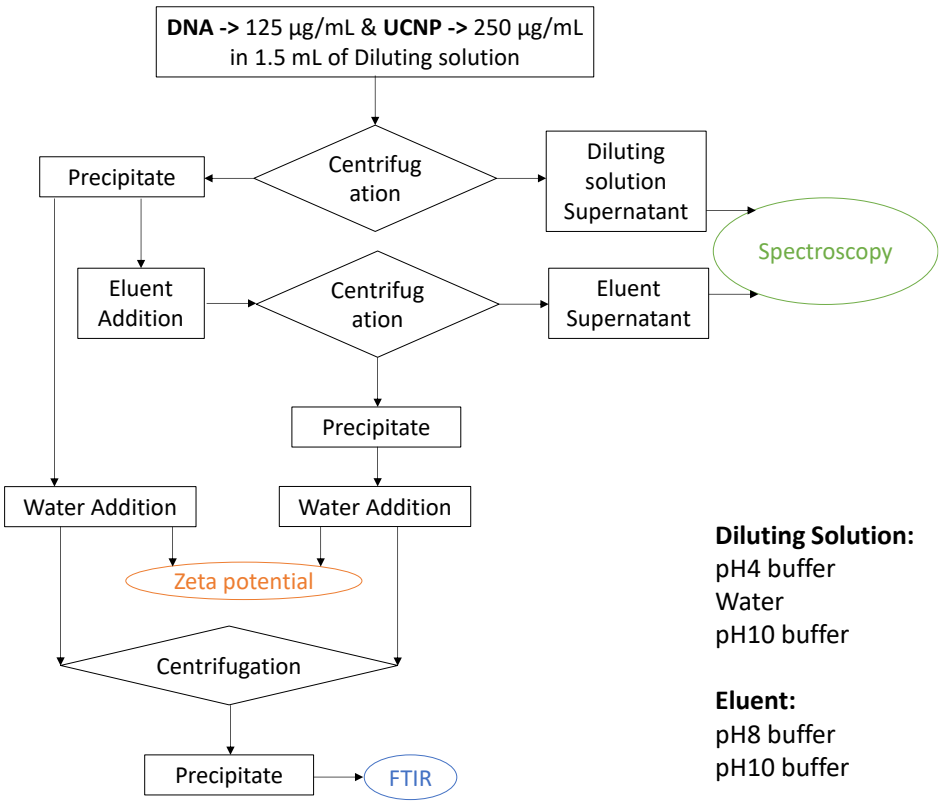

Figure 56. Experimental structure for testing DNA extraction by UCNPs.

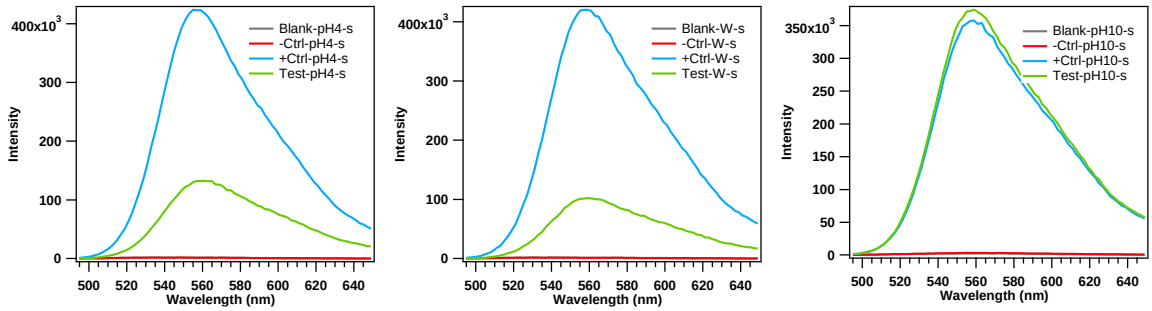

Figure 57. Spectra of DNA from various experiments.

The +Ctrl-W and +Ctrl-pH 4 have very comparable intensity suggests that the pH 4 buffer does not significantly alter the Dye response. However, the +Ctrl-pH 10 dye response decreased significantly indicates that the pH 10 is altering the Dye medium, which can be further confirmed from the slight increase in the intensity of Blank-pH 10 and –Ctrl-pH 10 compare Blank-W and –Ctrl-W in **Figure 58**.

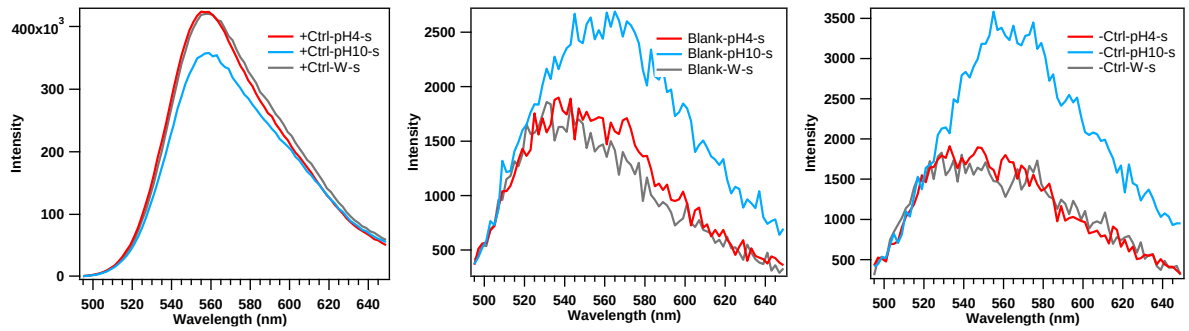

Figure 58. Spectra of DNA from various experiments.

The emission response of the Test (DNA+UCNP) specimen prepared from pH 4 and pH 10 media decreased significantly compared to their respective +Ctrl (DNA) specimen indicated that the quantity of the DNA in the supernatant is decreased. The loss of the DNA in the supernatant can be attributed to binding of the DNA to UCNP. The quantity of the 'bound' DNA is quantified using Equations 3 and 4:

$$DNA_{Test} = \frac{I_{Test}}{I_{+Ctrl}} \times 125\ ppm\ ; I = intensity; \tag{3}$$

$$\%\ DNA_{bound} = \frac{(DNA_{+Ctrl} - DNA_{Test})}{DNA_{+Ctrl}} \times 100 \tag{4}$$

The bound DNA was calculated to be 76% for Test-W and 69% for Test-pH 4, which is consistent with the previously observed value of 73% found previously. The amount of the DNA bound is 380 and 347 µg/mg of UCNP, respectively, for the specimen prepared in pH 4 buffer and water media.

The intensity of the DNA in the Test-pH 10 is in the same order of the +Ctrl-pH 10 suggests that the DNA binding to the UCNP in the pH 10 buffer is not favored.

The FTIR spectra of the Test-W, Test-pH 4, and Test-pH 10 (UCNP+DNA) were compared to -Ctrl-W, -Ctrl-pH 4, and –Ctrl-pH 10 (UCNP) for DNA specific features in the Test specimen. It is very apparent to observe strong DNA feature in the Test-pH 4 and in Test-W but not in the Test-pH 10 also confirms that the DNA is not binding to the UCNP in the pH 10 buffer medium. The FTIR spectrum for Test-pH 4 appears very similar to the DNA-UCNP in pH 4 reported previously, see **Figure 59**.

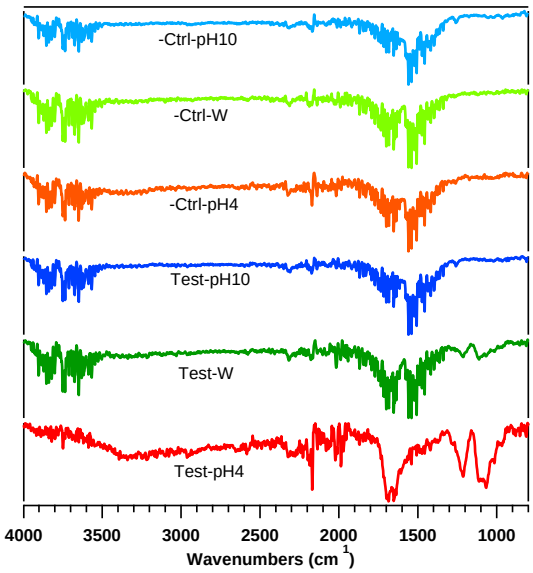

Figure 59. FTIR spectra of UCNPs with and without DNA from various experiments.

It is important to note that the Test and –Ctrl samples were washed with water before precipitating and drying for FTIR spectroscopy. The washing of the specimen might have removed all traces of the buffering agent, therefore, the FTIR response of the –Ctrl specimen appear clean from ligands.

The zeta potential of the Test and –Ctrl specimen were compared to evaluate the DNA-bound and un-bound UCNP. The –Ctrl-W, i.e., UCNP in water have zeta potential of +35mV, which is consistent with the previous reported value. However, the zeta potential of –Ctrl-pH 4 is +18 mV, which is significantly higher than the previously reported value of 'zero'. The high zeta potential for –Ctrl-pH 4 could be due cleaning off the surface ligand during the washing of the UCNP. The zeta potentials were acquired in the original buffer solutions, see **Figure 60**.

Nevertheless, the Test-W and Test-pH 4 specimen zeta potential is moved to -18 mV and -31 mV, respectively, also confirms that DNA is bound to the UCNP in the pH 4 buffer and in water. The zeta potential measurement of the Test-pH 10 and –Ctrl-pH 10 both fall in the negative region, therefore, no meaningful conclusion is arrived with the pH 10 specimen. Similar observations were made for the specimen in pH 10 buffer previously.

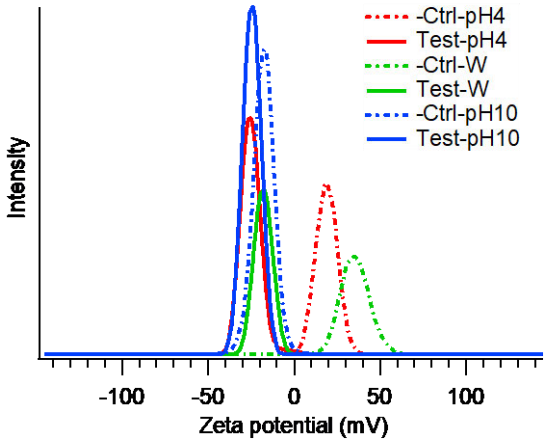

Figure 60. Zeta potential of UCNPs from various experiments.

DNA extraction from UCNPs: The precipitates from Test-W, Test-pH 4, -Ctrl-W, and –Ctrl-pH 4 were re-dispersed in pH 8 buffer (or pH 10 buffer) to release the bound DNA into buffering medium. The gray curves in the below spectra corresponds to the DNA in +Ctrl specimen. The red curves correspond to the intensity of the un-bound DNA in Test specimen. The green curve corresponds to the released DNA in the pH 8 buffer medium and the blue curve corresponds to the DNA released in the pH 10 buffer medium (**Figure 61**).

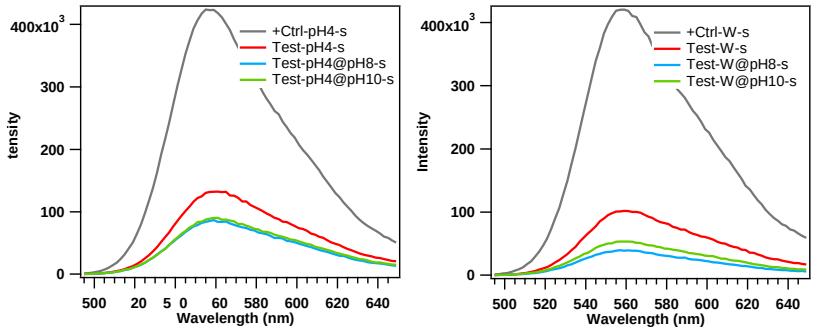

Figure 61. Spectra of DNA from various experiments.

Figure 61 clearly suggests that DNA is released in pH 8 and pH 10 buffering media for both, Test-W, and Test-pH 4 specimen. The amount of DNA released is quantified using Equations 5 and 6.

$$\%\, DNA_{released} = \frac{DNA_{conc}}{(DNA_{+Ctrl} - DNA_{Test})} \times 100 \quad (5)$$

$$\%\, Recovery = \frac{DNA_{conc}}{DNA_{+Ctrl}} \times 100 \quad (6)$$

The overall DNA recovery rate, shown in **Table 5**, of ~10% is achieved with the specimen prepared in water and ~20% is achieved with the specimen prepared in pH 4 buffer. Relatively greater release is achieved in pH 10 buffer compared to pH 8 buffer. The DNA release efficiency is 30% for Test-pH 4 and 12-16% for Test-W, which is comparable to their binding affinities of the DNA and UCNP in the original buffer solution. This implies that

Table 5. Recovery of DNA from various experiments.

	Bound	Released	Recovery
Test-pH 4	69%		
Test-pH 4@pH 8		29%	19.9%
Test-pH 4@pH 10		30%	20.9%
Test-W	76%		
Test-W-pH 8		12%	9.0%
Test-W-pH 10		16%	12.4%

the bound and un-bound DNA are in equilibrium at 3:1 ratio. However, the FTIR spectra of the Test-W@pH 8, Test-W@pH 10, Test-pH 4@pH 8, and Test-pH 4@pH 10 suggests absence of the DNA phosphate stretch in pH 8 and pH 10 buffer treated specimen, see **Figure 62**.

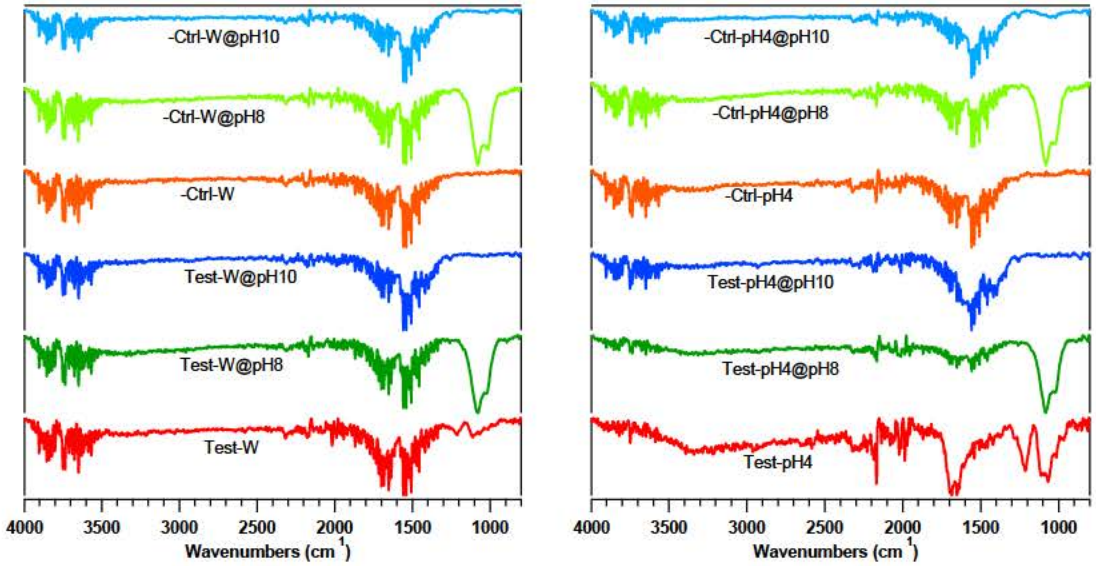

Figure 62. FTIR spectra of DNA showing adsorption and release of DNA from AAUCNPs.

Except for the –Ctrl-pH 4 and –Ctrl-W all specimen shows negative zeta potential. Presence of DNA on UCNP of course lead to negative zeta potential for Test-W and Test-pH 4 specimen, but the UCNP with and without DNA have negative zeta potentials in pH 8 buffer or pH 10 buffer (**Figure 63**). Therefore, no meaningful information can be attained from the zeta potential measurements.

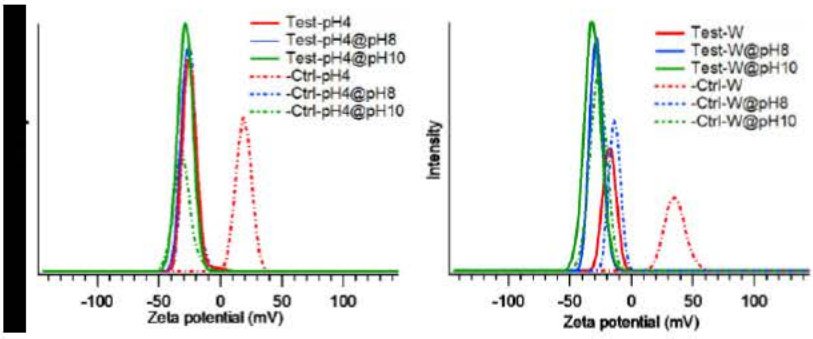

Figure 63. Zeta potential of DNA and AAUCNP solutions.

pH change protocol with developed fingerprints: AAUCNP developed fingerprints were sent from researchers in South Dakota (University of South Dakota (USD)) to New Mexico (New Mexico Tech (NMT)). Three total sets were received: Two sets of developed fingerprints (labeled as developed 1 and developed 2) and one set of undeveloped set containing no nanoparticles. Each set consisted of fingerprints for the left thumb, right thumb, left index and right index. The optimized double swab technique was used to collect DNA from all samples. Next the pH dependence protocol was performed on all developed fingerprint samples to release DNA from the nanoparticles. Concentrations for the samples before pH change protocol and after pH change protocol were taken. Undeveloped samples were also nano-dropped. Only samples after pH change protocol developed left index 2 (DLT-2) and developed right index 1 (DRI-1), had efficient 260/280 ratios. DLI-2 was 12.6 ug/ml and 260/280 of 1.53. DRI-1 was 422.7 ug/ml and a 260/280 of 1.42.

A polymerase chain reaction (PCR) was run to amplify the fingerprint DNA. These results are shown in **Figure 64**. DNA amplification was not seen in any of the fingerprints. It was theorized that the salt content of the samples was affecting amplification. Another theory for lack of amplification was nanoparticle inhibition.

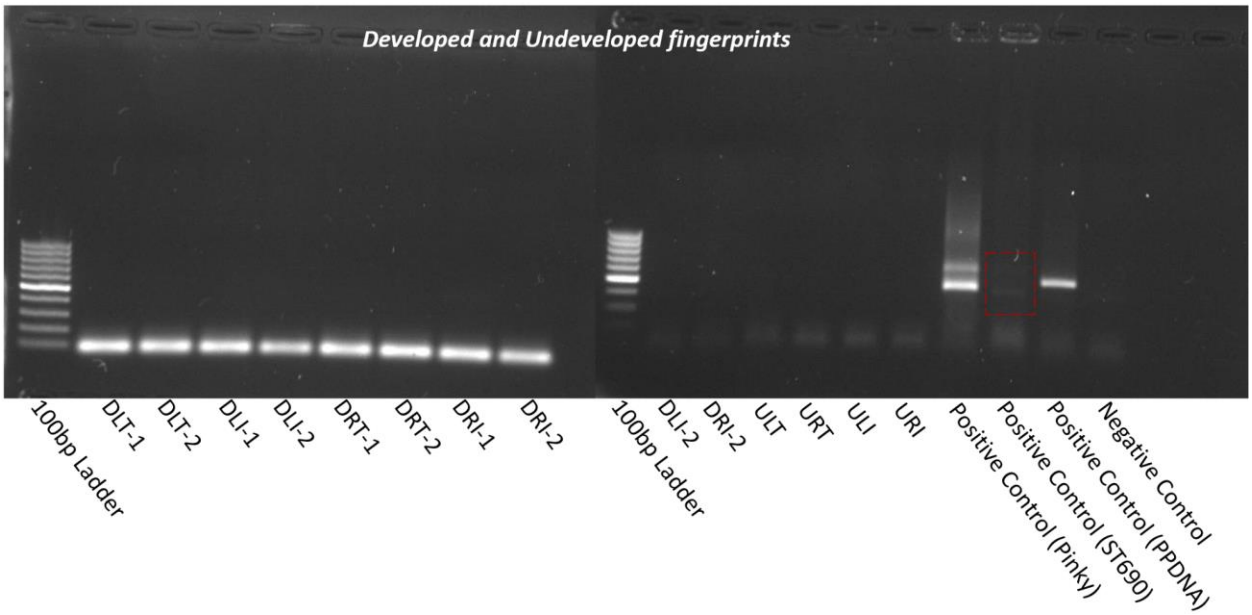

Figure 64. Examining pH change DNA isolation from Developed and undeveloped fingerprints. Labeling of wells: Developed (D), Undeveloped (U), first set of fingerprints (1) and second set (2), LT (left thumb), RT (right thumb), Left index finger (LI), and right index finger (RI). One possibility was that the AAUCNPs inhibited the PCR amplification.

Inhibition test of updated nanoparticles Next, freshly synthesized nanoparticles were sent from USD to NMT. These nanoparticles were tested via pH change protocol. Similar results were expected with amplification of basified supernatant. Three buccal cell samples were tested and recorded as follows: Pinky, PPDNA, and ST690. Positive control was the sample named Pinky. These results are shown in **Figure 65**.

This resource was prepared by the author(s) using Federal funds provided by the U.S. Department of Justice. Opinions or points of view expressed are those of the author(s) and do not necessarily reflect the official position or policies of the U.S. Department of Justice.

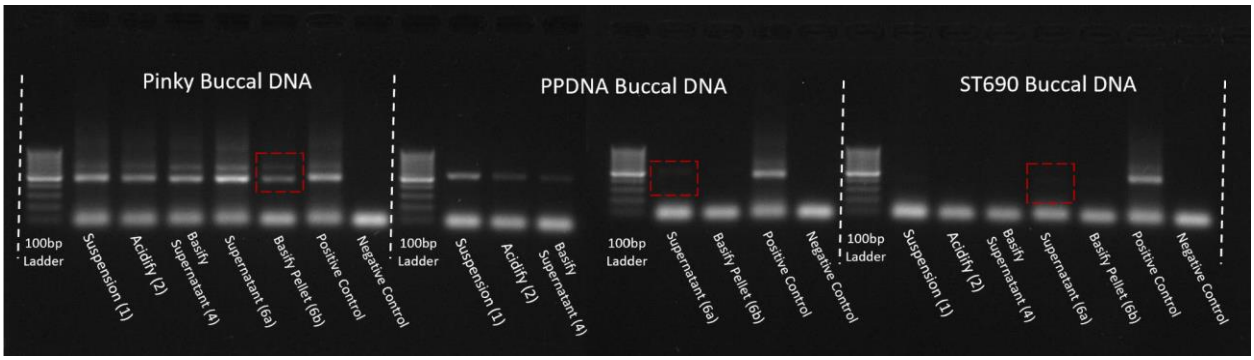

Figure 65. Acetic-acid capped nanoparticle inhibition test.

Amplification was present in each supernatant sample. There is no evidence of nanoparticle inhibition on PCR.

Task Research Summary:

Acetic acid-capped UCNPs (AAUCNPs) appear to bind DNA at pH 4, and to release some DNA at pH 8 and pH 10. However, DNA did not amplify when collected from developed fingerprints via AAUCNPs, this was not due to the presence of the AAUCNPs.

Task 9: Non-Powder Application Methods

Purpose: As dry nanoparticles may present health risks to the user, methods to apply the UCNPs in forms other than a dry powder were examined.

Research: The initial methods examined was placing split pieces of silicon or glass slides both with fingerprints into a bath of UCNPs dispersed in a solvent. Solvents used were toluene and chloroform, which we have previously used to disperse oleic acid-capped UCNPs similar to those used herein. **Figure 66** shows a comparison of fingerprints developed using dispersion of UCNPs in toluene (**Figure 66a**) and chloroform (**Figure 66b**). From **Figure 66**, it appears that toluene develops fingerprints better than chloroform, although more quantifiable results need to be determined to better understand this finding.

In addition to examining the dispersion solvent choice, the concentration of UCNPs in the dispersion was also examined in an attempt to determine the optimal UCNP concentration. Initially, dispersion concentrations of 0.5, 1 and 5 wt% in toluene were evaluated. **Figure 67** shows images of prints developed with 0.5 and 1 wt% UCNP in toluene dispersions. The 5 wt% dispersion was visually indistinguishable from the 1 wt % dispersion. The 0.5 wt% dispersions cleaned of excess UCNPs by dipping in toluene yielded the best visual images, although more quantifiable results need to be determined to better understand this phenomenon.

Soybean Oil Emulsion A second non-powder application technique utilized were emulsions developed for printing applications (Meruga et al., Langmuir, 2018, 34 (4), pp 1535–1541). This emulsion is a soybean oil in water emulsion. The emulsions were made at a nominal concentration of 1.5 wt% UCNPs (0.96 wt% after one day of settling by TGA). These emulsions were sprayed onto split fingerprints. Unfortunately, the soybean oil did not evaporate quickly and left a film on the print (see **Figure 68**) so visualization of latent fingerprints with this emulsion was not possible.

SDS Solution A method developed by M. Wang and published in RSC Advances, *"Latent fingermarks light up: facile development of latent fingermarks using NIR-responsive upconversion fluorescent nanocrystals"*, (Wang, RSC Advances, 2016, volume 6, pp. 36264-36268) was evaluated for applicability to the current project. In the referenced work, sodium dodecylsulfate (SDS) was used to solubilize stearate-coated upconverting nanoparticles (UCNPs) in water. As the UCNPs used in this work are coated with oleate molecules, considerable effort was expended to be able to use this method with the powders made for this grant. The first step in this evaluation

involved using a grinding procedure developed to separate the UCNPs for powder application (crush in mortar with pestle, vortex for 8 hours and pressing between weighing papers). This was followed by stirring the separated UCNP powder into water (one gram UCNPs in 10 ml of water) while sonicating, then mixing this sonicated suspension with an aqueous 3 wt% (0.0104 molal) SDS solution. The resulting mixed solution was stirred for a further 30 minutes, after stirring, some of the UCNPs settled from solution, but fewer settled than from the same procedure without SDS. The final solution was still cloudy, indicating that not all the UCNPs settled.

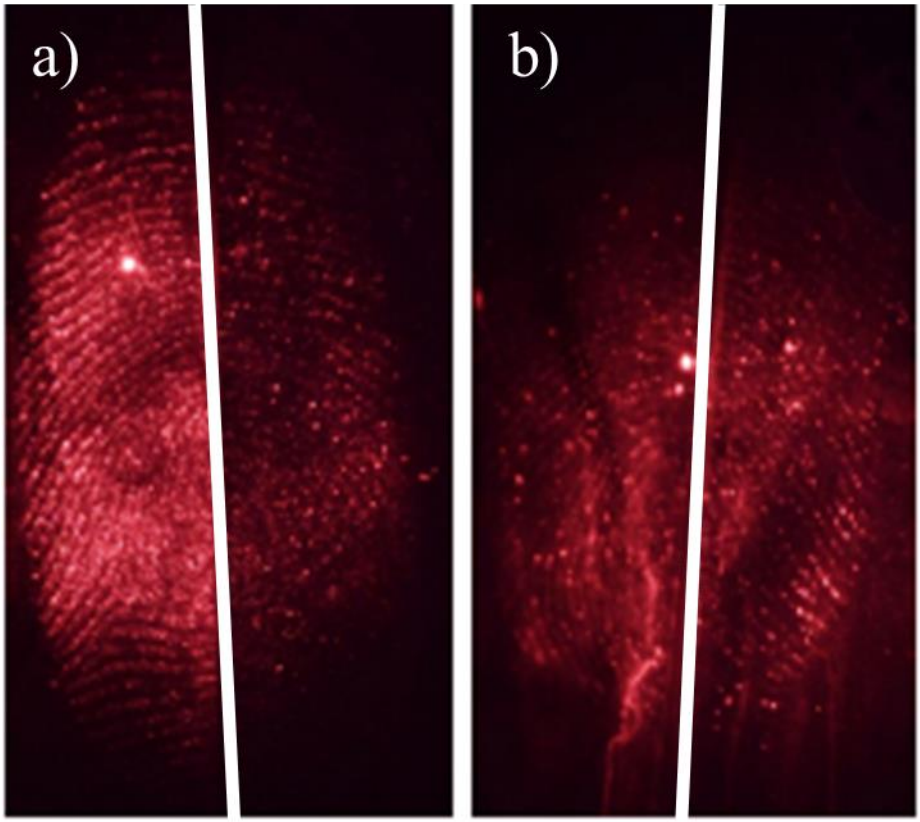

Figure 66. Split fingerprints of 48 nm UCNPs deposited from a) a 1 wt% UCNP in toluene dispersion and from b) a 1 wt% UCNP in chloroform dispersion. In both a) and b) the left split print was obtained by contacting the print with the dispersion for 3 minutes, while the right split print was obtained by contacting the print with the dispersion for 1 minute. Both images were obtained after 1 second of exposure to a 980 nm laser with a laser power density of a) 785 mW/cm^2 and b) 915 mW/cm^2.

To assess the technique, fingermarks were placed on glass slides. These marked glass slides were placed in the SDS/UCNP solution, while stirring, for 30 seconds. The glass slide was then removed from the UCNP/SDS solution, washed carefully with deionized water and dried open to the air at room temperature. Representative images of upconversion from the UCNPs attached to the fingermarks are shown in **Figures 69 and 70**. These images were obtained by illuminating the dried fingermarks with 980 nm laser light, using 1.45 W power and camera settings ISO 400 with f/3.2. **Figure 69** was collected with a 0.5 second exposure, while the exposure for **Figure 70** was 2 seconds.

Examination of **Figures 69 and 70** shows that ridges on the fingermark are observable. The 0.5 second exposure was insufficient to image the entirety of the print. In addition, bright spots, such as those seen in **Figure 69**, were often observed. While the cause of the bright spots has not yet been investigated in detail, one possible cause of these spots is large aggregates of UCNPs that were not removed by washing. These bright spots could make matching of the fingermarks problematic. The upconversion also appears to be non-uniform, which may make identifying minutiae more difficult.

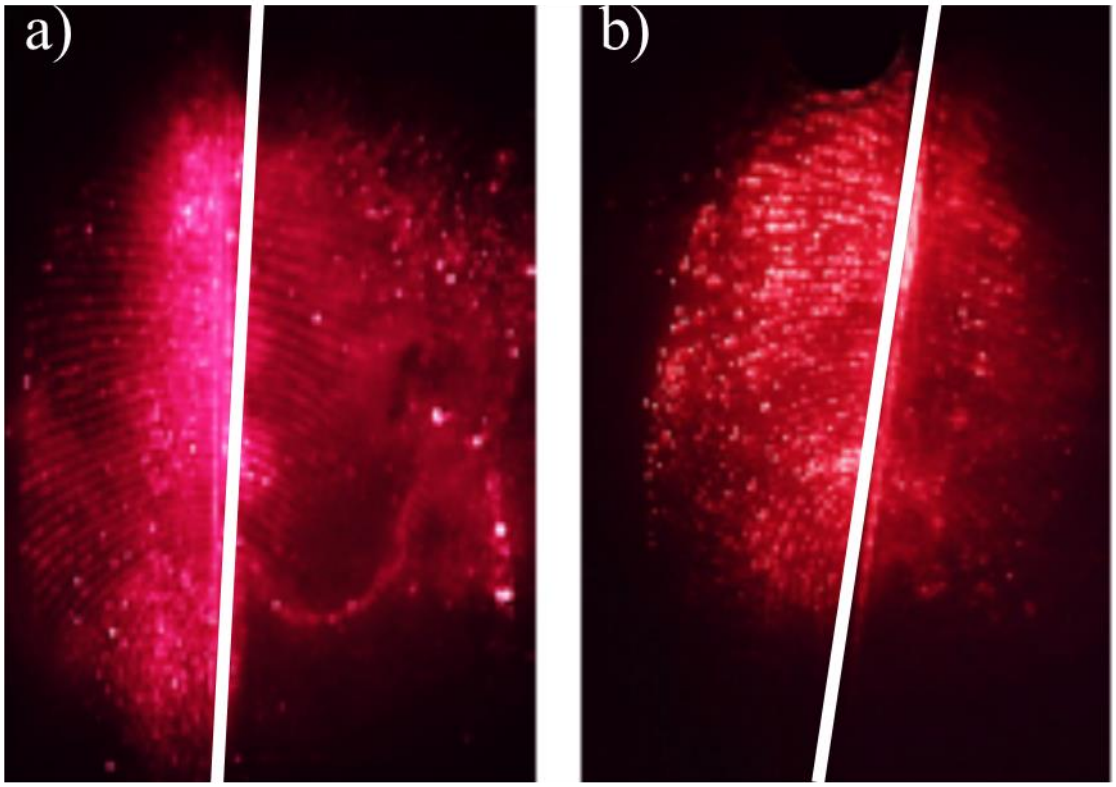

Figure 67. Split fingerprints of 48 nm UCNPs deposited from toluene dispersions with a) 1 wt% UCNPs and b) 0.5 wt% UCNPs. In both a) and b) the left split print was imaged after dipping the print in neat toluene, while the right split print was imaged by spraying the print with neat toluene. Both images were obtained after 0.5 seconds of exposure to a 980 nm laser with a laser power density of a) 600 mW/cm^2 and b) 686 mW/cm^2.

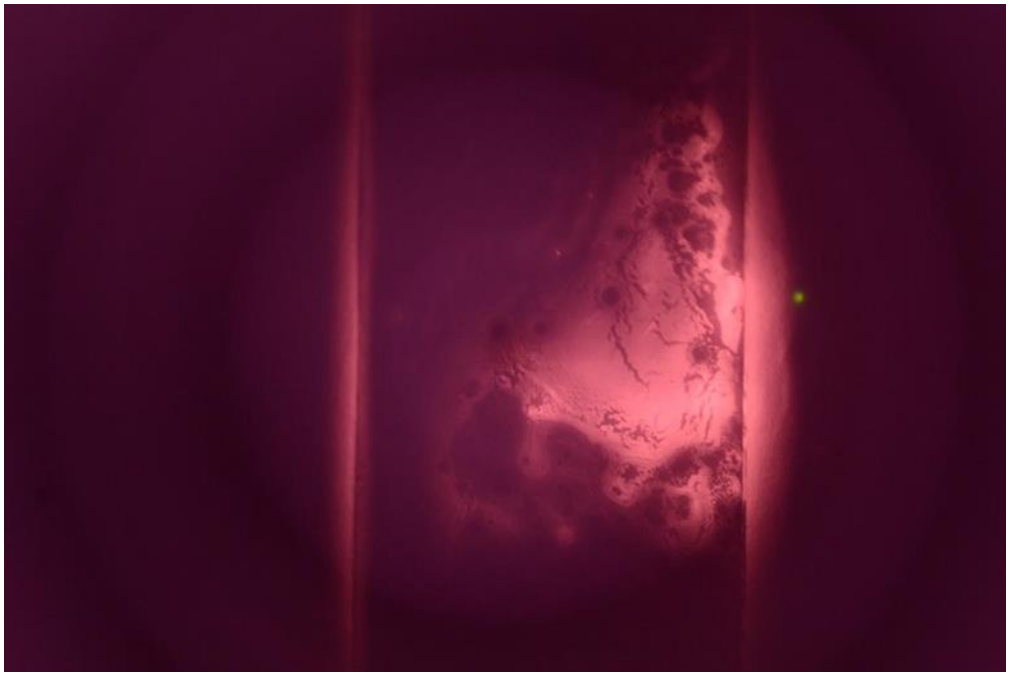

Figure 68. Fingerprint on glass slide substrate developed using UCNP soybean oil in water microemulsion, imaged with 980 nm laser.

Because of these issues, the PIs decided to re-explore use of emulsions to deposit the UCNPs. Emulsions were examined in a previous six month report, but had not worked well as the oil phase used had a tendency to obscure the fingermark. Thus, emulsion formulations were considered with an oil phase that dispersed the oleate coated UCNPs, yielded less residue and would evaporate relatively quickly. Eventually, toluene was chosen as a possible oil phase. A literature review found several possible candidate emulsion formulations. We focused on those stabilized by Tween 80 surfactant.

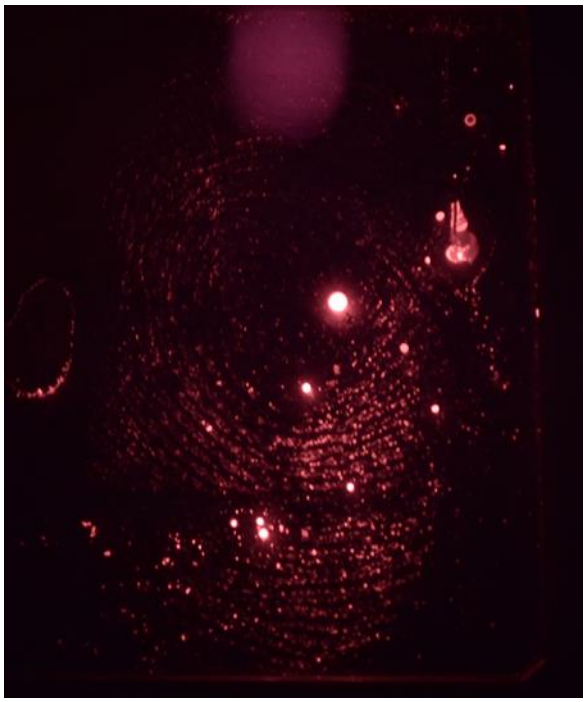

Figure 69. Upconversion image of UCNPs attached to a fingermark with image collection for 0.5 seconds.

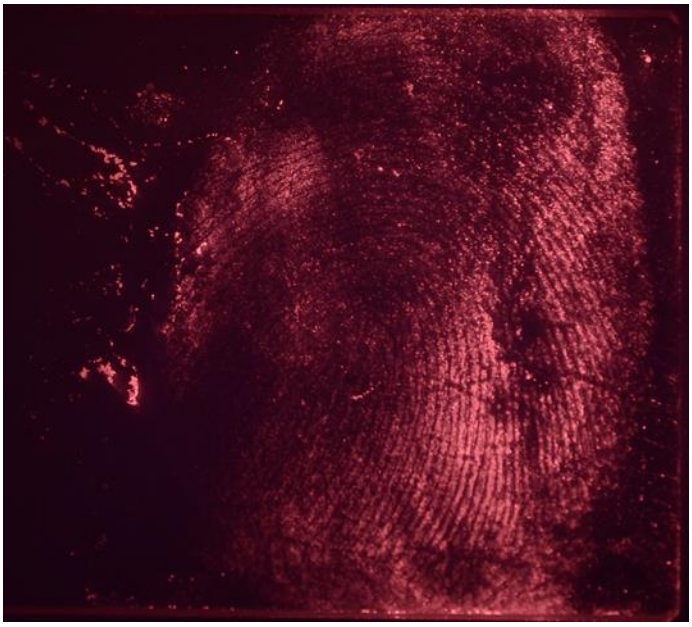

Figure 70. Upconversion image of UCNPs attached to a fingermark with image collection for 2 seconds.

Toluene Emulsion Non-powder application methods were examined in conjunction with a National Science Foundation Research Experience for Undergraduates research. In this work toluene-in-water emulsions were

made as soybean oil-in-water emulsions examined previously left a layer of oil covering the print. Toluene was thought to be a good replacement for soybean oil, as the UCNPs are known to be easily dispersible in toluene, and toluene has a high evaporation rate. To make an emulsion, the surfactants need to have a hydrophilic-lyophilic balance (HLB) specific for each oil. For toluene-in-water, the recommended HLB=15 [ICI Americas, Inc., "The HLB System: a time saving guide to emulsifier selection", published 1980, accessed 7-31-2019, http://www.scientificspectator.com/documents/personal care spectator/The HLB Book ICI.pdf]. One common surfactant that has HLB=15 is Tween 80. Therefore, initial emulsions with 80 % water, 10 % toluene and 10 % Tween 80. UCNPs were added to the toluene at a nominal concentration of 1.5 wt% UCNPs in the emulsion. Some settling of the UCNPs occurred as the emulsion was left standing for 24 hours before use, see **Figure 71**. After the emulsion was formulated and allowed to stand for 24 hours, the weight fraction of UCNP found by thermogravimetric analysis was 0.26 wt%. The emulsion droplets were found to be 350 ± 70 nm in diameter. This emulsion did not work particularly well for print analysis, likely due to the low amount of UCNPs present.

Better results were obtained using an emulsion with 70 % water, 20 % toluene (including 1.5 wt% UCNPs) and 10 % Tween 80. A new sonicating tip was also used for this emulsion allowing for longer sonication. Fingerprints were developed by dipping in the emulsion for up to one minute and then imaging before and after rinsing the substrate with non-UCNP containing toluene-in-water emulsions (see **Figure 72a**), as shown in **Figure 72c**. Pure toluene was also tried as a rinsing agent, but have not yet yielded sufficient fingerprint detail (**Figure 72b**).

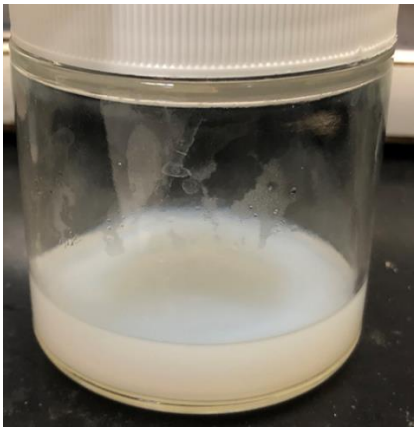

Figure 71. Toluene-in-water emulsion after 24 hours of settling. Some UCNP settling is observed.

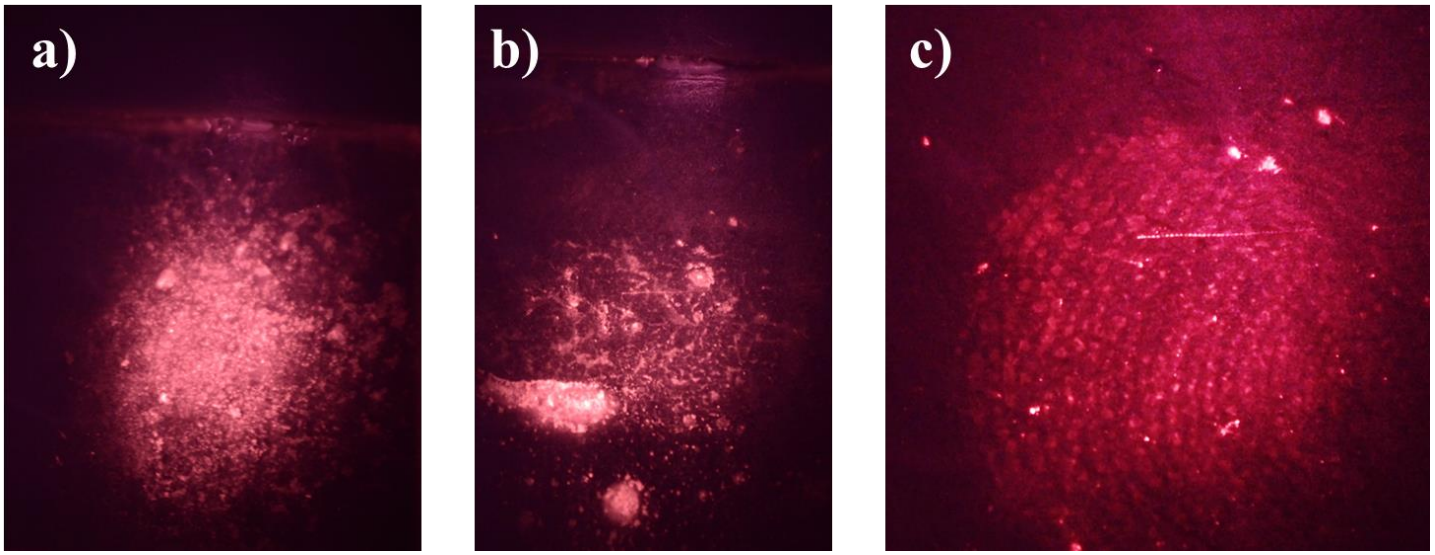

Figure 72. Fingerprints developed using UCNP containing toluene-in-water emulsion. a) unrinsed developed fingerprint little fingerprint detail is observable; b) fingerprint rinsed in pure toluene, some ridges are observable; c) developed fingerprint rinsed in particle-less toluene-in-water emulsion, ridges are more easily observable.

Tape Application Non-powder application methods were examined in conjunction with a National Research Traineeship grant. As application of UCNPs using emulsions had given results that were not particularly promising, the research shifted to examining tape application methods. The goal in this work is to apply UCNPs to a tape product, apply the UCNP/tape to the fingerprint and have the UCNPs transfer to the fingerprint from the tape. It is likely that there is an optimal level of tape adhesion strength for this to occur. While the initial tape adhesion strength is sometimes known, the effect of the method of putting the UCNPs onto the tape on the adhesion strength of the tape is important to know. The first application method to be examined was printing as the research team has a history in printing these UCNPs from toluene solutions. In addition, printing can be performed such that large areas can be covered rapidly.

Initial work in this area has involved obtaining a series of tapes having varying backings and adhesion strengths then testing these tapes with toluene to understand whether toluene, the primary component of the ink to be used, alters the adhesive strength of the tape. Pure toluene was printed with a Sono-Tak printer and a piece of tape is covered with the toluene ink. The ink treatment of the tape was, in some cases, performed multiple times. The toluene is allowed to evaporate, and after the final toluene treatment the tape is removed applied to a piece of cardboard and the adhesion estimated for both the treated piece of tape and an untreated piece of tape. The tapes used and the results are shown in **Table 6**. In general, for the tapes tested thus far, up to 16 toluene treatments do not greatly affect the adhesion strength of the tape, nor do these treatments destroy the tape backing materials.

An important aspect of this work is to find methods by which the upconverting nanoparticle powders (UCNPs) can be used to develop latent fingerprints using the UCNPs in a manner that is not dry powder. Dry nanopowder may pose health risks for users. Previously, we had examined emulsions as a possible delivery method. More recently, we have focused on tape-based and direct write printed application methods. In addition, we switched to a polyvinyl chloride (PVC) cards as the fingerprint substrate to improve UCNP visualization. The first step in using these cards is to determine if they exhibit any 800 nm light under 980 nm illumination. These tests results are shown in **Figures 73-75**. The card by itself after tape contact nor the card after tape contact or printing followed by rinsing or fingerprint brushing exhibited significant light at 800 nm.

Satisfied that the PVC card should work well, the next step was to include UCNPs. For the tapes used, UCNPs were added by printing 10 passes of the UCNPs using the Sono-tek printer with a 1 wt% UCNP ink in toluene. In addition, the UCNPs were directly printed onto the fingerprint. As **Figures 76-78** indicate, neither a five second toluene rinse, nor a five second brushing were sufficient to reveal the fingerprints.

To investigate this further as the initial trials were inconclusive, the tape-based application was stopped and various experiments were performed using Sono-tek printing to add UCNPs to the fingerprint. The first area tested was the number of printing passes used to deliver UCNPs to the fingerprint followed by toluene rinsing or brushing. As five passes were inconclusive, fewer passes were tested. Figure 79 shows these results for a five second toluene rinse of either one or four passes (layers). The rinse clearly removes UCNPs as indicated by the decrease in color intensity, but no fingerprints are observed. **Figure 80** shows similar results for brushing with a standard fingerprint brush. While some removal occurred, this did not successfully reveal any fingerprints. As soaking in toluene had been successful in delivering UCNPs to fingerprints, the procedure was modified to allow for longer contact of the UCNP printed fingerprint with toluene. **Figure 81** shows the results for using a small droplet pool of toluene for up to two minutes, while **Figure 82** shows the results for soaking in toluene for up to three minutes. Again, UCNPs were likely removed but no fingerprints are apparent. As **Figure 83** shows, fingerprint ridges are observable after a two minute toluene soak under oblique visible lighting.

Table 6. Tapes, Adhesive Strength, Toluene Treatments and Effects.

Brand	Part Number	Type	Peel Strength	Similar 3M Product Number	Similar Product Peel Strength	Tested (Toluene Passes)	Result
3M	2080	Masking (Delicate)				7	No noticeable difference from fresh tape
3M	2090	Masking				16	
3M/Scotch	3650	Packaging		309	8 N/ 25 mm	16	
universalop.com		Masking Tape				16	
3M	2979	Duct		1900	15.0 N/ 25 mm	16	
3M/Scotch	810	Regular Scotch				16	
3M/Scotch		Low Tack Artist Tape				16	
3M/Scotch		Foam Mounting Tape				7	
Blue Hawk		Painters Tape				16	
3M	8979	Outdoor Clean-Release Duct Tape	5.3 N /25mm				
3M	471	Floor Marking Tape (Vinyl)	25 N / 100 mm				
3M	Super 33+	Electrical Tape		471	25 N/100 mm		
3M/Scotch	2090	Masking Tape					
3M/Scotch	232	Masking Tape					
McMaster-Carr		Conductive Aluminum Foil Electrical Tape		1436	12 N/100 mm		
Saint-Gobain		Low-Friction Uhmw Tape		5423	39 N/100 mm		
3M	VHB 4905	Optically Clear Foam Mounting Tape					
3M	924	Glue-On-A-Roll	5 N/cm				
3M	928	Glue-On-A-Roll Repositionable					

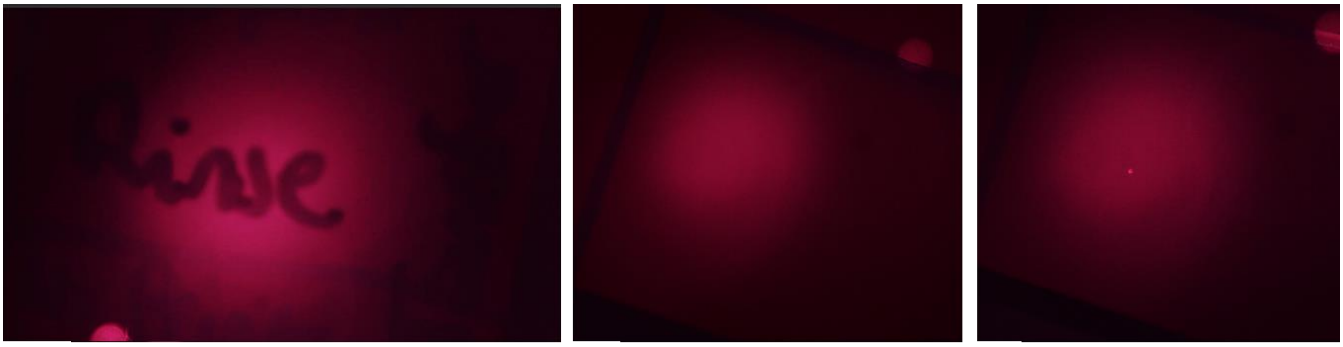

Figure 73. PVC card after contact with low tack artists tape having no UCNPs and then rinsed or brushed.

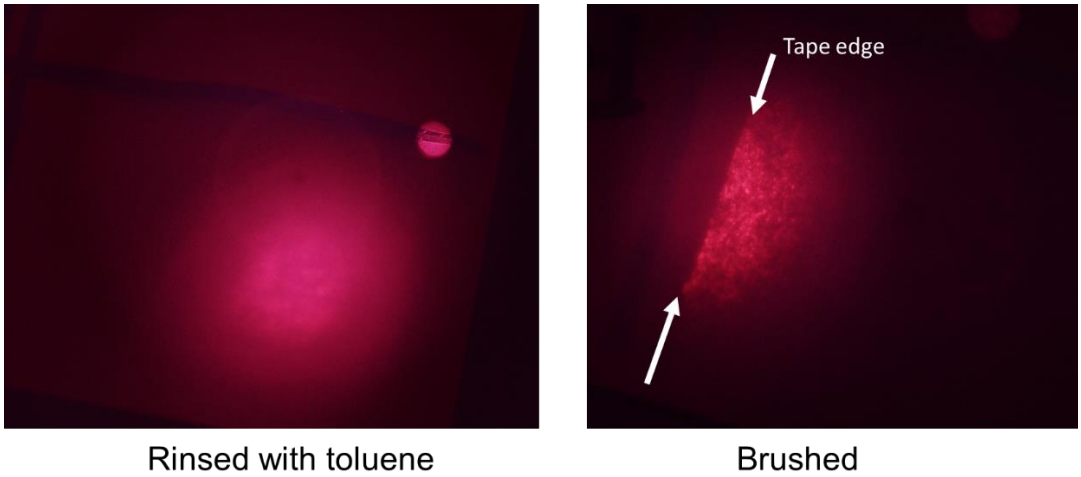

Figure 74. PVC card after contact with painter's tape having no UCNPs and then rinsed or brushed.

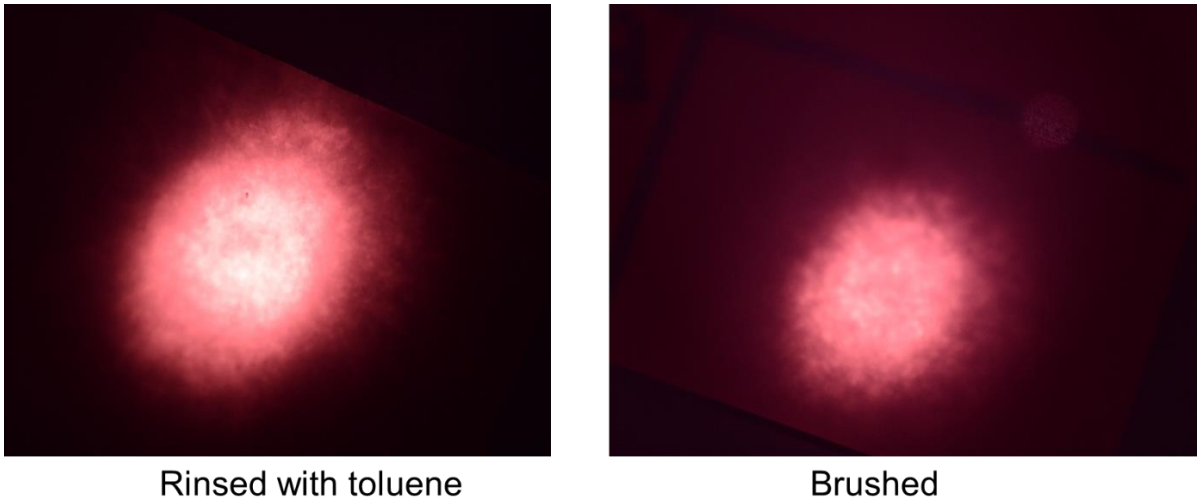

Figure 75. PVC card after Sono-tek printing of toluene having no UCNPs and then either rinsed or brushed.

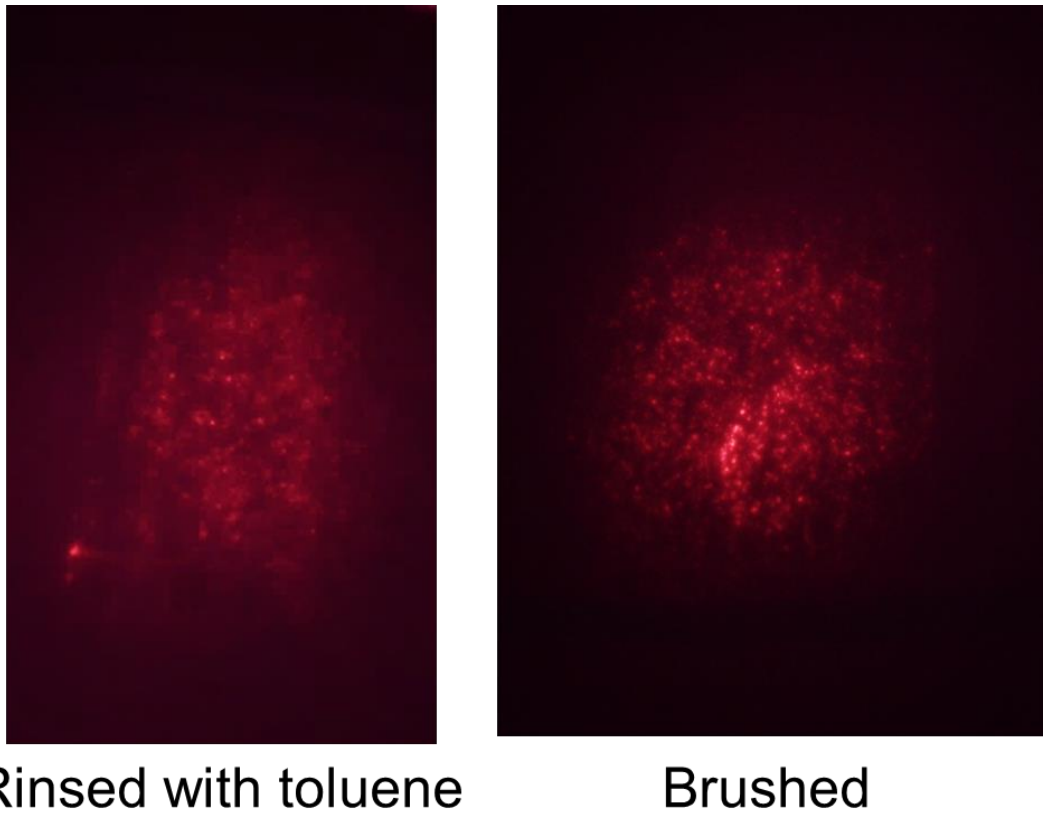

Figure 76. PVC card with a fingerprint after contact with low tack artists tape having UCNPs and then either rinsed or brushed.

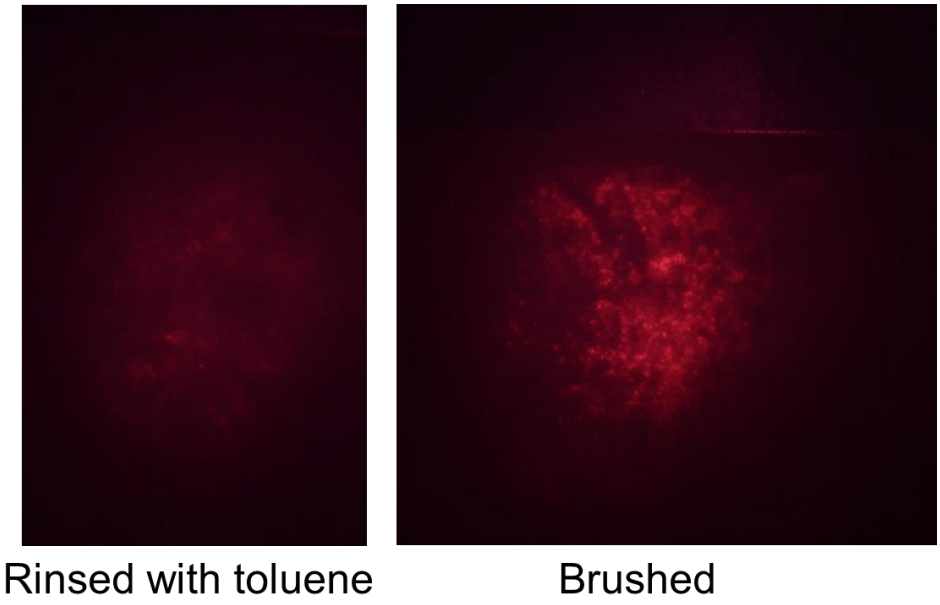

Figure 77. PVC card with a fingerprint after contact with painter's tape having UCNPs and then either rinsed or brushed.

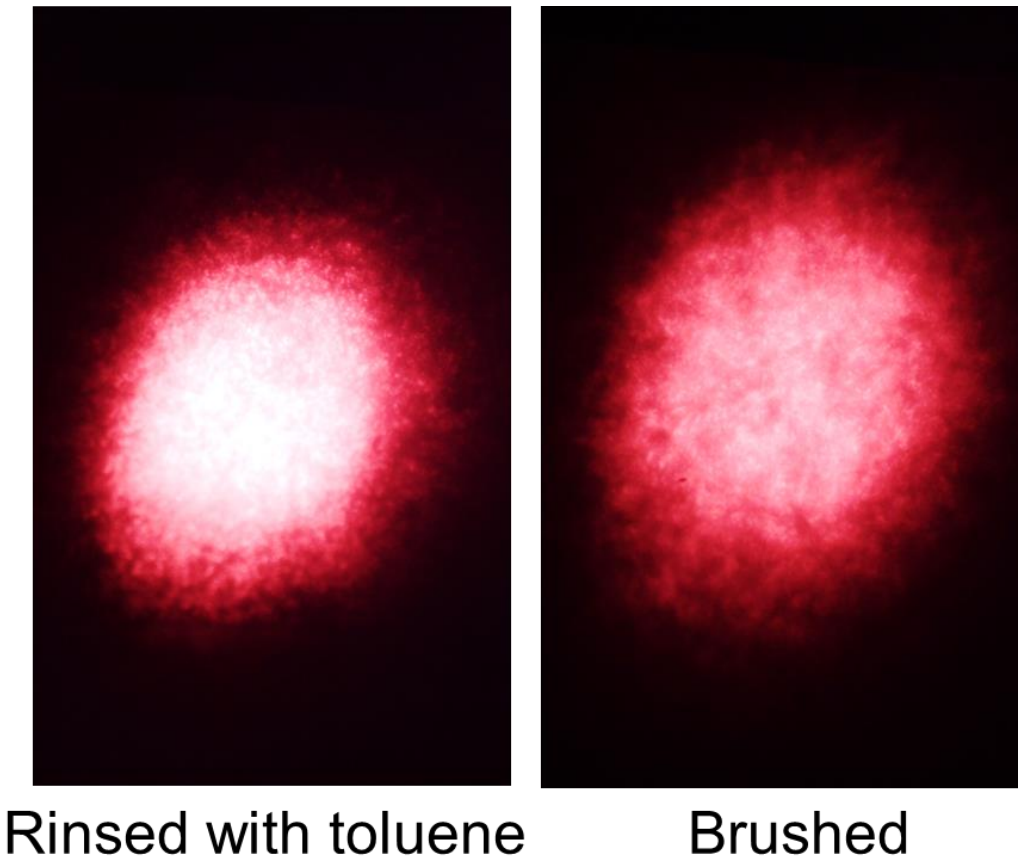

Figure 78. PVC card with a fingerprint after Sono-tek printing of five passes of a toluene solution with 1 wt% UCNPs and then either rinsed or brushed.

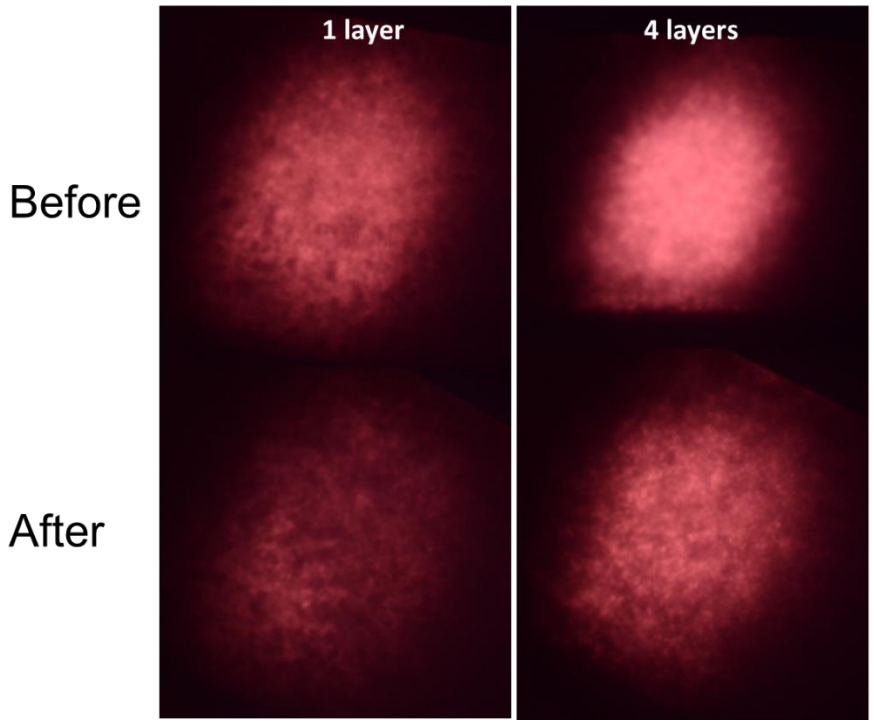

Figure 79. PVC card with a fingerprint after Sono-tek printing of toluene with 1 wt% UCNPs. The number of layers indicates the number of times the print head passes over the fingerprint. After indicates the fingerprint with UCNPs was rinsed in toluene for five seconds to help remove unattached UCNPs.

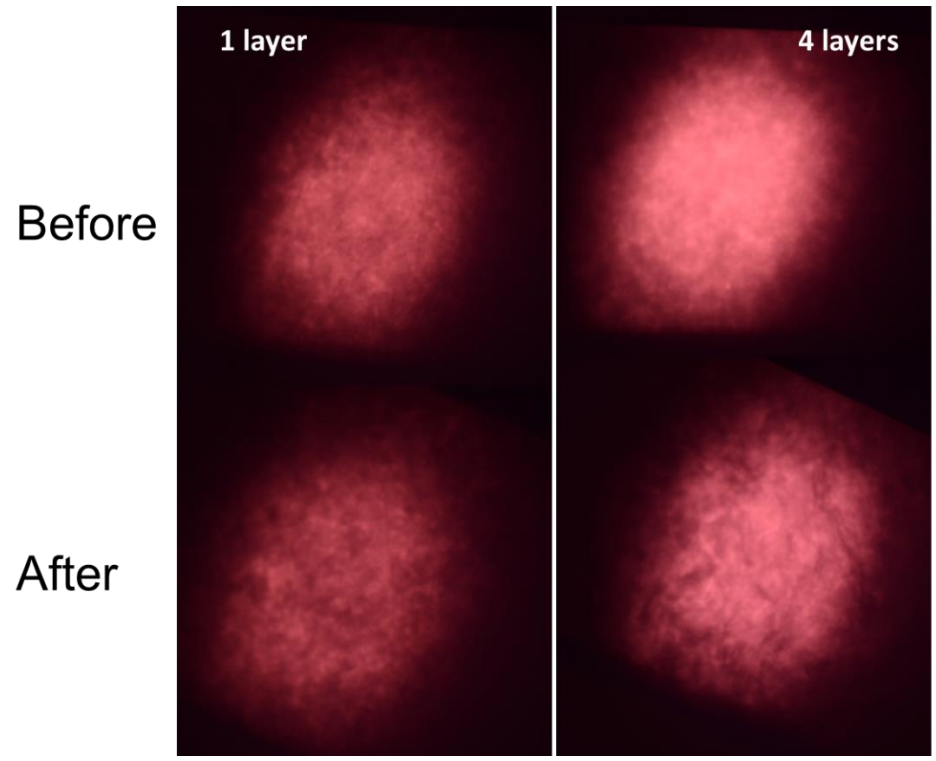

Figure 80. PVC card with a fingerprint after Sono-tek printing of toluene with 1 wt% UCNPs. The number of layers indicates the number of times the print head passes over the fingerprint. After indicates the fingerprint with UCNPs was rinsed in brushed for five seconds to remove excess UCNPs.

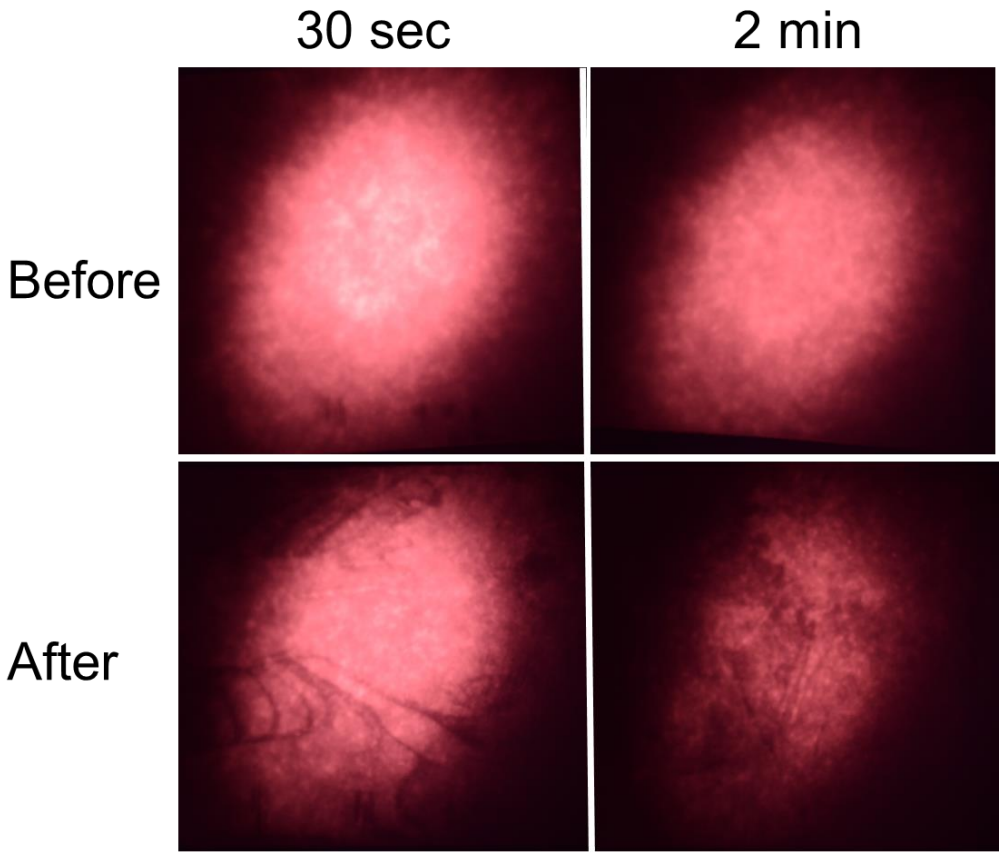

Figure 81. PVC card upconversion from a fingerprint after Sono-tek printing of toluene with 1 wt% UCNPs. Two layers of UCNPs were printed over the fingerprint. After indicates the fingerprint with UCNPs was rinsed in toluene and a drop of toluene was allowed to pool on the print for the indicated time to help remove unattached UCNPs.

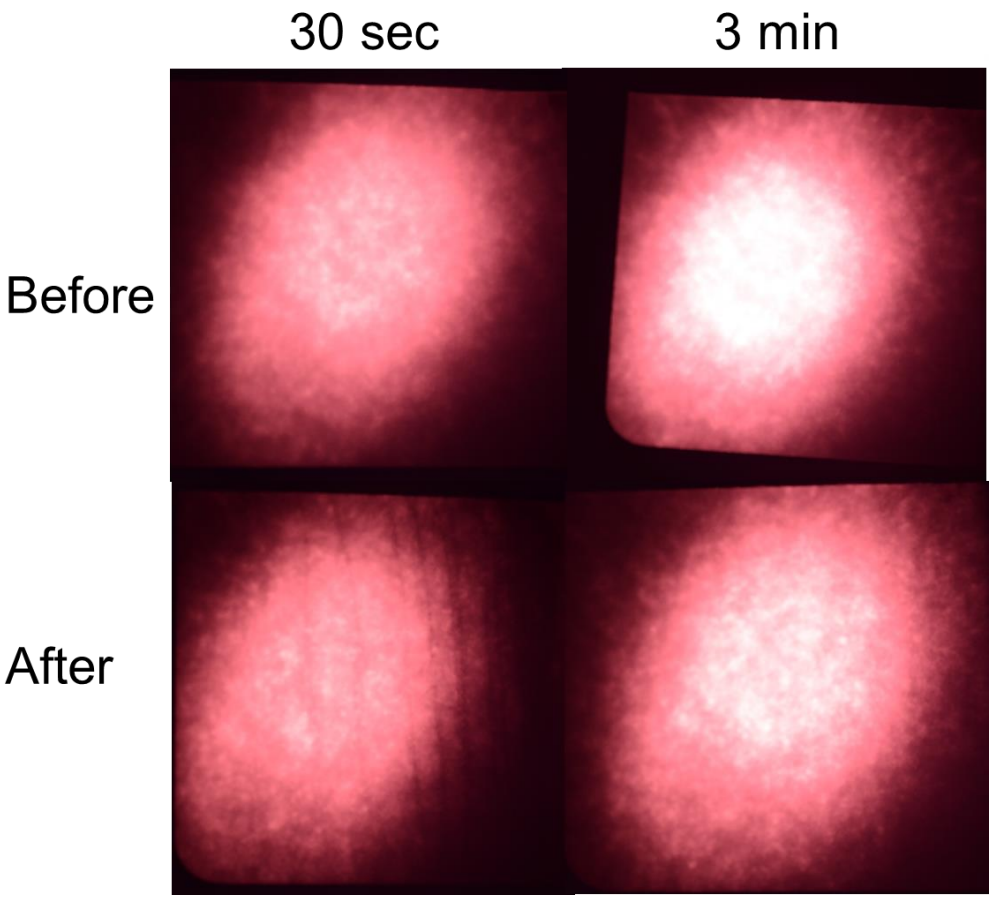

Figure 82. PVC card upconversion from a fingerprint after Sono-tek printing of toluene with 1 wt% UCNPs. Two layers of UCNPs were printed over the fingerprint. After indicates the fingerprint with UCNPs was soaked in toluene for the indicated time to help remove unattached UCNPs.

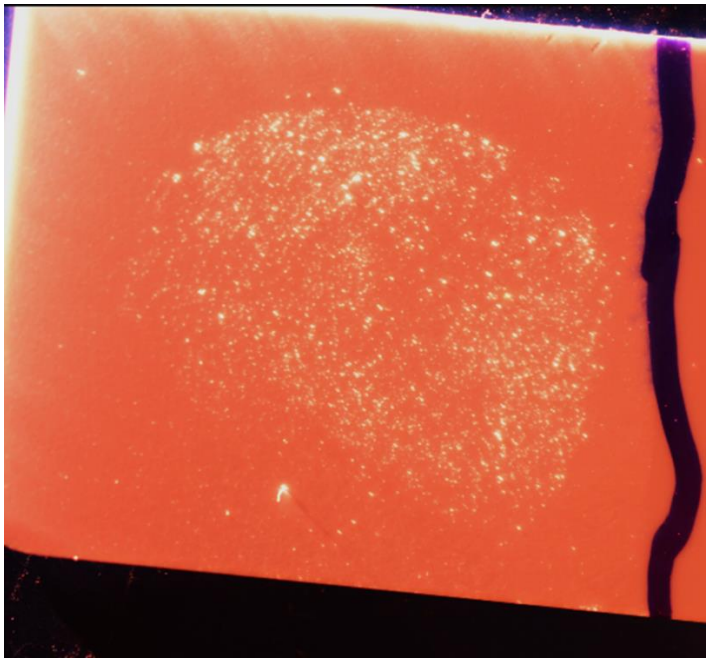

Figure 83. PVC card upconversion from a fingerprint after Sono-tek printing of toluene with 1 wt% UCNPs. Two layers of UCNPs were printed over the fingerprint. After indicates the fingerprint with UCNPs was soaked in toluene for two minutes to help remove unattached UCNPs.

With tape application we next focused on direct write printed application methods. While this has yet to be fully successful, as we have battled problems with removing the printed particles from the fingerprints following deposition of the upconverting nanoparticles (UCNPs), see **Figure 84**. In addition, as the DNA may be able to be collected using acetic acid-capped UCNPs (AAUCNPs), we have investigated non-powder based methods for AAUCNP application to fingerprints. The main issue in this portion of the work appears to be that the AAUCNPs prefer to stay dispersed in the solvents rather than deposit on the fingerprints, see **Figure 85**.

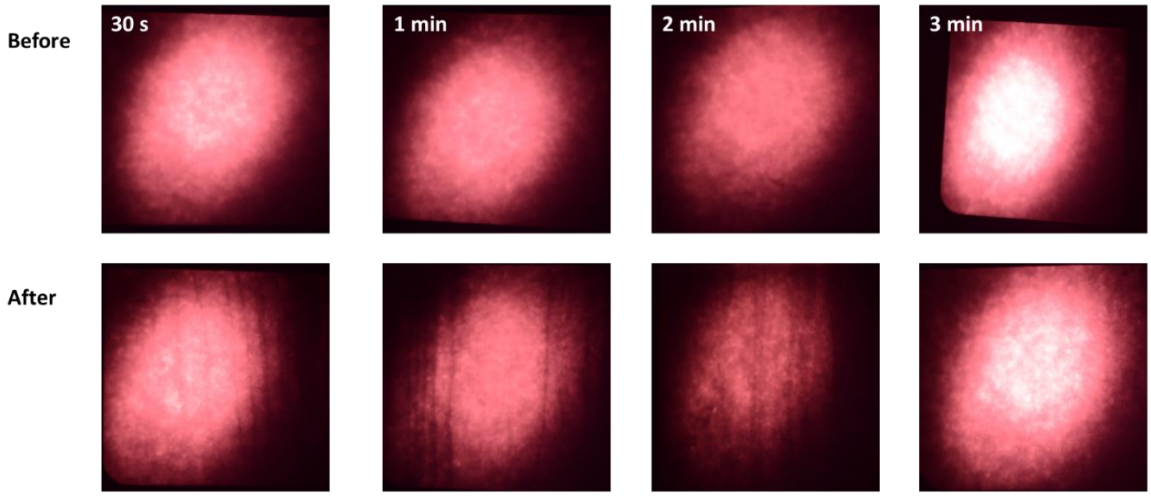

Figure 84. Laser upconversion of oleic acid-capped UCNPs (OAUCNPs) direct write printed onto fingerprints before and after rinsing in toluene. The times show the amount of rinsing time used. Little change is observed in the amount of upconversion.

Figure 85. Laser upconverted images of 1 wt% AAUCNPs deposition after 45 seconds in water solution. The text on each image indicates attempts to remove un-fingerprint attached AAUCNPs. Little upconversion is observed.

A Sono-Tek ultrasonic printer was used to apply the UCNPs usually at 0.25 wt% in toluene. The angles used were 30, 45 and 60 degrees from flat, as shown in **Figure 86**. The results for one set of fingerprints are shown in **Figure 87.**

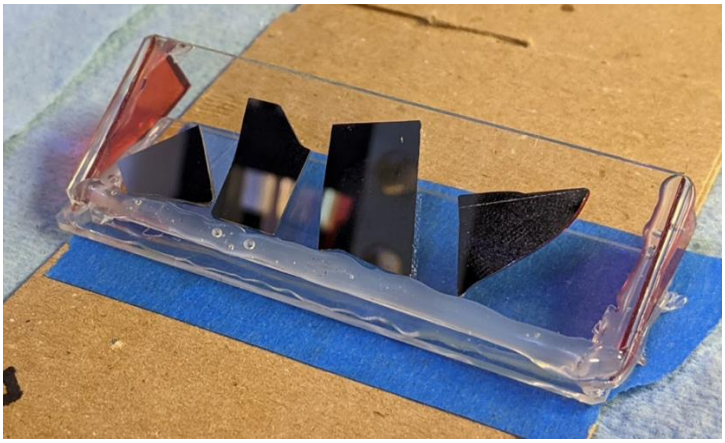

Figure 86. Fingerprint laden silicon wafer samples tilted at 30 degrees to flat prior to UCNPs being applied.

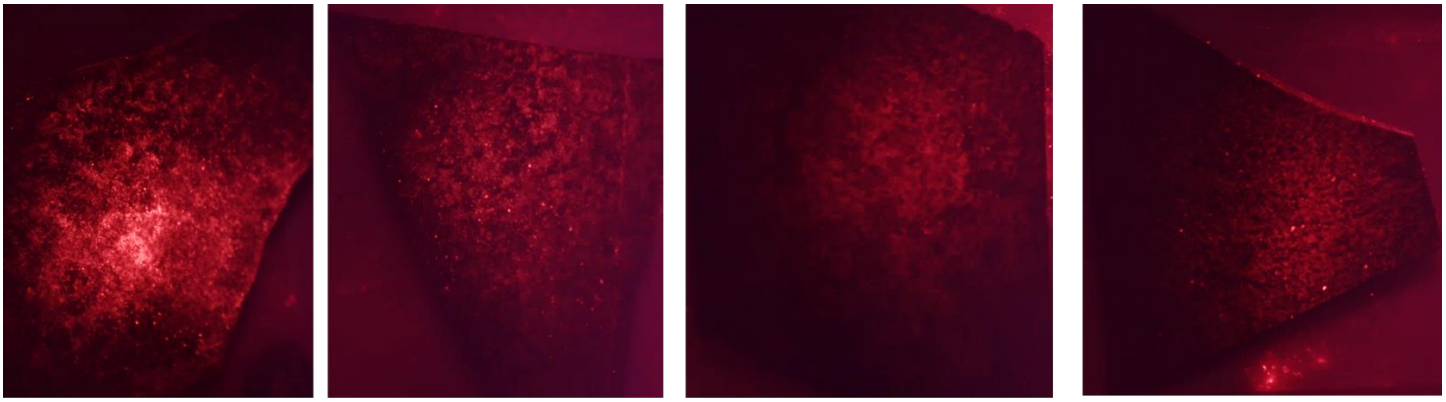

Figure 87. Developed fingerprints after UCNP application and rinsing. The numbers under the pictures represent to angle at which the UCNPs were applied.

The results from the use of angling the samples show that there was a little help to fingerprint development with angling, but that this was not particularly significant.

In addition, fingerprints were placed onto silicon wafers and examined by scanning electron microscopy (SEM) prior to being exposed to UCNPs. **Figures 88-92** show there was sometimes some deposited crystals, likely NaCl, and that the silicon substrate sometimes exhibited a film after cleaning.

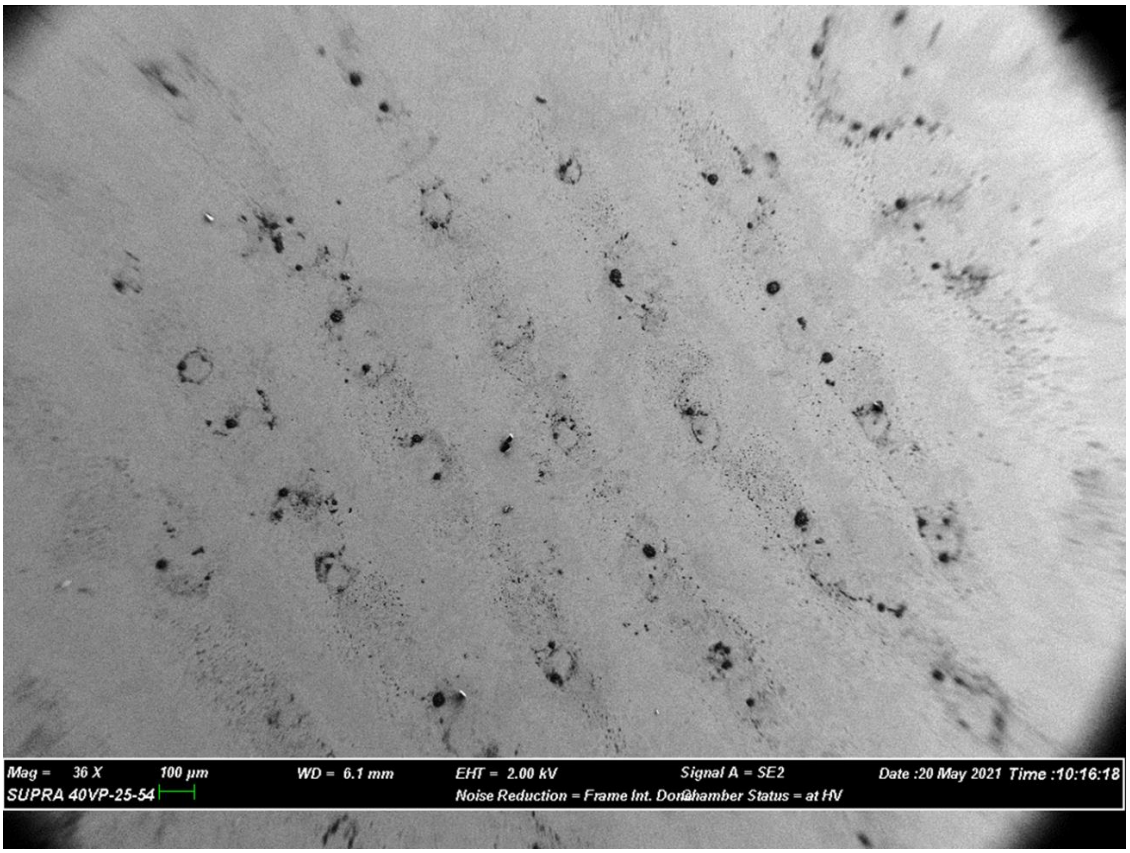

Figure 88. Undeveloped fingerprint on silicon prior to rinsing. SEM image taken at 2 kV exciting voltage and 36x.

Figure 89. Undeveloped fingerprint on silicon after a five second toluene rinse. SEM image taken at 1 kV and 88x magnification. Some crystals are observed on this image. In addition, the area between the ridges is much clearer after rinsing in toluene.

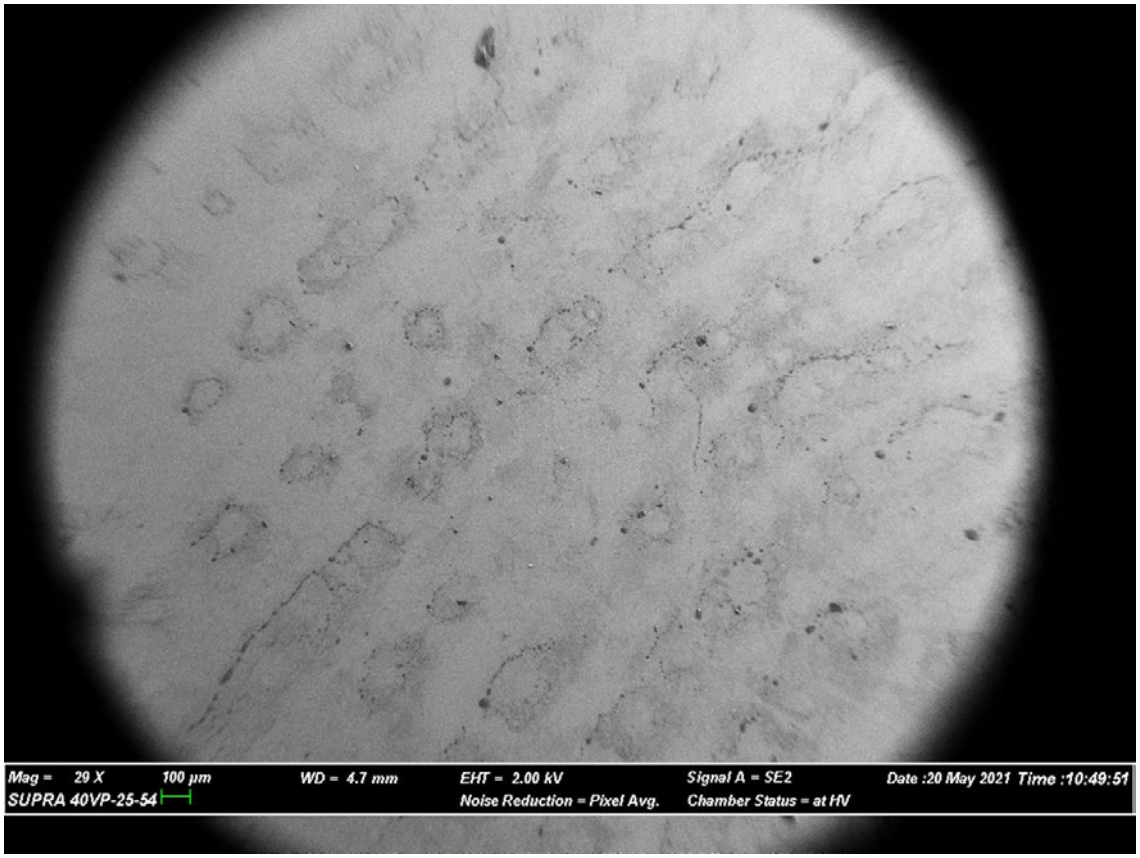

Figure 90. Undeveloped fingerprint after being sprayed with toluene by the Sono-Tek printer and rinsed for five seconds with toluene. Print is much cleaner than the original print (**Figure 88**) and the treatments did not remove the deposited fingerprint. Image obtained at 29x and 2 kV.

Figure 91. Undeveloped fingerprint after Sono-tek treatment and toluene rinse at one kV. The low voltage used allows greater surface sensitivity and much excess material can be observed here.

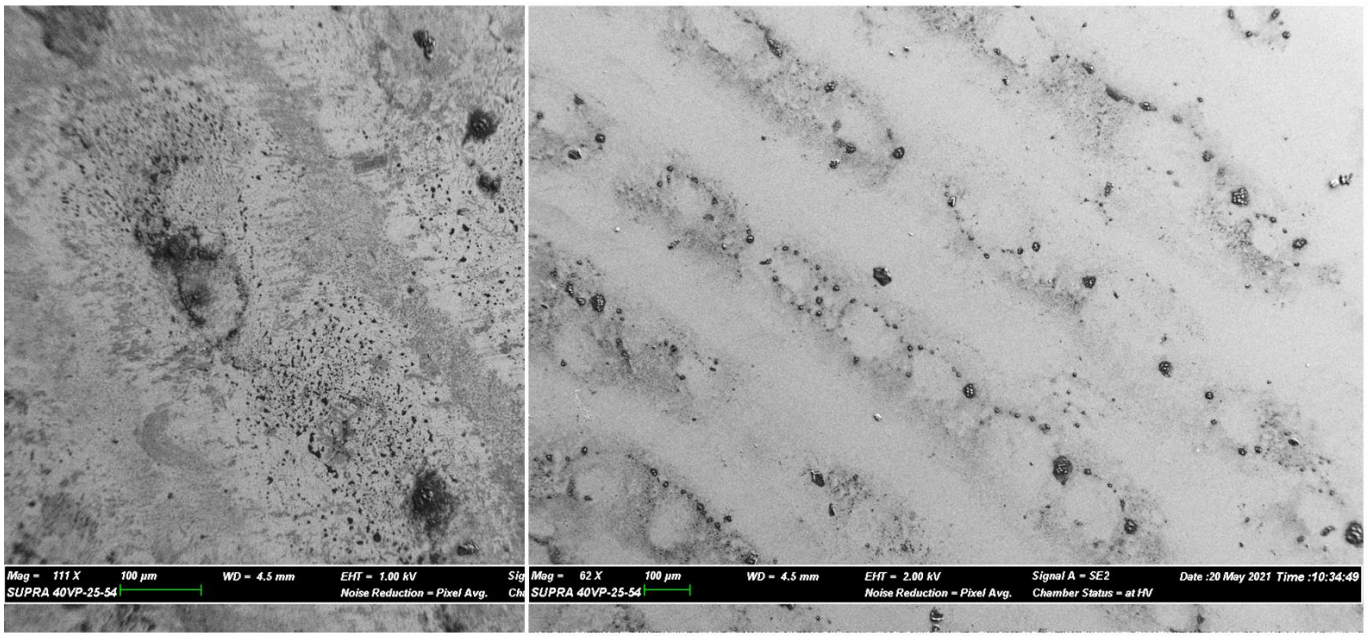

Figure 92. Undeveloped fingerprint comparing before rinsing with toluene (left) and after rinsing with toluene (right). The right image is much cleaner.

Task Research Summary: A variety of non-powder application methods were tested. These methods imclude dipping a substrate having a fingerprint in a solution containing UCNPs, spraying an emulsion containing UCNPs on the fingerprint, and applying UCNPs via tapes. Unfortunately, these methods either did not work well (emulsions and tape application) or are impractical for many types of samples (solution dipping).

Task 10: Data Collection and Analysis/Complete System Development

Purpose: The data collection and analysis were primarily focused on developing software techniques for developing and identifying fingerprints using a mobile phone particularly with respect to minutiae identification, while the complete system development focused on building reader systems capable of stimulating and collecting upconversion images for collecting fingerprint images

Research:

Minutiae Identification NBIS Software was created by the National Institute of Standards and Technology (NIST) for automated fingerprint recognition. This software works by extracting and using level 2 features (from fingerprint images to compare and match fingerprints. The NBIS Software does a great job of extracting minutiae and matching fingerprints. Therefore, we are using it as a benchmark to evaluate the performance of our methods.

Specifically, the tool that extracts the minutiae in this software is called MINDTCT, which creates an intermediate file containing the details of all the extracted minutiae from the fingerprint image. It will generate a .xyt file containing the positions and orientations of all minutiae extracted. It takes the .xyt files generated by MINDTCT, and then computes a score indicating how well two images match to each other. The output of the BOZORTH3 algorithm for a single pair of fingerprint image is shown below:

58 mindtctOutput/notBlurred_0_1532_1.xyt mindtctOutput/1532_12.xyt

In the above example, the first number indicates the matching score between the two fingerprints. The following two file paths are the names and the filepaths of the images being compared. Although the output of a single match is straight forward, it can be difficult and time consuming to analyze the matching results when running the software on larger datasets for testing purposes. An example of this is shown in **Figure 93**.

```
499 mindtctOutput/notBlurred_0_1532_1.xyt mindtctOutput/1532_1.xyt
58 mindtctOutput/notBlurred_0_1532_1.xyt mindtctOutput/1532_12.xyt
556 mindtctOutput/notBlurred_0_1532_10.xyt mindtctOutput/1532_10.xyt
60 mindtctOutput/notBlurred_0_1532_10.xyt mindtctOutput/1532_6.xyt
541 mindtctOutput/notBlurred_0_1532_11.xyt mindtctOutput/1532_11.xyt
58 mindtctOutput/notBlurred_0_1532_12.xyt mindtctOutput/1532_1.xyt
499 mindtctOutput/notBlurred_0_1532_12.xyt mindtctOutput/1532_12.xyt
499 mindtctOutput/notBlurred_0_1532_13.xyt mindtctOutput/1532_13.xyt
87 mindtctOutput/notBlurred_0_1532_13.xyt mindtctOutput/1532_2.xyt
634 mindtctOutput/notBlurred_0_1532_14.xyt mindtctOutput/1532_14.xyt
55 mindtctOutput/notBlurred_0_1532_14.xyt mindtctOutput/1532_3.xyt
```

Figure 93. Matching results example output from BOZORTH3 algorithm.

The above example shows part of the matching results when two small datasets were being compared against each other. This format makes it difficult and time consuming to analyzing the results when run against larger data sets. To solve this problem, a small program was written to analyze and compile the above results into a more readable format. **Figure 94** shows an example of part of the output produced by this tool.

The creation of this tool will help expedite verification of the matching results from testing. In addition, it will greatly assist the research time in testing and validating any changes made to the software of the automated fingerprint recognition system.

The proposed minutiae extraction method has successfully extracted various types of minutiae by thinning the ridges of an enhanced fingerprint image and then scanning them using predefined 3 by 3 masks. While this process was able to identify most of the valid minutiae in the fingerprint image, it also resulted in the identification of some false minutiae. In order to reduce the number of false minutiae, the current work is focused on using convolutional neural networks to verify the minutiae extracted from the algorithm described above. Next, we created a dataset of 1000 manually labeled images sample of true and false minutiae. Each image is at the size of 50 by 50 pixels with unthinned ridges. The examples of true and false minutiae are shown in **Figure 95**.

```
================================================================
Summary of Results
----------------------------------------------------------------
Correctly identified 96% of all correct matches
  Identified 58 of 60 correct matches
Failed to identify 3% of all correct matches
  Failed to identify 2 of 60 correct matches
Falsely identify 19% of all generated fingerprint matches
  Falsely identified 14 of all 72 generated fingerprint matches

Matching of fingerprint images to the same fingerprint image
----------------------------------------------------------------
Successfully matched 100% identical fingerprint images
  Successfully matched 26 of 26 identical fingerprint images
Failed to match 0% identical fingerprint images
Failed to match 0 of 26 total matches for the control
```

Figure 94. Output from tool created to aid in analyzing results from BOZORTH3 matching results on datasets.

(a) (b) (c) (d)

Figure 95. Examples of true minutiae (a, b) and false minutiae (c, d).

This dataset has been used to train a convolutional neural network (CNN) to classify images as either true minutiae or false minutiae. The preliminary results show that a great portion of false minutiae can be eliminated from the features in **Figure 96**.

(a) (b)

Figure 96. Extracted minutiae (a) before CNN verification (b) after CNN verification.

In order to further improve the accuracy and generality of the minutiae extraction, we are currently experimenting CNN verification of thinned and unthinned images at size of 25 by 25 pixels to find the optimal parameters for the methods.

In addition to the minutiae's (x,y) coordinates in the fingerprint image, the BOZORTH3 algorithm also requires the orientation angle for each minutiae. The angle of orientation as specified by the ANSI/NIST standard is marked as angle "A" in the illustration below.

The next step is to compute the minutiae orientation using the following algorithm. Thinned fingerprint images (the image where the ridges in the fingerprint were thinned down to 1 pixel wide) will be used. In order to find the minutiae orientation angle for ridge endings, 2 reference points will be use. The coordinate of the minutiae will be the first reference point (x_1, y_1). Then the pixel located 10 pixels away, while walking along the ridgeline will be used as the second reference point (x_2, y_2). After these two points are found, the minutiae orientation for ridge endings (in degrees) can be found by using the following equation. Note the that values of x and y below are in reference to the origin (0, 0) located in the top left of the image.

$$ridge\ ending\ orientation = \begin{cases} (\tan^{-1}\frac{|y_1 - y_2|}{|x_1 - x_2|} * \frac{180}{\pi} + 180)\ \%\ 360\ , & y_2 \leq y_1\ and\ x_2 > x_1 \\ \left(180 - \left(\tan^{-1}\frac{|y_1 - y_2|}{|x_1 - x_2|} * \frac{180}{\pi}\right) + 180\right)\ \%\ 360\ , & y_2 \leq y_1\ and\ x_2 < x_1 \\ \left(180 + \left(\tan^{-1}\frac{|y_1 - y_2|}{|x_1 - x_2|} * \frac{180}{\pi}\right) + 180\right)\ \%\ 360, & y_2 > y_1\ and\ x_2 \leq x_1 \\ \left(360 - \left(\tan^{-1}\frac{|y_1 - y_2|}{|x_1 - x_2|} * \frac{180}{\pi}\right) + 180\right)\ \%\ 360, & y_2 > y_1\ and\ x_2 \geq x_1 \end{cases}$$

Finding the minutiae orientation for bifurcations was a little more complicated. A bifurcation is defined by 3 ridges converging at a single point, so the first reference point will be the convergence point. Then, the orientation of all three ridges will be found using the same algorithm as for ridge ending. Finally, the ridge orientation with the highest absolute difference from the other 2 ridge orientations will be chosen to serve as the minutiae orientation for the bifurcation.

Fingerprint segmentation Segmentation is an important step in automatic fingerprint recognition to limit the number of false minutiae generated. Although we came up with a solution for this that worked reasonably well in the previous reports, the solution found was computationally expensive. This made it impractical for use on larger datasets, since it would take considerable time to complete. Work on improving the efficiency of this step was recently done. This work is currently on going, but so far, the improvements decreased the runtime significantly while being able to segment the fingerprint from the background.

The current solution first constructs a bounding box around the fingerprint by measuring the image vertically and horizontally. Following this, the whole image is block processed multiple times using block sizes of 10 by 10 and 15 by 15 pixels. The result is then run through multiple averaging filters of different sizes before having a threshold applied to create a mask identifying areas in the image with high standard deviations (which are likely to be part of the fingerprint).

Several different convolutional neural network (CNN) models were trained using different datasets, which included models trained using input images of thinned, binarized minutiae patch that were 25 by 25 and 50 by 50 pixels in size. Although visual inspection showed a reduction in the number of false minutiae from using the neural networks, it would be more convincing to test the performance of the improved minutiae extraction algorithm, and thus several experiments were conducted by employing popular minutiae based matchers to test the extracted minutiae features.

In practice, comparative testing was carried out on the two models, which included a deep neural network that classified thinned binarized images of 25 by 25 pixels in size, and a deep neural network that classified thinned binarized images of 50 by 50 pixels in size. The following test was performed. The minutiae identified from the minutiae extraction algorithm described above were assigned a score by each of the neural networks, indicating the probability that a minutia is true. The minutiae were then sorted in decreasing order of probability. The matching performance of the BOZORTH3 and MCC matchers were evaluated at varying numbers of minutiae, n, made available for matching. The value of n ranged from 5 to 185 and were increased by 5 at each step. For any value of n, the first n minutiae with the highest assigned probabilities of be true minutiae were selected to be used for the matching step.

BOZORTH3 is a fingerprint matching algorithm included in the NIST Biometric Image Software (NBIS). It is a minutiae-based fingerprint matching algorithm which will do both one-to-one and one-to-many matching operations. It is designed to accept minutiae generated by the MINDTCT algorithm which is a tool in NBIS for minutiae extraction. The NBIS software was made available by NIST.

Minutiae Cylinder Code (MCC) Matcher is another popular minutiae-based fingerprint matcher. The MCC matcher software was made available by the Biometric System Laboratory at the University of Bologna, and more information on this tool can be found on their website.

To test our minutiae extraction algorithm, we modified our program to output the minutiae in the format of MINDTCT output and BOZORTH3 input. Both matchers were experimented with, and their performance was compared using a small dataset of 23 images of fingerprints obtained using the NIR-to-NIR upconverting nanocrystals.

The minutiae made available to the matchers were extracted using the following method. The fingerprint was filtered and enhanced to a binary image, which was then converted to a thinned binary image. The minutiae were extracted by scanning the thinned binary image with a 3-pixel by 3-pixel mask containing a set of predefined minutiae patterns. Other than segmenting the fingerprint during the fingerprint segmentation step, no steps were taken to limit the false minutiae extracted using this method.

In addition to the two models of minutiae selection described previously, a randomly selected minutiae set was made for comparison. This set was chosen at random from the entire minutiae population at the same quantity levels as used for testing the other two models. At each level, the random sampling was done 5 times and the results from different samples were averaged together to get each matcher's performance at each level. Both matchers work by reading files containing the extracted minutiae from each fingerprint, and the number of minutiae made available at each level would increase from 5 to 185 minutiae at a step size of five.

The performance of the two matchers was compared by varying the number of minutiae available for matching. The better fingerprint matcher should be able to maintain its matching accuracy when performing matching with fewer minutiae. The number of extracted minutiae from each fingerprint made available during the matching step was capped at varying levels to examine which matcher could perform better using fewer minutiae.

A comparison of the BOZORTH3 and MCC matchers performance of finding true matches are shown in **Figure 97**. The results indicate MCC was able to consistently identify more True Positives than BOZORTH3 with less than 140 minutiae available for matching.

Figures 98-100 show the positive matches including false positives for the BOZORTH3 and MCC matchers using the deep neural network classified minutiae. In these results, both the MCC and BOZROTH3 matchers tend to have increased performance when a trained deep neural network was used to select the minutiae for use in the matching step over randomly selecting minutiae. Both matchers were able to identify more true positives while using the neural network. In addition, by looking at the number of false positives identified by the BOZORTH3 matcher in **Figure 99**, one can see that the number of false positives increase after using more than 140 minutiae for matching. This may mean that a neural network could be used to reduce the number of false positive matches, but further testing is needed on larger datasets to confirm this.

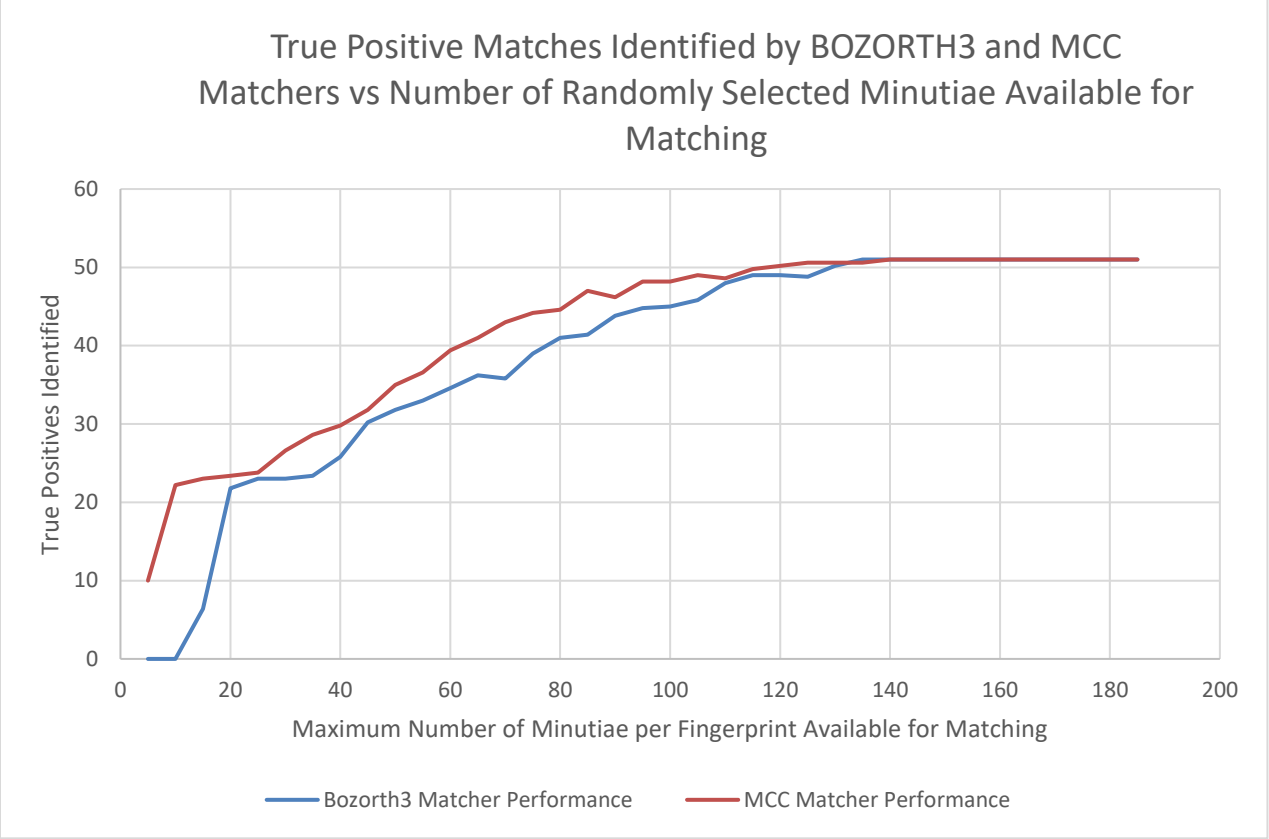

Figure 97. Performance comparison of the MCC and BOZORTH3 matchers.

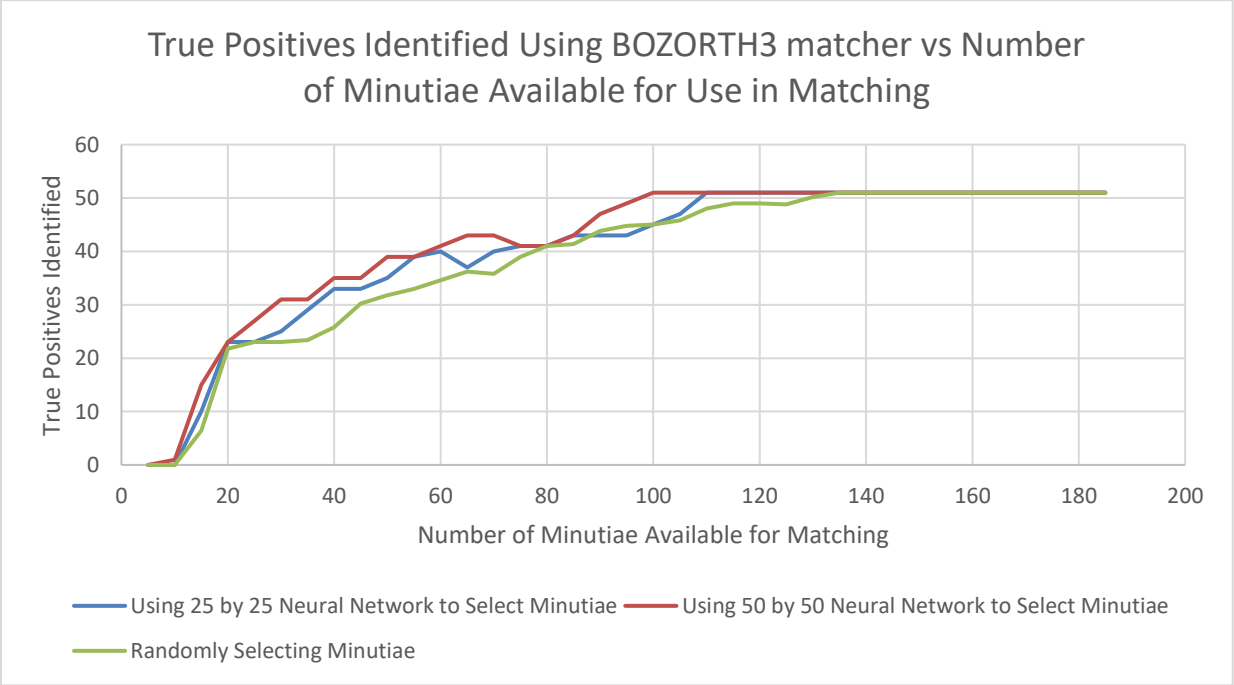

Figure 98. True positives identified by BOZORTH3 matcher using neural networks to select varying numbers of minutiae for use in matching.

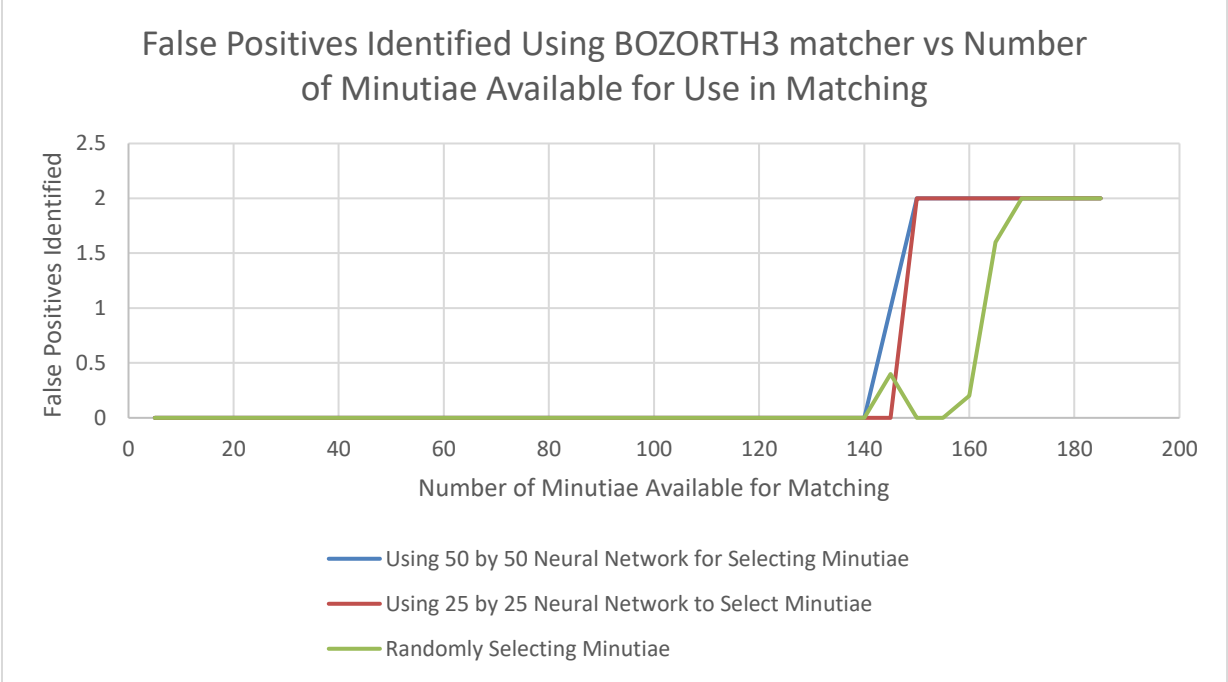

Figure 99. False positives identified by BOZORTH3 matcher using neural networks to select varying numbers of minutiae for use in matching.

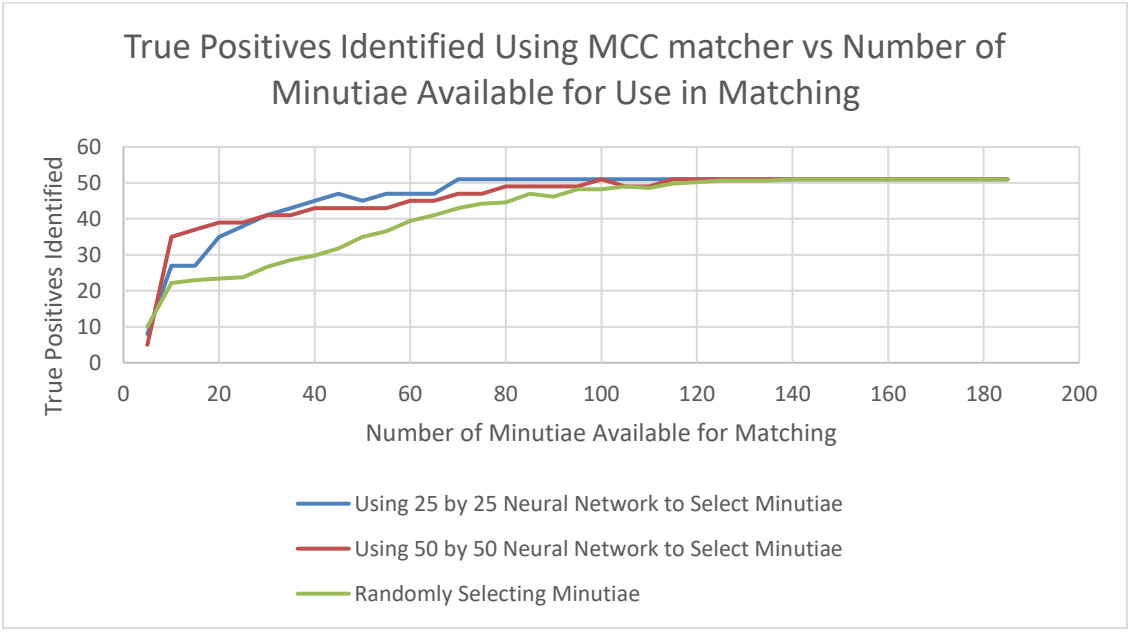

Figure 100. True positives identified by MCC matcher using neural networks to select varying numbers of minutiae for use in matching.

Automatic Fingerprint Recognition Software Platform Multiple tasks have been accomplished for the automatic fingerprint recognition software platform of the Portable Field Fingerprint Reader system. These

include using Deep Learning for fingerprint segmentation, the development of Generative Adversarial Networks to enhance latent fingerprints, and the generation of a database of synthetic fingerprints which include over 1,000,000 images. First, the work for the fingerprint segmentation will be discussed followed by the development of the Generative Adversarial Networks. Finally, we will discuss the database of synthetic fingerprints that were generated.

Fingerprint segmentation is an important step in automatic fingerprint recognition. It identifies the foreground in the image to ensure that the following steps done to identify the fingerprint are conducted on the Fingerprint itself and not on the background. Up until this point, the fingerprint segmentation was accomplished by block processing the image to measuring the standard deviation of the pixel values in each block. Following this, a threshold would be applied to determine which blocks were part of the foreground and which were part of the background. This works in most cases, but there are cases where the algorithm will consider certain types of background noise to be considered as part of the foreground. To correct this, work was done to develop a Neural Network and deep learning methods to Segment Fingerprints (see **Figure 101**).

The development of Generative Adversarial Networks (GAN) to enhance images of latent fingerprints was started. This was done to help overcome the poor image quality commonly observed for latent fingerprints. Most latent fingerprints collected from crime scene contain some distortions, damages, or noise which significantly affect feature extraction and matching. Leveraging the advancement of GAN, we expect to build a deep learning model for enhance the quality of image, reconstruct fingerprint from poor quality image, and/or correlate the acceptable portion of the latent fingerprint with its corresponding region in stored fingerprint patterns for partial matching. The building and tuning of deep GAN model is time-consuming.

In addition, a Siamese neural network was used with the GAN to enforce similarity between the generated images and the original structure. As a proof of concept, this model use used to enhance images of celebrity's faces obtained from the freely available. Artificial noise such as Gaussian blur, bright spots, black dots, and elastic distortion were added to these images. Then the GAN along with the Siamese neural network were used to enhance the images. The results given in **Figure 102** show potential for application to images of latent fingerprints.

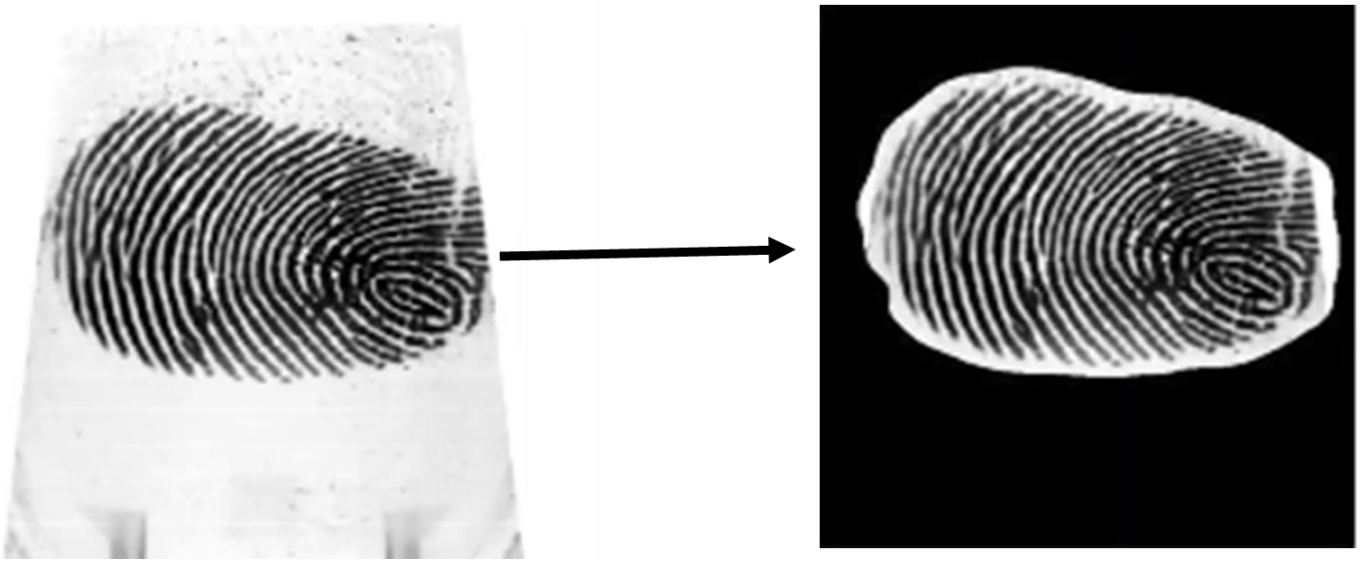

Figure 101. Segmentation using deep learning model.

This resource was prepared by the author(s) using Federal funds provided by the U.S. Department of Justice. Opinions or points of view expressed are those of the author(s) and do not necessarily reflect the official position or policies of the U.S. Department of Justice.

Figure 102. Results from using GAN and Siamese neural networks to enhance noisy images.

Figure 103 shows the loss from training the GAN and the Siamese neural network together. As you can see, the training loss for the Enhancer (blue) seems to diverge over time. This is due to the Siamese neural network outperforming the Enhancer and Discriminator networks. On solution to this is to pretrain the Siamese neural network before training the GAN. Then when training the GAN, the Siamese neural network is just used to enforce similarity between the generated and the real images in the dataset.

To successfully train a GAN, many images are needed. To train the GAN for our purposes, synthetic fingerprints were generated using the Anguli fingerprint generation software. This software was used to generate 10,000 unique fingerprint templates. From these templates, 100,000 good quality fingerprints, similar to **Figure 104**, and 1,000,000 bad quality fingerprints, similar to **Figure 105**, were generated.

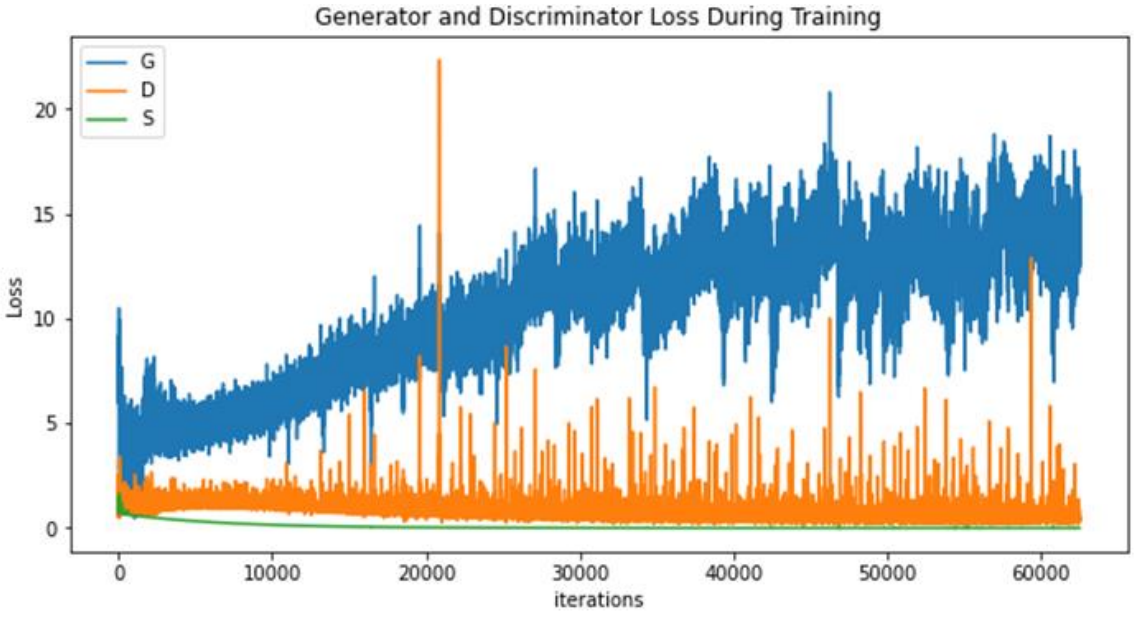

Figure 103. Training loss for model. The blue line shows the enhancer loss; the orange line indicated the discriminator loss, while the green line displays the Siamese neural network loss.

This resource was prepared by the author(s) using Federal funds provided by the U.S. Department of Justice. Opinions or points of view expressed are those of the author(s) and do not necessarily reflect the official position or policies of the U.S. Department of Justice.

Figure 104. Good quality generated fingerprint image.

Figure 105. Bad quality generated fingerprint image.

A platform to run automatic fingerprint recognition software consists of a server that runs the fingerprint recognition software, a database management system that manages the datasets and metadata, and finally an android app that connects to the server and uploads images to be processed. The user interfaces with the software from a mobile app, where they can either take pictures of fingerprints using the device camera, or they can import images from a separate device. The app will allow the user to select images to analyze, and once they do, the image gets uploaded to a server that runs the automatic fingerprint recognition software on it. It will perform image enhancement on the fingerprint, and then it will attempt to extract the minutiae from the enhanced image. The server will then use the extracted features to try and match the uploaded fingerprint against a database of known fingerprints. The server will query the database for a list of fingerprints to match the uploaded fingerprint against. Once the server has completed the matching step, it will return the results back to the android app, which will display the results to the screen. A general overview of the app system is given in **Figure 106**.

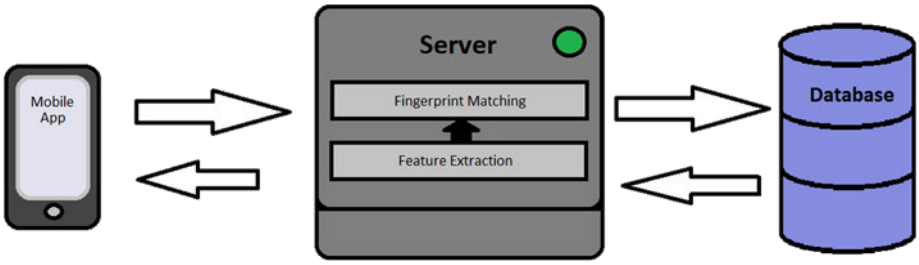

Figure 106. High level overview of the whole system.

Although this software is not yet considered to be complete, it should gave the research team a good platform for running and testing other fingerprint recognition software on it.

Android App An android application is the main way the user will interact with the fingerprint recognition software. An overview of the application activities is shown in **Figure 107**. The main activity page will provide the user with the option to upload images or obtain general information about the software and project itself. Selecting "Upload Fingerprint" will bring the user to the "Upload Activity" page. This allows the user to capture

a fingerprint using the device camera or select an image from storage. Selecting “Select Photo” will bring the user to the “Select Photo Activity” page. This page contains all images stored on the device in the app, and it will allow the user to select one of the images. Alternatively, if the user selects “Capture Photo” from the “Upload Activity” page, it will bring the user to the “Camera Activity” page, which allows the user to use the camera to capture an image of a fingerprint. Once the user either selects an image from storage or captures and image using the camera, the image will be displayed back on the “Upload Activity” page, and then the user will have the option to analyze the fingerprint. Once the user selects this option, then the android app will upload the selected image to the server, that will run the automatic fingerprint recognition software on it.

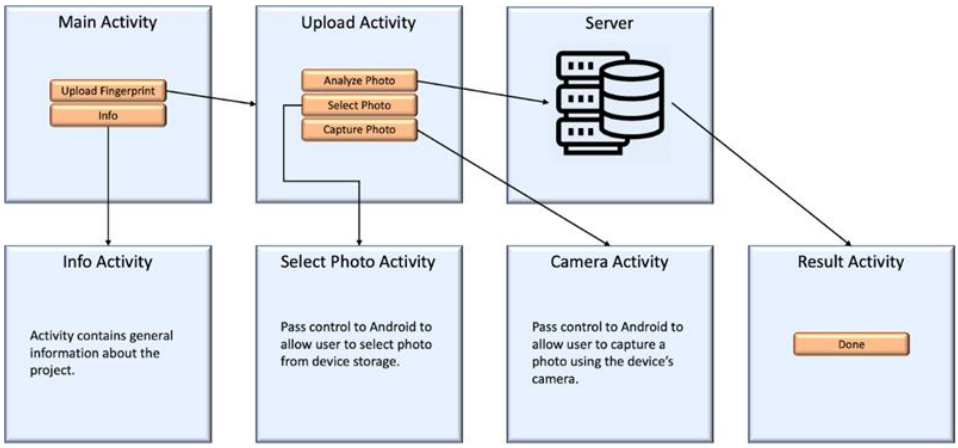

Figure 107. Overview of Android application activities.

Once an image is uploaded to the server, then the automatic fingerprint recognition will be run on it, as overviewed in **Figure 108**. The software will first attempt to perform image enhancement on the fingerprint. It will segment the fingerprint and attempt to convert the image into a binary format where the ridges in the fingerprint are one value (pixel value of 1), while the valleys and background of the image are another value (pixel value of 0).

Once the image is enhanced, the server will attempt to extract the minutiae from the image. For this, it will skeletonize the binary image and then scan the resulting image with a 3 by 3 window looking for predefined minutiae patterns. Once one is found, its location is recorded, and its minutiae orientation is calculated. Following this is an optional step where each candidate minutiae is classified by a network as valid or invalid. This neural network is trained using TensorFlow and can be used to help limit the number of false minutiae. Past testing has shown that this can help reduce the number of false positives identified by the system.

After the minutiae are extracted from the image, the server will query the database for a list of fingerprints stored in the database to match the uploaded print against. The server currently uses NIST’s BOZORTH3 to perform the matching. The server will use this tool to match the uploaded print against the database. Once this is completed, the server will return the results back to the android application.

This resource was prepared by the author(s) using Federal funds provided by the U.S. Department of Justice. Opinions or points of view expressed are those of the author(s) and do not necessarily reflect the official position or policies of the U.S. Department of Justice.

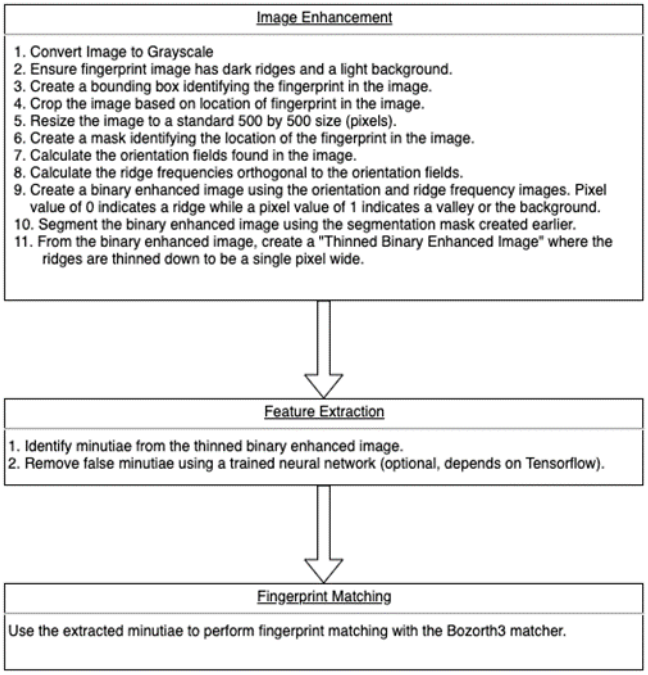

Figure 108. General overview for the fingerprint processing and matching algorithms.
Database.

A database management system, as overviewed in **Figure 109**, is used to manage the fingerprints and the fingerprint's metadata. Currently, it stores the original images, the extracted features for each of the originals, and the finger index for each fingerprint image (if known). The ability to easily store the subject id for each print will help with testing and evaluating the performance of the system, because it allows developers an easy method to determine if a match made by the system was truly correct or not. Additionally, the matching speed of the system could be significantly improved by storing the Level 1 classification of the fingerprint itself. Level 1 classification for fingerprint includes the general ridge orientation of the fingerprint. Some examples of these are loops, whorls, arches, and tented arches. It is possible to determine the class of the fingerprint by executables provided by NIST. By using and storing this information in the database, the system could potentially determine the class of the uploaded fingerprint, and then the system would only need to match the uploaded fingerprint against fingerprints stored in the database that are of the same Level 1 classification. This technique is already commonly done in most automatic fingerprint recognition systems.

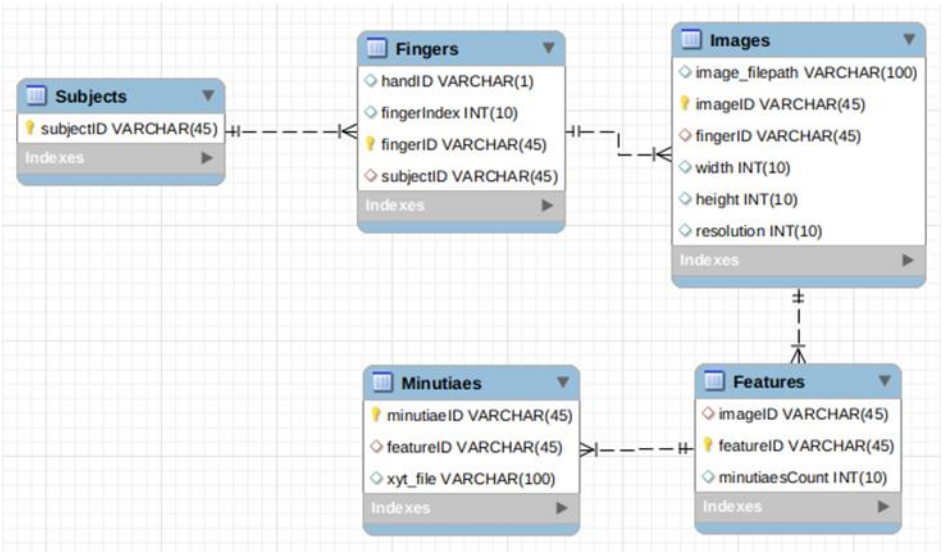

Figure 109. Overview of the database structure.

This resource was prepared by the author(s) using Federal funds provided by the U.S. Department of Justice. Opinions or points of view expressed are those of the author(s) and do not necessarily reflect the official position or policies of the U.S. Department of Justice.

The final aspect of this work was the design of a physical fingerprint reader system. Two versions of this reader system were developed, one for use in a laboratory setting and one for use in the field. Illumination and excitation of ceramic nanoparticles is traditionally done with lasers. However, very powerful and effective lasers have many downsides. Using a laser to search for markings or fingerprints is similar to reading a book in the dark using a laser pointer. Ideally, if one were to find themselves reading in the dark, a flashlight with a broad soft light would be much easier to use than a laser pointer. This simple principle was the drive for the development of a light emitting diode (LED) based reader system.

Development of the LED reader system was divided into two directions and developed in parallel. It was decided by the team that a stationary instrument for laboratory use and a mobile platform for field use would be the most useful devices to move forward with. **Figure 110** shows the complete initial LED reader system with its carrying case.

The laboratory instrument (**Figure 110**) was dubbed the *Illuminir 1.0* and is designed with a scientist or engineer user in mind. The user has the ability to adjust the input voltage and current on the controller and see their values along with diode temperature in real-time on digital displays. High precision 20-turn potentiometers with locking knobs are used for all adjustments. The body of the *Illuminir 1.0* was designed to be robust and industrial, so a TIG welded aluminum shell was fabricated and powder coated with a tough wrinkle texture to ensure proper protection of the diode and its heatsink and fan. An *Illuminir* logo and warning label are laser engraved on the top of the device. On the bottom of the body is an adjustable base with a ¼ - 20 female mount that fits onto any photography-style tripod head.

A multitude of optics were developed for use with the *Illuminir*, in particular, a 25° parabolic reflector and a 60° lens. There are many challenges involved in the optics, primarily related to the wavelength and distribution of the infrared light. Although the average wavelength emitted is 980 nm, other wavelengths (940 nm, 1000 nm etc.) present an issue when the markings are imaged on a digital camera because of the tuning of the filters on the camera and the emitted light from the excited particles. To solve this, a filter (**Figure 111**) is used on the LED to ensure that only the desired wavelength is emitted from the device.

Figure 110. Complete LED Reader System.

This resource was prepared by the author(s) using Federal funds provided by the U.S. Department of Justice. Opinions or points of view expressed are those of the author(s) and do not necessarily reflect the official position or policies of the U.S. Department of Justice.

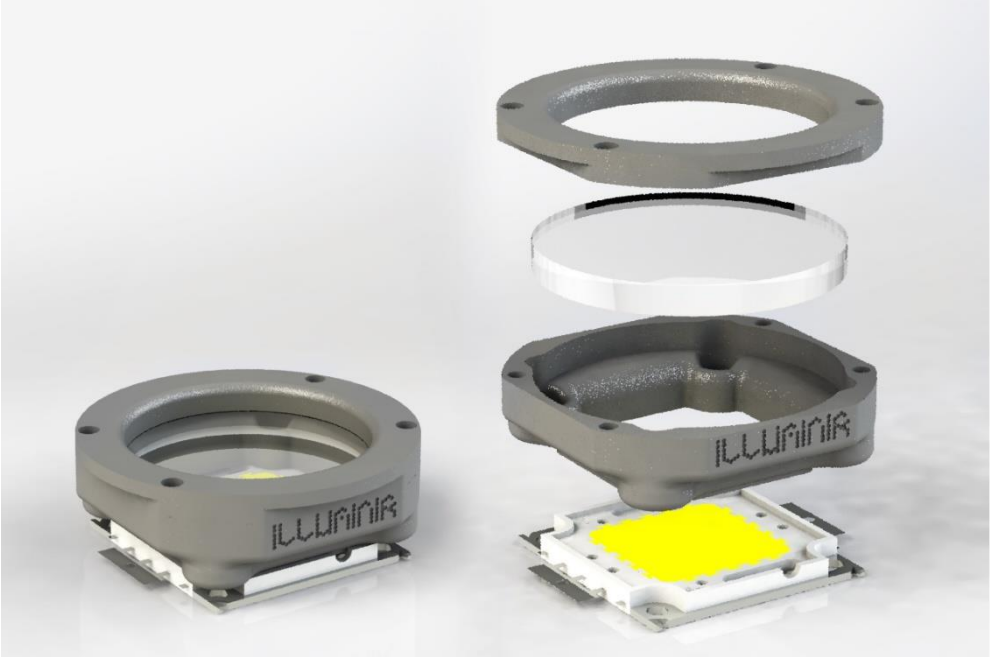

Figure 111. Filter for LED output.

A second reader design was developed. This reader design used laser illumination and is therefore better used in a laboratory environment. In addition, a miniaturized version of the LED-based *Illuminir 1.0* reader developed previously was constructed.

Laser-based fingerprint reader A mobile latent fingerprint development imaging system for laboratory deployment was developed. This was used our knowledge gained from developing anti-counterfeiting reader systems. The imaging system includes a fingerprint development kit, NIR-filter removed, cellular phone camera, 980 nm laser diode excitation source and appropriate filters for band-selective imaging of NIR (800 nm) upconversion. **Figure 112** shows the various components of this reader.

Light emitting diode (LED)-based fingerprint reader A mobile latent fingerprint imaging system for laboratory and field deployment. The imaging system includes a 980 nm light emitting diode (LED) excitation source mounted on a heat sink, a parabolic reflector to collimate the LED light, and appropriate filters for band-selective imaging of NIR (800 nm) upconversion.

The major upgrade from the *Illuminir* 1.0 design was to reduce the size and weight of the heat sink and the parabolic reflector. The new heat sink, LED, parabolic reflector design is shown in **Figure 113**. **Figure 114** shows the manufactured design, both assembled and disassembled. **Figure 115** compares the size of the previous *Illuminir 1.0* version with the much smaller newer *Illumnir 2.0* version.

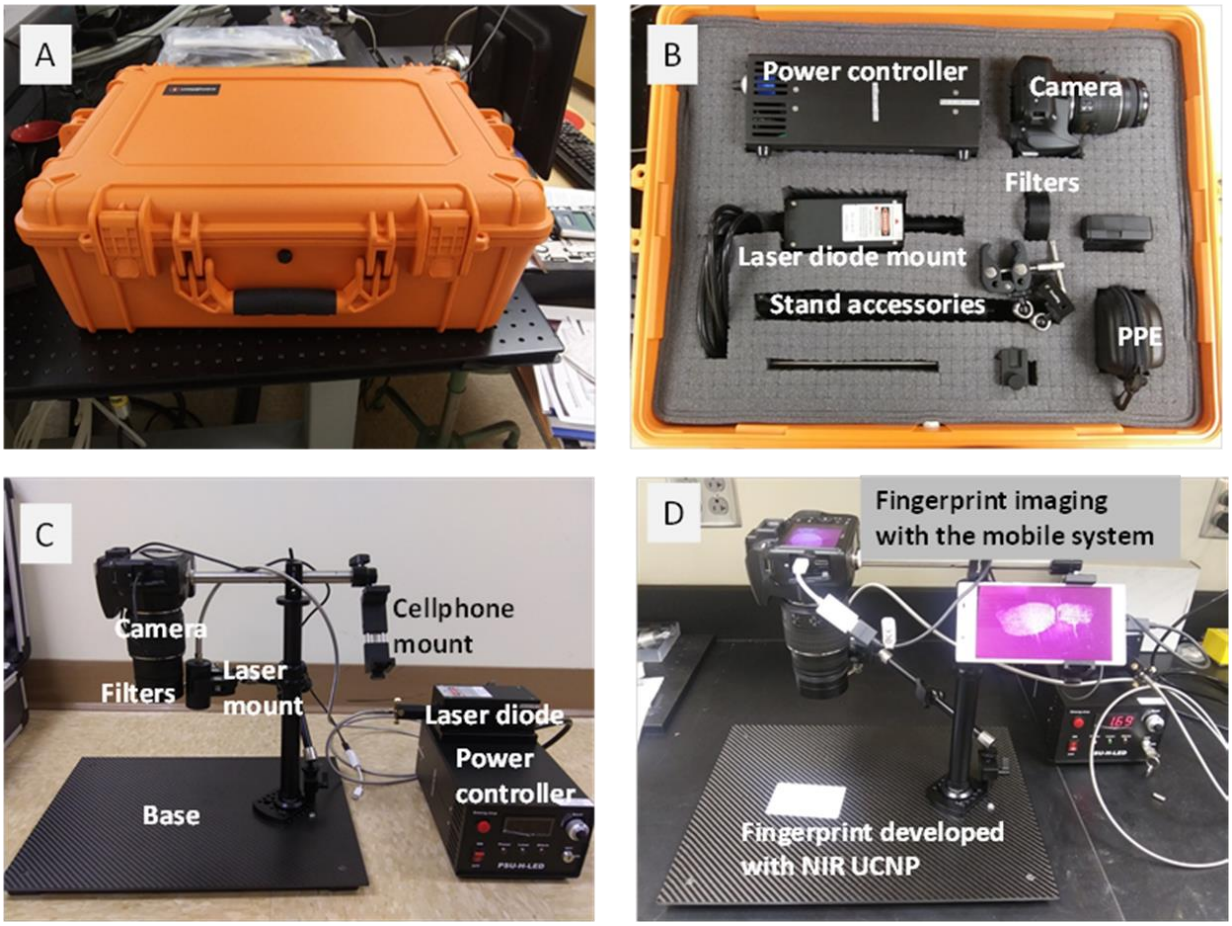

Figure 112. A) A mobile box consists of fingerprint imaging system, B) The components of the fingerprint imaging system, C) The fingerprint imaging system post assembly, and D) the fingerprint imaging system in action.

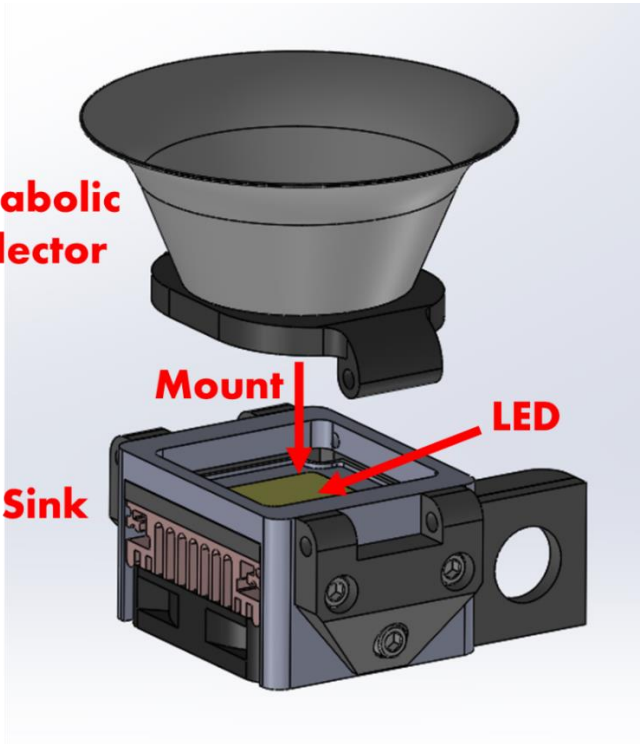

Figure 113. Schematic model of heat sink, LED light, and parabolic reflector.

This resource was prepared by the author(s) using Federal funds provided by the U.S. Department of Justice. Opinions or points of view expressed are those of the author(s) and do not necessarily reflect the official position or policies of the U.S. Department of Justice.

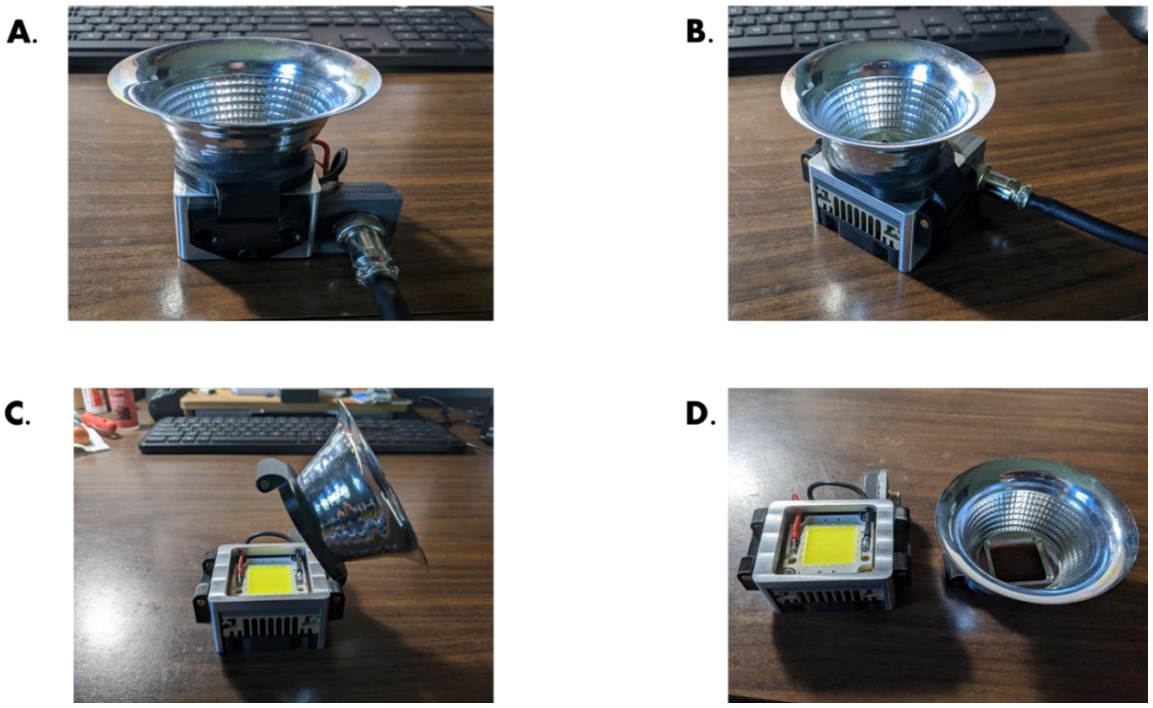

Figure 114. Manufactured heat sink device, A. and B. fully assembled, C. removing the parabolic reflector, D. the parabolic reflector removed.

Figure 115. Comparison of *Illuminir 1.0* (left), and *Illuminir 2.0* (right).

As the laser-based system was essentially complete, our research group focused on improving the LED-based reader system by increasing the distance from the LED to the sample to allow better imaging of the fingerprints. This necessitated increasing the power of the LED, as the LED being further from the fingerprints needed more power to activate the UCNPs on the fingerprint because of the spreading of the light cone produced. However, this extra power caused the LED to heat considerably entailing imaging to be performed only in very short bursts. To counter this, the LED was set in a water-cooled jacket to lower the temperature of the LED. In addition, the parabolic reflector was removed as it wasn't reducing the beam size at the fingerprint sufficiently to be useful. This increased the distance available for taking pictures of the fingerprints to about 3 inches from about 1.5 inches. **Figures 116-119** show the *Illuminir 2.1* system, and its use for fingerprints. **Figure 119** indicates that the image capture may need more pixels to properly obtain the fingerprint image.

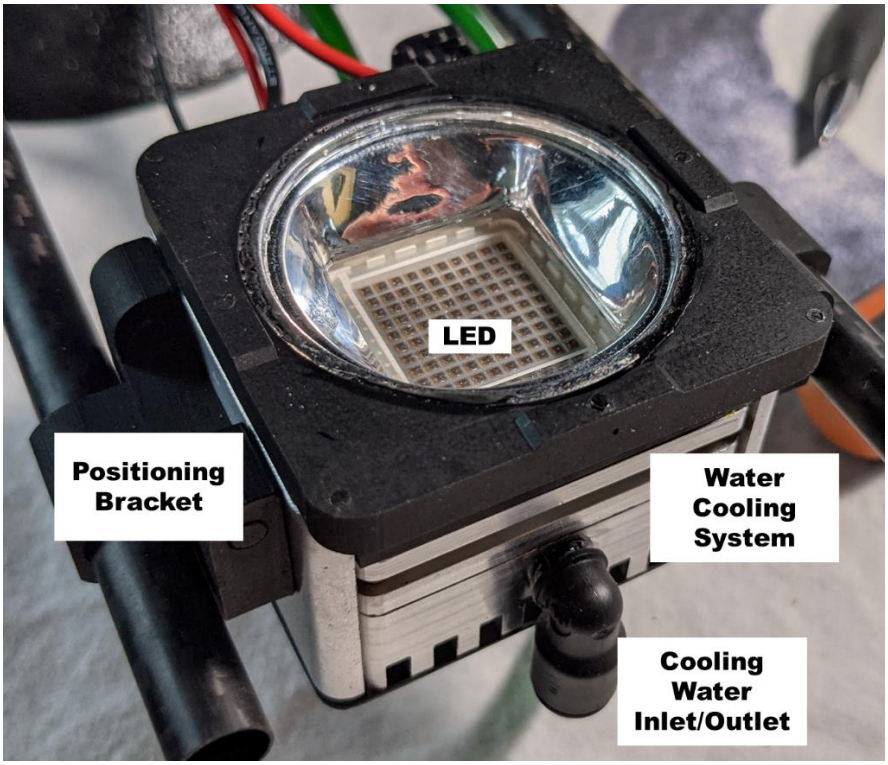

Figure 116. Disassembled *Illuminir 2.1* showing LED and cooling system.

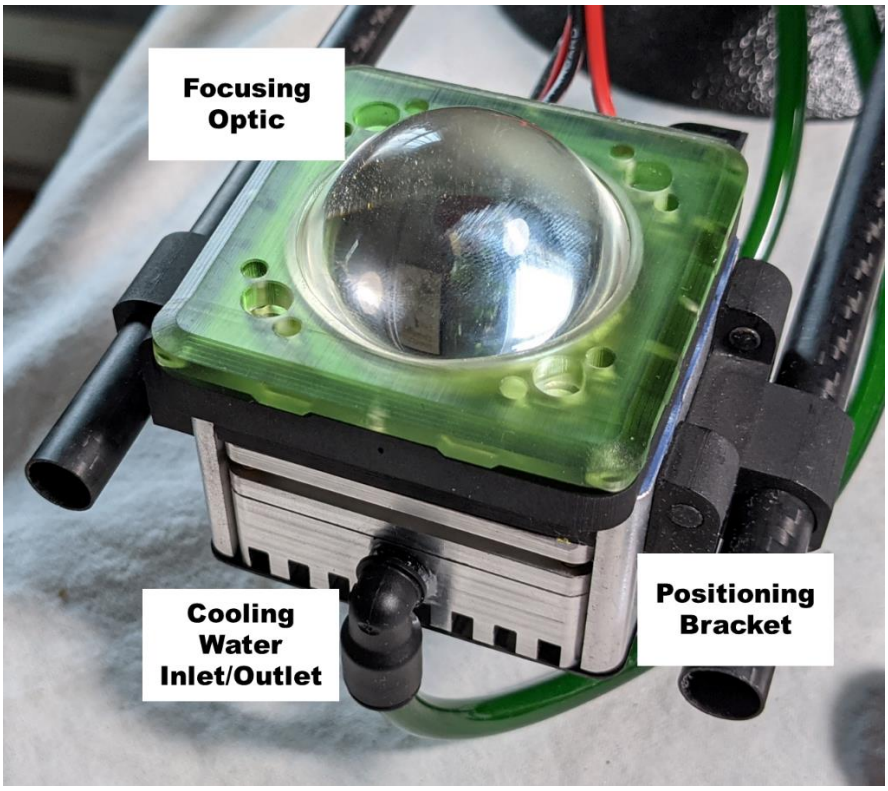

Figure 117. *Illuminir 2.1* with attached hemi-spherical focusing optic.

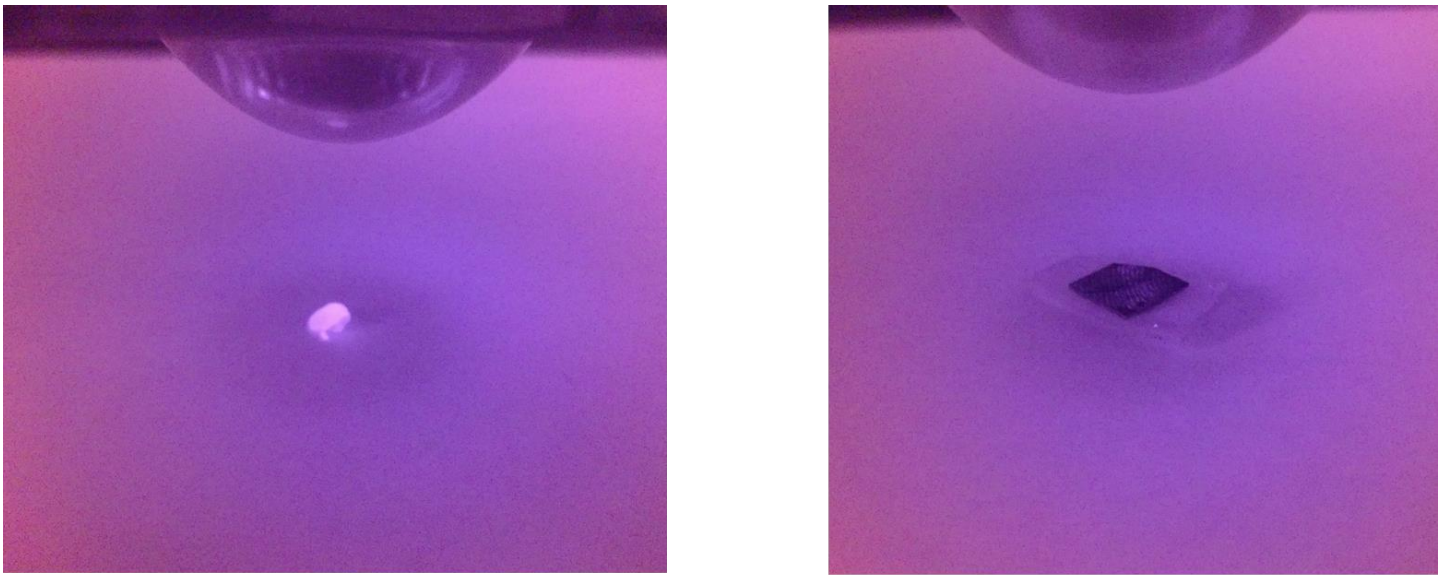

Figure 118. *Illuminir 2.1* in use. Images captured with a Google Nexus 5.0 NIR enabled phone with 12.3 megapixels. Image A shows a small pile of UCNPs, while image B is a fingerprint on a piece of silicon.

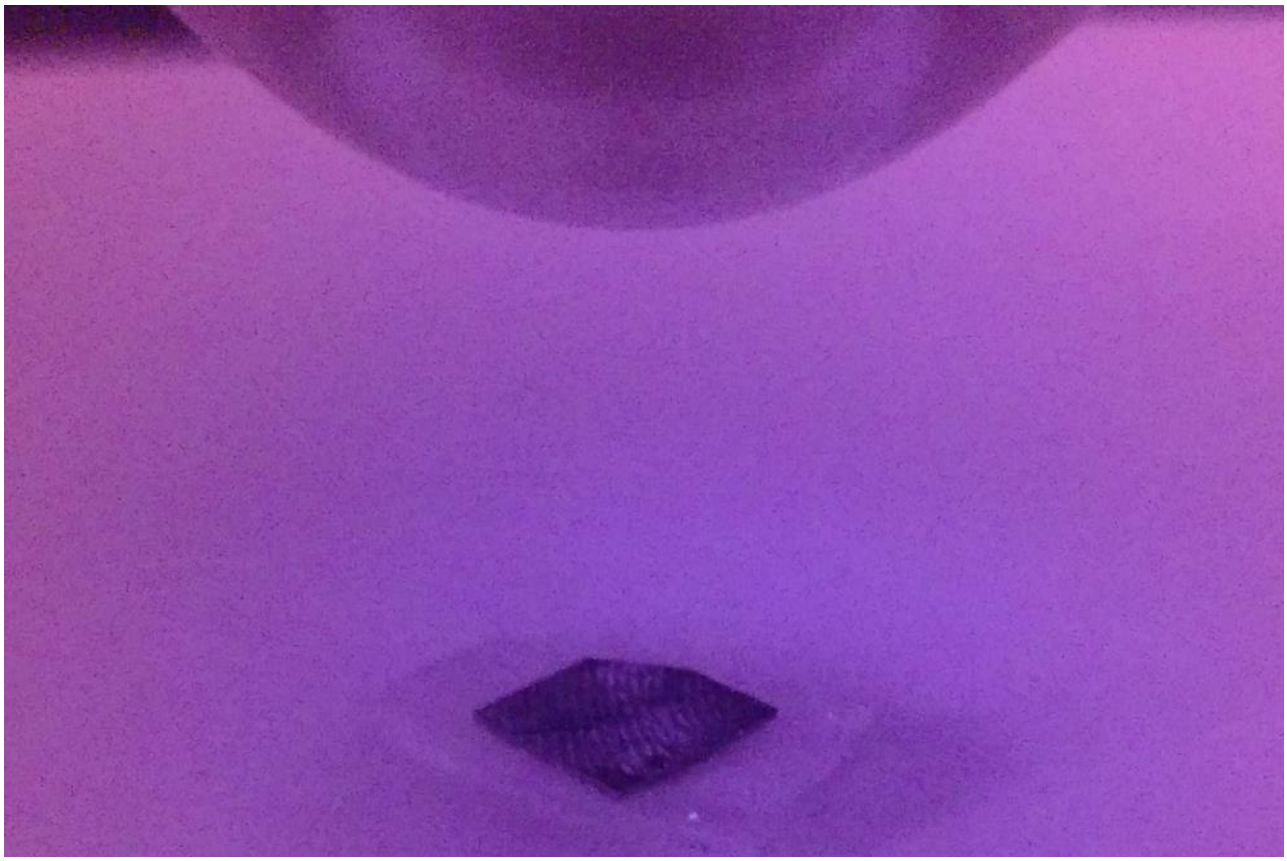

Figure 119. A blown-up image of the fingerprint in image B in **Figure 118**.

To finish the *Illuminir 2.1* reader device, research focused on improving the LED-based reader system by adding a recirculating water cooler system to reduce the LED temperature, while also utilizing a new camera having its NIR filter removed. Removing the NIR filter necessitated using a visible light filter.

The size of the LED unit, including its heat sink and collimating lens were greatly reduced. Unfortunately, this caused the LED unit to heat considerably, particularly at high LED Wattages (approaching 100 Watts) faster allowing operation for a few seconds at a time. To solve this problem a water-cooling system was designed for the Illuminir system. **Figure 120** shows the LED with the cooling water nozzle. This cooling system was run off tap water but could be run off a portable water system. This cooling system allowed the LED to run for more than 30 minutes consecutively without heating significantly.

Figure 120. LED unit of Illuminir reader design showing a cooling water inlet.

The next step to be performed for the *Illuminir* system was to change cameras, as fingerprint development was limited by the camera. Previously we had utilized a Google Nexus 5x phone as the camera system, but the size of this six year old phone limited the ability to get the camera close to the fingerprint, particularly when using a visible light filter. This new camera chosen was a Nikon D3000 with 10 megapixels. The near-infrared (NIR) filter was removed from the camera as shown in **Figure 121**.

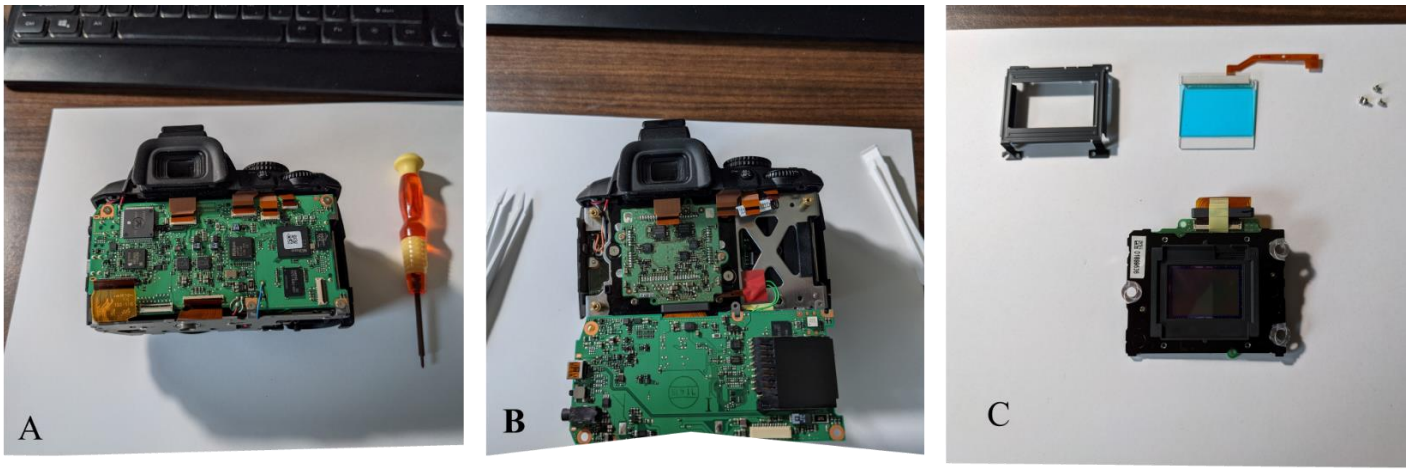

Figure 121. Removal of the NIR filter. A. Removal of the camera's rear panel; B. Camera circuit board removal; C. Camera sensor assembly after NIR filter (blue square) removal.

The filterless-NIR camera was tested as shown in **Figure 122**. The collected images are shown in **Figures 123-125**. As can be seen in **Figure 123**, the images could only be collected for very short time intervals, no longer than 1/50 seconds as considerable background light is visible in the images. As this background light likely stems ambient room light, a high pass filter that blocked light with wavelengths less than 800 nm wavelength was added to the camera. Note the longer time interval of collection with the visible light filter. This additional time may be important, as the UCNPs are not particularly strong emitters.

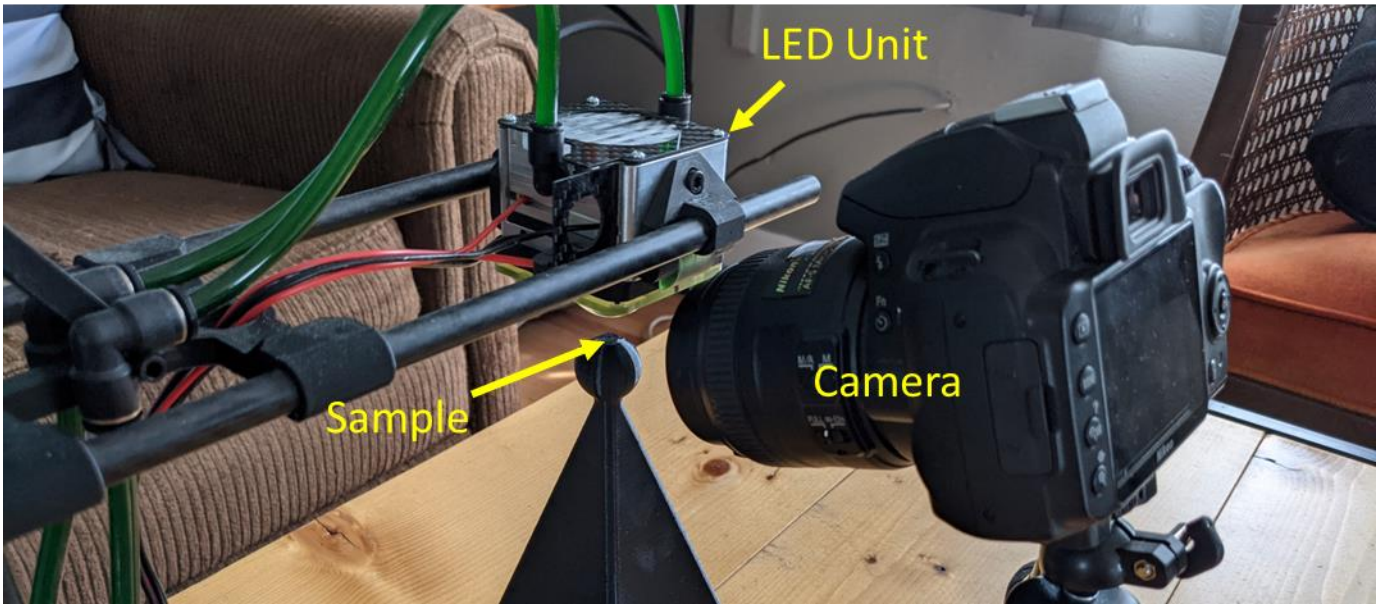

Figure 122. Imaging setup for NIR filterless fingerprint development.

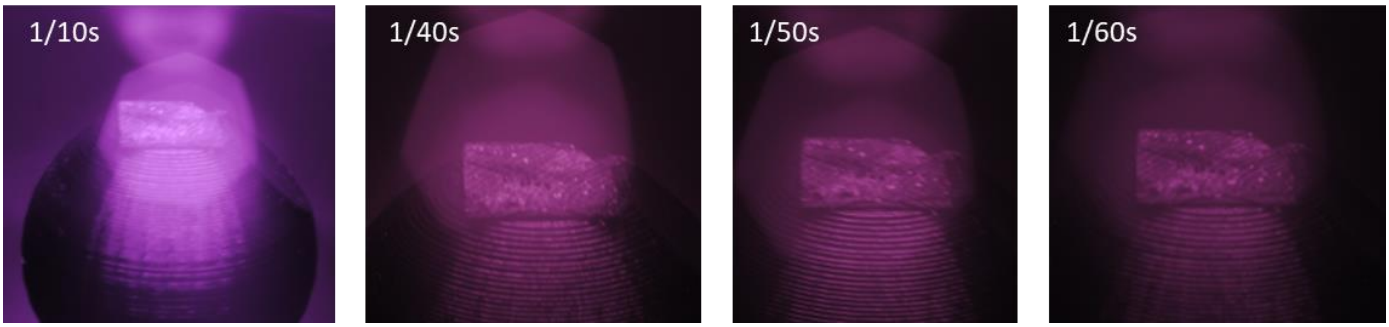

Figure 123. Captured images for system in **Figure 122** with no filters.

Figure 124. Captured images for system in **Figure 122** with a visible light filter but no NIR filter.

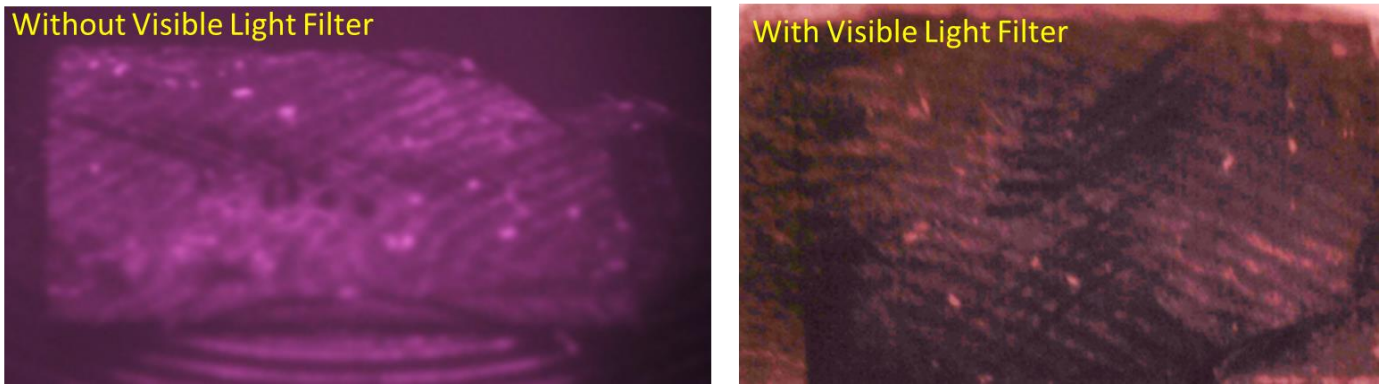

Figure 125. Fingerprint images from **Figure 122** (left) and **Figure 124** (right).

The background light in the images with no visible light filter made observing the developed fingerprint more difficult when compared to fingerprints developed using a visible light filter, as observed in **Figure 125**. A final point relevant to **Figure 124** is that the fingerprint images appear to be slightly distended, which may affect fingerprint identification. This aspect is the result of the positioning of the LED unit and the camera.

As observed in **Figure 122**, the camera is at an acute angle to the sample. The remedy for this was to design a slightly different setup in which the camera is perpendicular to the fingerprint sample, with the LED unit at an angle to the sample. To accomplish this a mount for the camera lens was designed using CAD (see **Figure 126**), printed using 3D printing of the component (**Figure 127**) and then evaluated (**Figures 128-130**). As shown in **Figure 11**, the miniaturization of the LED unit made this design much easier to accomplish. **Figures 128** through **130** show that the system works very well for imaging fingerprints relatively quickly (< 2 seconds) at reasonable power (~60 Volts).

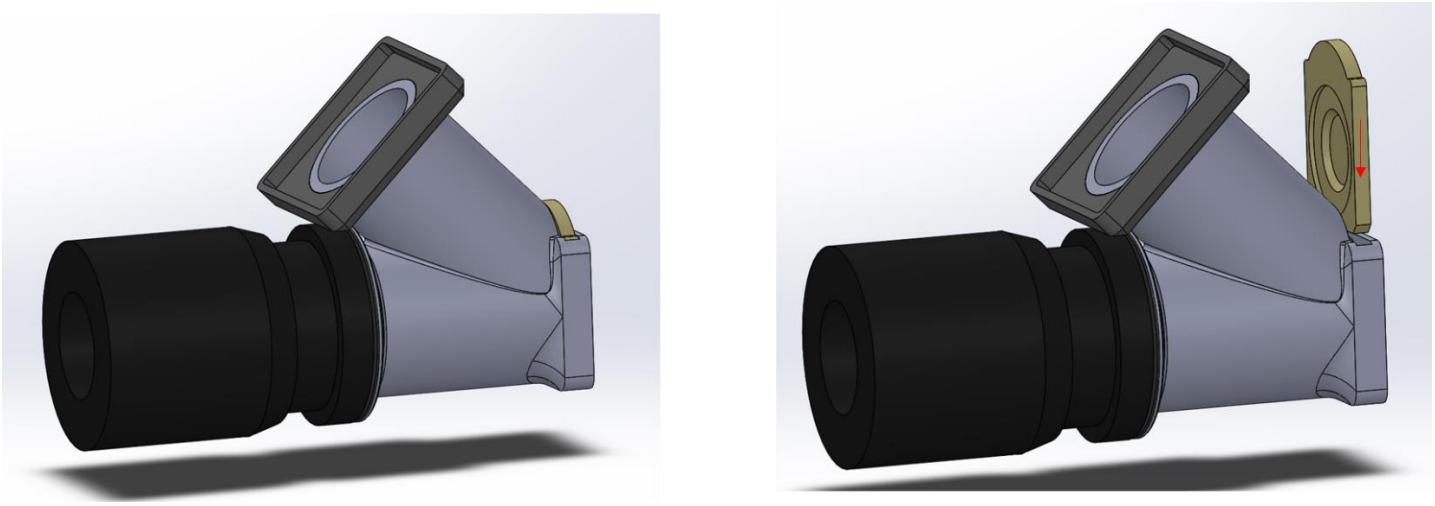

Figure 126. CAD model of the camera mount to join camera and LED unit. The right image shows the visible light filter positioning.

This resource was prepared by the author(s) using Federal funds provided by the U.S. Department of Justice. Opinions or points of view expressed are those of the author(s) and do not necessarily reflect the official position or policies of the U.S. Department of Justice.

Figure 127. Camera mount connecting the LED unit to the camera.

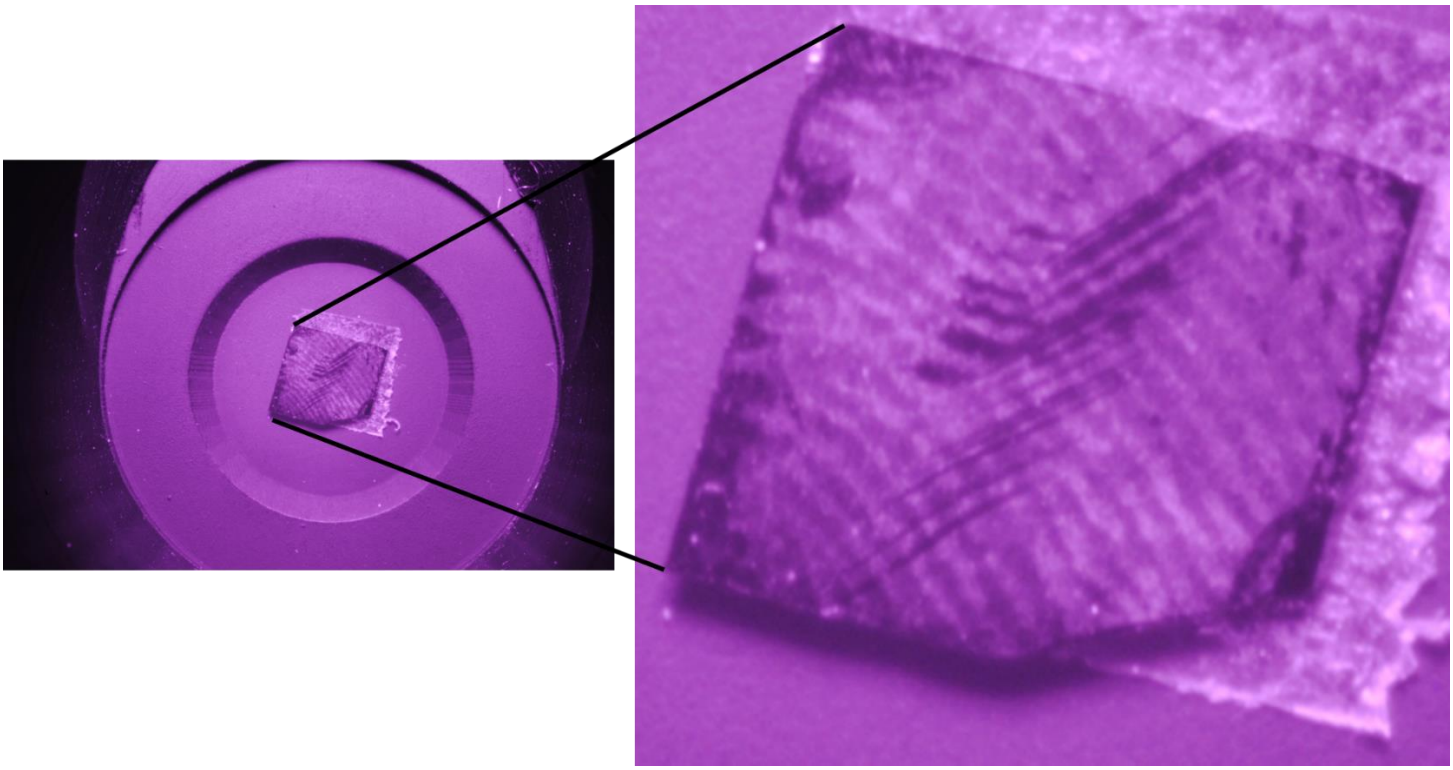

Figure 128. Example fingerprint imaged using the camera and camera mount.

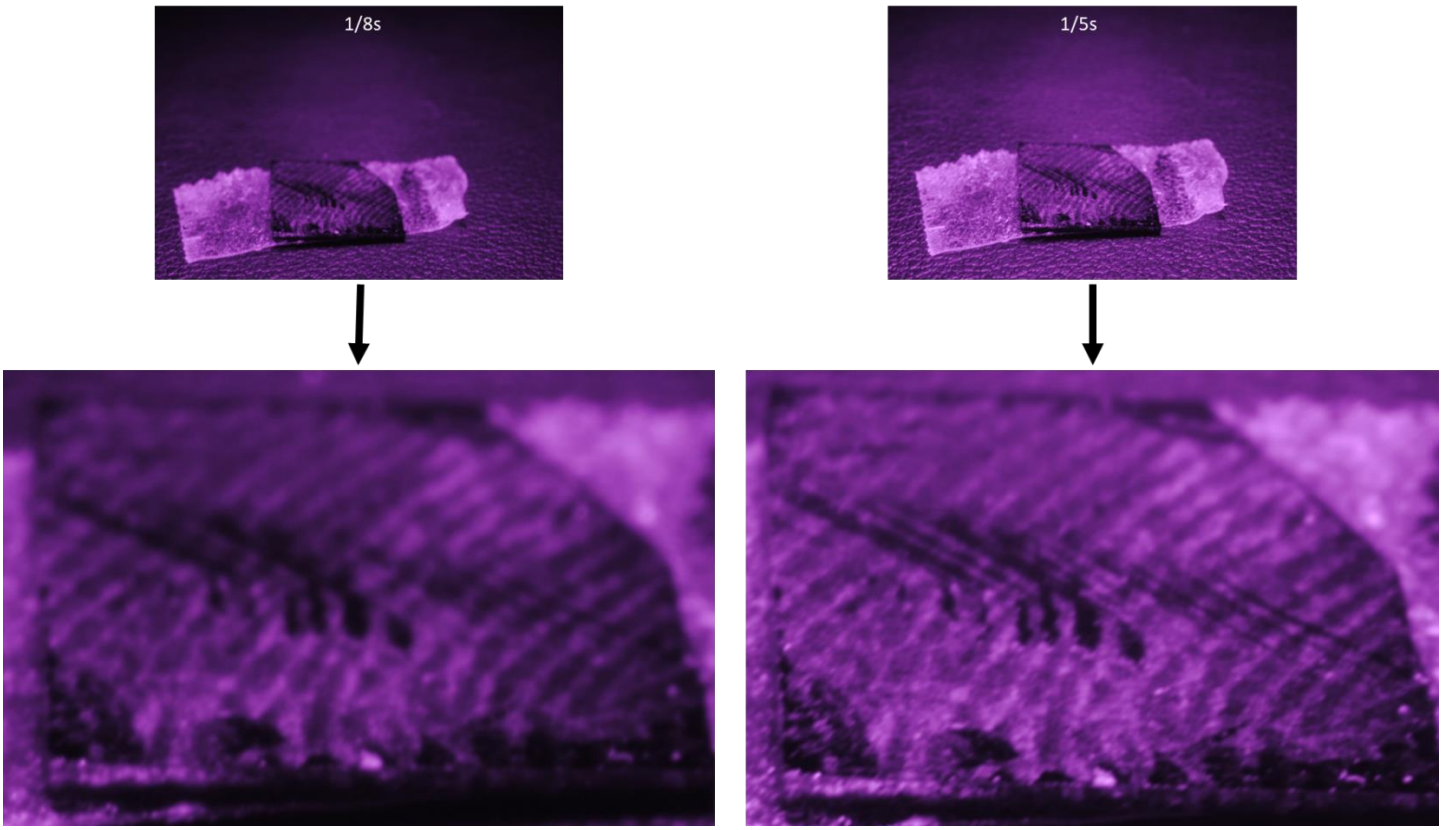

Figure 129. Fingerprints imaged with the new camera mount system, imaged at two different times.

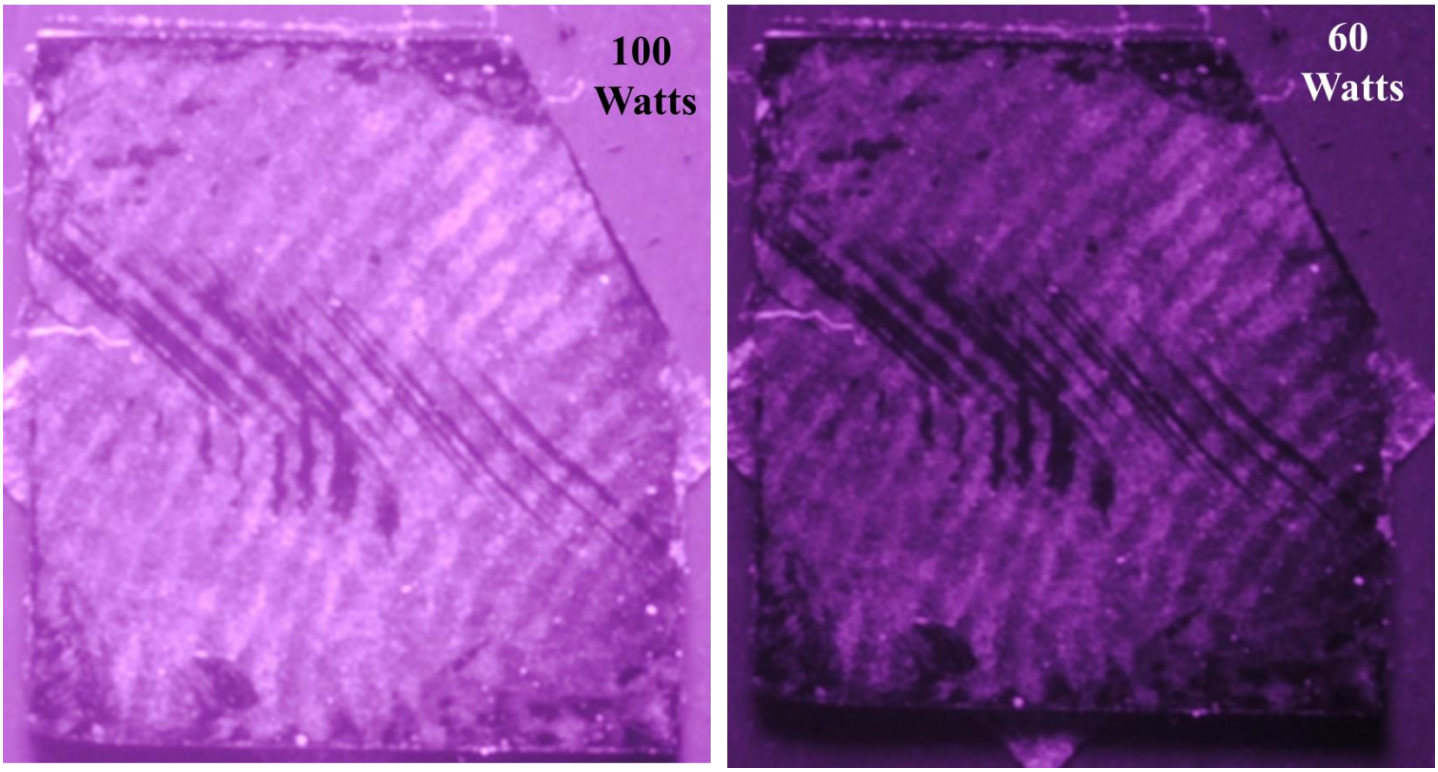

Figure 130. Fingerprints imaged using the new camera mount at two different LED Wattages.

Task Research Summary:

A reader system was designed, tested, and shown to work at reasonable collection times and LED Wattages.

3. What opportunities for training and professional development has the project provided?

Ms. Sierra Rasmussen, a Ph.D. student involved with the NIJ research was selected to participate in a National Science Foundation (NSF) National Research Traineeship (NRT) program, Cyber-Physical-Social System for Understanding and Thwarting the Illicit Economy. The NRT programmatic elements will provide Ms. Rasmussen with the scientific knowledge and the professional skills and training needed to become a next-generation leader in the fight against the illicit economy. In addition, Ms. Rasmussen will receive professional and leadership training within the framework of a unique, collaborative cyber-physical-social model. The NRT model takes a comprehensive approach that factors in not only the technical aspects of the cyber strategies and physical methods used to combat the illicit economy, but also whether these strategies and methods are compatible with human behavior. The NRT model will allow trainees such as Ms. Rasmussen to solve complex problems, where the solutions must tightly integrate cyber, physical, and social interactions in real-time.
In addition, Ms. Rasmussen mentored two National Science Foundation Research Experience for Undergraduate students.

Mr. Dennis Kovarik, as an undergraduate researcher in Computer Science and Engineering used this research as a platform for his Senior Design Project.

At NMT, the project has provided an undergraduate research experience for Ms. Esparza. This experience has prepared them for further research in a molecular biology or forensic DNA lab.

4. What do you plan to do during the next reporting period to accomplish the goals and objectives?

This is the last reporting period.

5. What has the project produced?

The project has produced two reader systems for utilizing upconverting nanoparticles to develop fingerprints.

6. What are the project outcomes?

Two systems were developed, one utilizing a laser to excite the upconverting nanoparticles (UCNPs) and a modified cellular phone as a camera to read the upconversion. The UCNPs were tested and worked excellently on a wide variety of substrates, including fluorescent surfaces and under room lighting. A platform for interpreting the fingerprint minutiae and matching fingeprints was also developed. A second light emitting diode (LED)-based system was also developed to read the upconversion from the UCNPs on fingerprints. This utilized a 100 Watt, 980 nm emitting LED and a modified camera to collect the upconversion light. The LED system also included a water-cooling setup to keep the LED emitting light for longer.

Finally, UCNPs were modified to be more attractive to DNA molecules. Acetic acid was used to modify the surface of the UCNPs. Acetic acid modification allowed the UCNPs to pick up DNA at low pH and to shed this DNA when the pH was raised sufficiently. This resulted in the recovery of 15-20% of the DNA. In addition, at low DNA concentrations, polymerase chain reaction (PCR) of the DNA seemed to be inhibited by the presence of UCNPs or contaminants from the UCNPs that are present when UCNPs are used.